US Army Corps of Engineers

(2)

THE ATCHAFALAYA RIVER DELTA

Report 2

FIELD DATA
SECTION 2. SETTLING CHARACTERISTICS OF BAY SEDIMENTS

by

Allen M. Teeter, Walter Pankow

Hydraulics Laboratory

DEPARTMENT OF THE ARMY
Waterways Experiment Station, Corps of Engineers
3909 Halls Ferry Road, Vicksburg, Mississippi 39180-6199

September 1989

Report 2 of a Series

Prepared for US Army Engineer District, New Orleans
New Orleans, Louisiana 70160-0267

HYDRAULICS LABORATORY

REPORT DOCUMENTATION PAGE

Form Approved OMB No. 0704-0188

1a. REPORT SECURITY CLASSIFICATION Unclassified	1b. RESTRICTIVE MARKINGS
2a. SECURITY CLASSIFICATION AUTHORITY	3. DISTRIBUTION/AVAILABILITY OF REPORT Approved for public release; distribution unlimited.
2b. DECLASSIFICATION/DOWNGRADING SCHEDULE	
4. PERFORMING ORGANIZATION REPORT NUMBER(S) Technical Report HL-82-15	5. MONITORING ORGANIZATION REPORT NUMBER(S)
6a. NAME OF PERFORMING ORGANIZATION USAEWES Hydraulics Laboratory 6b. OFFICE SYMBOL (If applicable) CEWES-HE	7a. NAME OF MONITORING ORGANIZATION
6c. ADDRESS (City, State, and ZIP Code) 3909 Halls Ferry Road Vicksburg, MS 39180-6199	7b. ADDRESS (City, State, and ZIP Code)
8a. NAME OF FUNDING/SPONSORING ORGANIZATION USAED, New Orleans 8b. OFFICE SYMBOL (If applicable) LMNED	9. PROCUREMENT INSTRUMENT IDENTIFICATION NUMBER
8c. ADDRESS (City, State, and ZIP Code) PO Box 60267 New Orleans, LA 70160-0267	10. SOURCE OF FUNDING NUMBERS PROGRAM ELEMENT NO. / PROJECT NO. / TASK NO. / WORK UNIT ACCESSION NO.

11. TITLE (Include Security Classification)
The Atchafalaya River Delta; Report 2, Field Data; Section 2: Settling Characteristics of Bay Sediments

12. PERSONAL AUTHOR(S)
Teeter, Allen M.; Pankow, Walter

13a. TYPE OF REPORT	13b. TIME COVERED	14. DATE OF REPORT (Year, Month, Day)	15. PAGE COUNT
Report 2 of a series	FROM _____ TO _____	September 1989	119

16. SUPPLEMENTARY NOTATION
Available from National Technical Information Service, 5285 Port Royal Road, Springfield, VA 22161.

17. COSATI CODES			18. SUBJECT TERMS (Continue on reverse if necessary and identify by block number)
FIELD	GROUP	SUB-GROUP	Atchafalaya Bay (La.) (LC); Numerical analysis (LC); Hydrodynamics; Sedimentation; Mathematical models (LC)

19. ABSTRACT (Continue on reverse if necessary and identify by block number)

The Wax Lake Outlet and Atchafalaya River deltas in Louisiana have grown dramatically, and concern for their impacts has led the US Army Corps of Engineers to conduct an investigation to predict how the deltas will evolve over the next 50 years. The overall study task was to determine the impacts of that growth on navigation, flood control, salinity, and sedimentation. Within this series of reports, this report documents field, laboratory, and theoretical studies on the settling characteristics of bay sediments. Tests were performed using resuspended bed samples and samples of suspended material, and covered a wide concentration range. The effects of settling height, salinity, suspension concentration, and turbulence were tested.

20. DISTRIBUTION/AVAILABILITY OF ABSTRACT ☒ UNCLASSIFIED/UNLIMITED ☐ SAME AS RPT ☐ DTIC USERS	21. ABSTRACT SECURITY CLASSIFICATION Unclassified
22a. NAME OF RESPONSIBLE INDIVIDUAL	22b. TELEPHONE (Include Area Code) / 22c. OFFICE SYMBOL

PREFACE

The work reported herein was performed in the Hydraulics Laboratory (HL) of the US Army Engineer Waterways Experiment Station (WES) as a part of the overall investigation to predict the evolution of the Atchafalaya Bay delta. The study design (Phase I of the study) was authorized by the US Army Engineer District, New Orleans (LMN), on 18 July 1977. The implementation of the study plan (Phase II) was authorized by LMN on 21 May 1979. This report presents work done under Phase II, in support of numerical modeling of the delta evolution.

This study was conducted under the direction of Messrs. H. B. Simmons and F. A. Herrmann, Jr., former and present Chiefs, HL; R. A. Sager, Assistant Chief, HL; W. H. McAnally, Chief, Estuaries Division; G. M. Fisackerly, Chief, Estuarine Processes Branch; and R. A. Boland, former Chief, Hydrodynamics Branch. The plan of study of which this task is one part was developed by Messrs. McAnally and Samuel B. Heltzel, Estuarine Engineering Branch. This study was performed by Mr. A. M. Teeter, Estuarine Processes Branch, assisted by Messrs. B. G. Moore and D. M. White, Estuaries Division. Gratitude is extended to Dr. R. Ariathurai and Mr. McAnally for consultation. Consultants to the project were Mr. L. R. Beard, Dr. C. R. Kolb, Dr. R. B. Krone, and Mr. F. B. Toffaletti. This report was written by Messrs. Teeter and Walter Pankow, Estuarine Processes Branch, and edited by Mrs. M. C. Gay, Information Technology Laboratory, WES.

Commander and Director of WES during preparation of this report was COL Larry B. Fulton, EN. Technical Director was Dr. Robert W. Whalin.

CONTENTS

LIST OF FIGURES

CONVERSION FACTORS, NON-SI TO SI (METRIC) UNITS OF MEASUREMENT

Non-SI units of measurement used in this report can be converted to SI (metric) units as follows:

Multiply	By	To Obtain
cubic feet	0.02831685	cubic metres
feet	0.3048	metres
inches	2.540	centimetres
knots (international)	0.5144444	metres per second
miles (US statute)	1.609347	kilometres
pounds (force) per square inch	703.1	kilograms per square metre
pounds (mass) per cubic foot	16.01846	kilograms per cubic metre
tons (2,000 pounds, mass)	907.1847	kilograms

THE ATCHAFALAYA RIVER DELTA

FIELD DATA

Section 2. Settling Characteristics of Bay Sediments

PART I: INTRODUCTION

Background

1. The main energy source to the Atchafalaya Bay system is the Atchafalaya River. The river captures about 30 percent of the latitude flow (combined flow of the Mississippi River and Red River at the latitude of 31° N) at the Old River Diversion Structure (Figure 1), and carries with it an average of about 100 million tons* of sediment in suspension each year. Over the past several decades, the suspended sediment has filled in the Atchafalaya basin floodway between its natural levee systems and is now depositing rapidly in Atchafalaya Bay (Figure 1). As shown, two deltas are forming in Atchafalaya Bay: at the mouth of Lower Atchafalaya River and at Wax Lake Outlet (WLO). The evolving deltas became subaerial and vegetated in 1973 and have since become one of the most dynamic currently active delta systems in the world. The evolving deltas have converted shallow bays into marshes and continue to generate a great deal of interest in deltaic processes. The primary benefit from these two deltas has been the addition of new land to the coast of Louisiana in areas otherwise experiencing land loss. The primary concerns with the evolving deltas have been siltation in the navigation channels and backwater flooding in the surrounding low-lying coastal parishes of southern Louisiana. Fine-grained sediments predominate in the Atchafalaya Bay system.

2. Phenomenal growth of the subaerial Atchafalaya River delta and the emerging WLO delta led the US Army Engineer District, New Orleans, to request that the US Army Engineer Waterways Experiment Station (WES) conduct an investigation to predict future growth of the deltas and effects of that growth.

---

* A table of factors for converting non-SI units of measurement to SI (metric) units is presented on page 4.

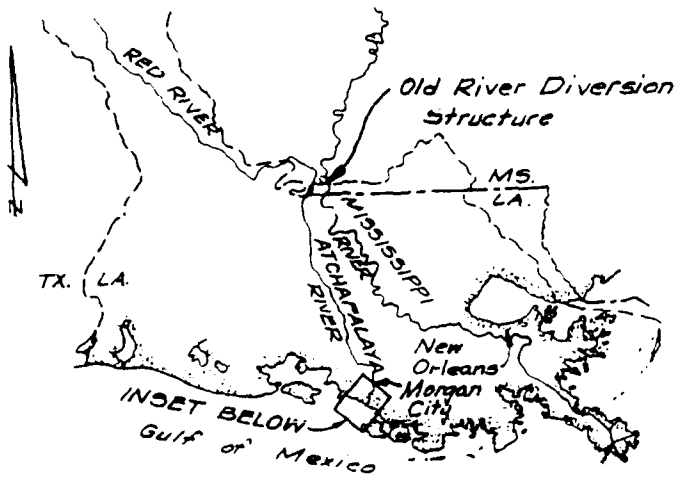

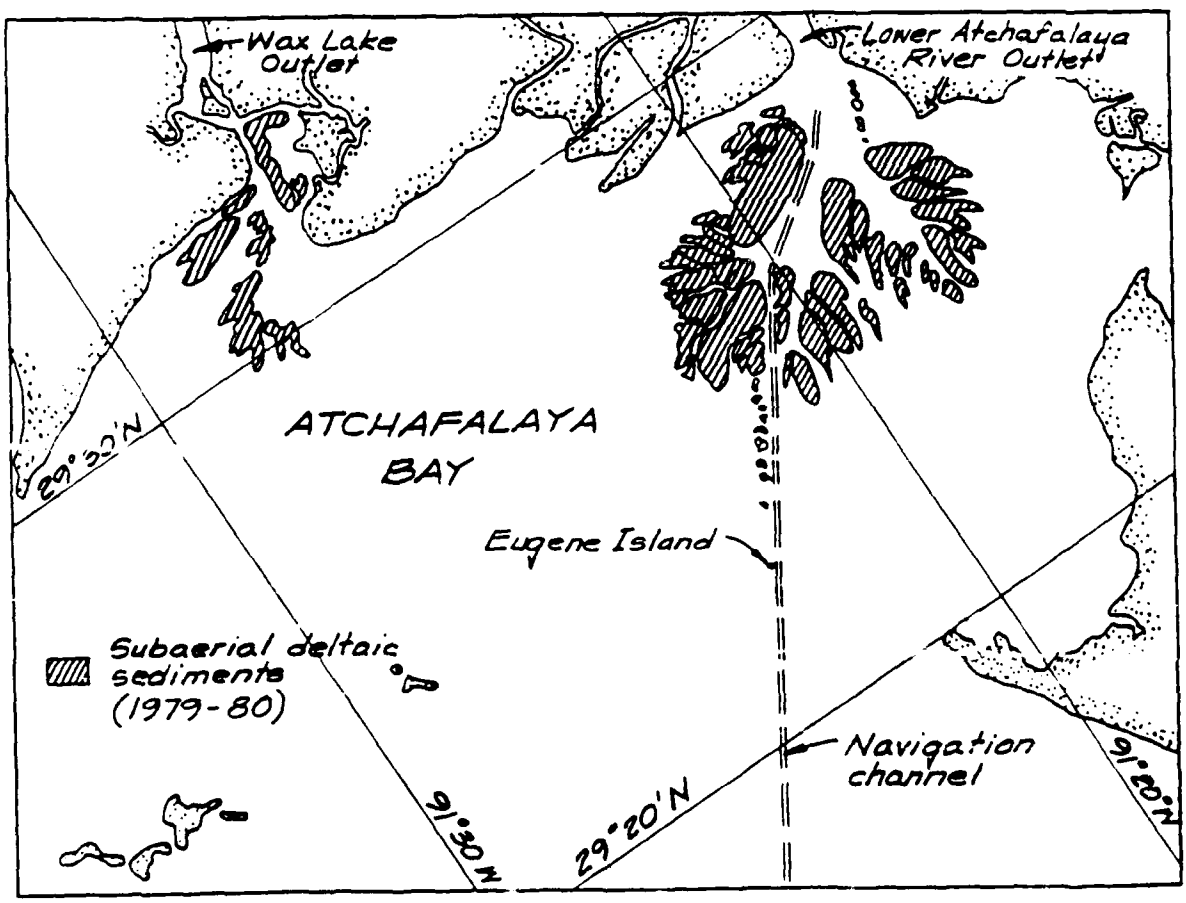

Figure 1. Vicinity sketch showing the Atchafalaya River and Wax Lake Outlet deltas

Objective

3. The overall objective of the Atchafalaya Bay investigation is to predict future evolution of the delta system. Specific answers are sought to these questions:

a. For existing conditions and no actions other than those already practiced (i.e., maintenance of navigation channels), how will delta deposits evolve over the short-to-medium term (10-15 years) and the long term (50 years)?

b. How will the delta's evolution affect:

(1) Flood stages?

(2) Maintenance dredging of the navigation channel?

(3) Salinity, sedimentation, and circulation in the Atchafalaya Bay system?

c. What would be the impact of various navigation/flood-control structural alternatives on all of the above?

4. This report summarizes studies conducted by the WES Hydraulics Laboratory to characterize sediments depositing in Atchafalaya Bay, Louisiana. These studies were undertaken as part of a comprehensive investigation of the deltaic evolution occurring in Atchafalaya Bay. Objectives were to describe field conditions and to generate information needed by the WES numerical sediment transport modeling effort for the prediction of delta evolution. The depositional properties of sediments were the primary subject. These properties include the settling velocity distributions of sediments found in suspension and in bed deposits, the concentration of newly deposited sediments, and the rates of consolidation of newly deposited bed sediments.

Approach

5. The plan of the overall investigation includes multiple techniques to predict delta growth. Each method builds upon prior work and employs predictive techniques using progressively greater degrees of sophistication, including the following:

a. Extrapolation of observed bathymetric changes into the future.

b. A generic analysis that predicts future growth by constructing an analogy between behavior of the Atchafalaya Delta and other deltas in similar environments.

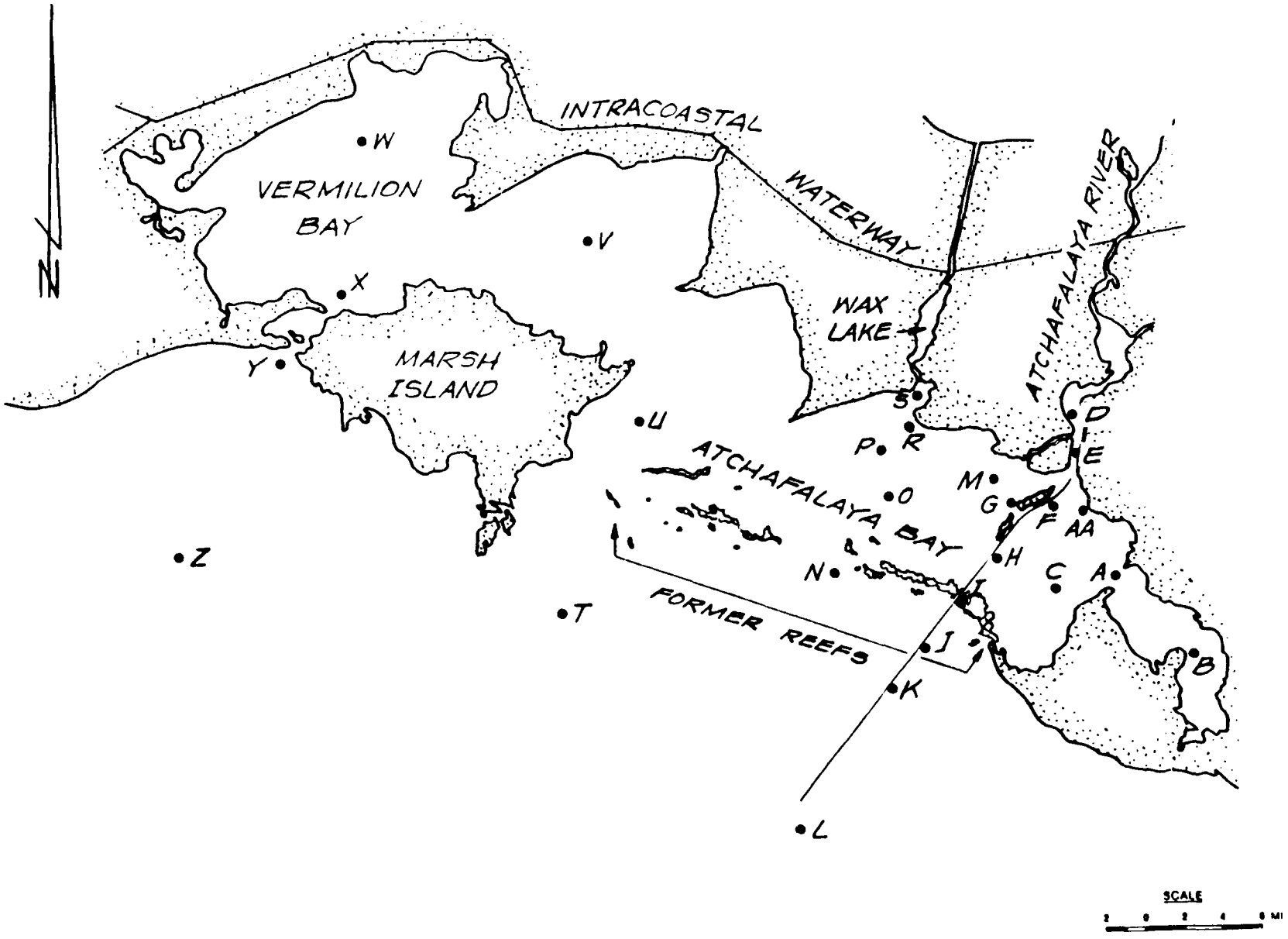

Figure 2. Sampling stations in the Atchafalaya Bay system, Louisiana

properties of the sediments themselves, conditions under which deposition and erosion occur in Atchafalaya Bay are of interest for a general understanding of sedimentation processes in the system and also for numerical sediment modeling efforts. Data on flows and sediment concentration distributions were used to identify these conditions. Separate laboratory studies were also conducted on this subject (Dixit, Mehta, and Partheniades 1982). Data on the grain size and radiograph analysis of sediment samples collected throughout the bay system are presented in Report 2, Section 3, of this report series (in preparation).

9. Settling tests are covered in Part II along with data on the initial bed densities of sediment settling from suspension. Consolidation of bed sediments in dense suspensions by hindered settling consolidation is covered in Part III. Part IV covers field data on the distributions of TSM and settling velocity, vertical TSM stratification, bed shear stress, and the bulk wet densities and cation exchange capacities of bed sediments.

PART II: SETTLING TESTS

10. Settling tests were performed in settling tubes and by numerical methods. Settling tube tests are indirect methods of determining settling velocity. The settling characteristics of quiescent suspensions were observed over time in the laboratory and in the field. Numerical models added turbulence and varying bottom boundary conditions to the study of the settling of suspensions. Because sediments were tested under various concentrations, salinities, heights, and turbulence, the laboratory behavior of sediments was observed and extended to the field behavior.

Basic Concepts and Definitions

11. Several interrelated factors influence the behavior of sediment particles suspended in a fluid. The factors can be categorized in two groups: the properties of the sediment and the conditions in which the sediment exists. Both of these groups are important in the classification scheme for suspended sediment and can be studied in the laboratory using a quiescent settling tube. For some purposes, the sediment grain size in itself is a useful classification scheme; however, a more useful classifier for suspended sediment is settling velocity. Basically, settling velocity is caused by the imbalance of gravitational forces and the viscous drag experienced by suspended particles and aggregations of particles. Settling velocity takes into account the effects of shape, density, and physical-chemical characteristics in addition to the particle size. To classify the behavior of particles in turbulent suspensions, certain properties of the flow must also be considered, namely, depth and turbulence. The particle Peclet number combines the effects of settling and flow conditions. This number is the ratio of settling time to vertical mixing time and can be related to suspension stratification and mass flux to the bed.

12. Particle grain size distribution and mineral composition are important factors in the settling velocity of fine-grained sediments. Other conditions that affect the settling velocity of fine-grained sediment include concentration, settling height, salinity, temperature, and turbulence. Most of these conditions can be reproduced in the laboratory. After testing, settling velocities can be converted into equivalent quartz spherical diameters

for comparison to mineral grain sizes by using Stokes' law of settling. Examples of such equivalent diameters for a particle density of 2.65 g/cu cm are shown in the following tabulation:

Settling Velocity, mm/sec	Stokes Equivalent Diameter, μm
0.0009	1
0.0038	2
0.0160	4
0.0600	8
0.2400	16
0.9800	32
3.8000	64

Figure 3 shows an example comparison of grain size distribution (determined by hydrometer test) plotted with a series of settling tests made on bed material from station F with varying concentrations. The largest differences are in the slow-settling or fine-grained range. These small particles have high

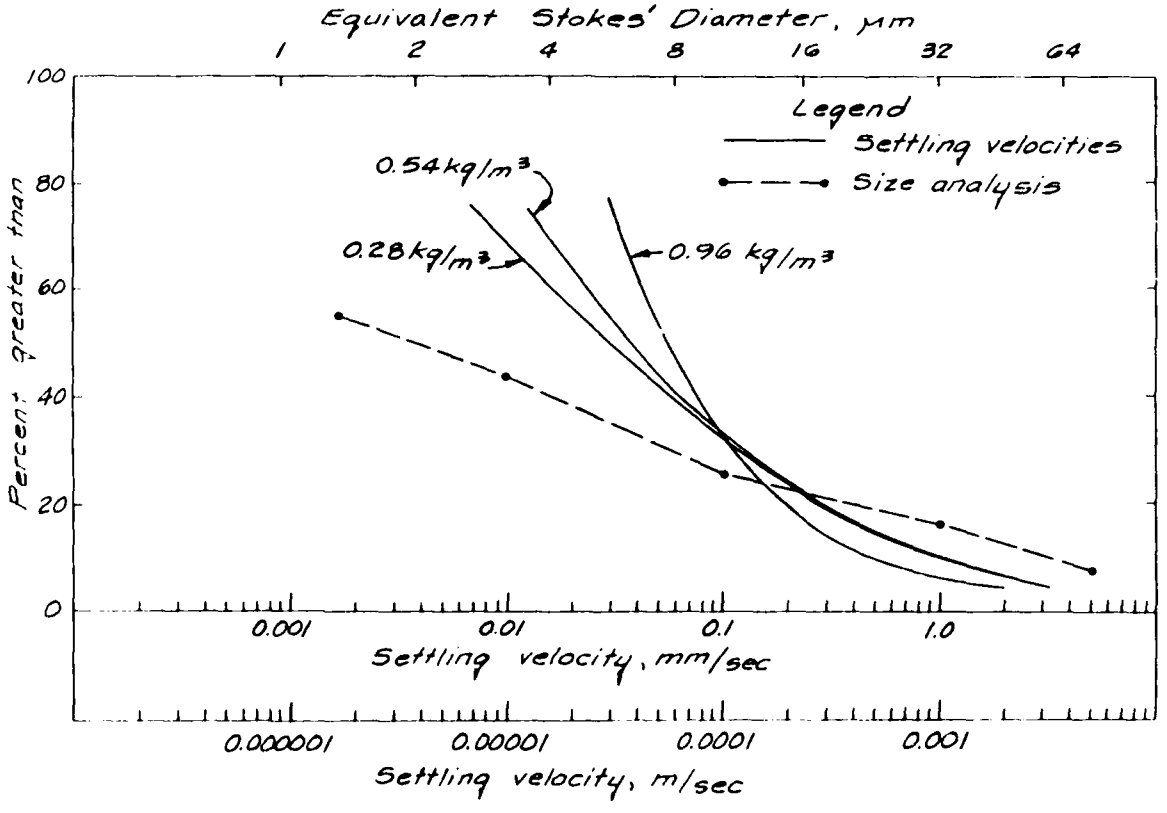

Figure 3. Comparison between grain size and settling velocity distributions for station F

surface-area-to-volume ratios and surface electrical charge densities. If conditions bring them into close contact or if ionic concentrations reduce repulsive forces, they will adhere to one another. The strength of this adhesion depends on interparticle distances. In the example shown in Figure 3, concentration has affected the settling velocity distribution. Thus the settling velocity distribution cannot be deduced directly from dispersed grain size distribution.

13. Dispersed grain size distributions for stations F and M are shown in Figure 4. They are characteristic of the area. A compilation of grain size distributions for hundreds of locations in the bay system is given in Report 2, Section 3, of this report series (Donnell, in preparation). Bed sediments were found generally to be silty, fine-grained materials with varying amounts of clay and sand.

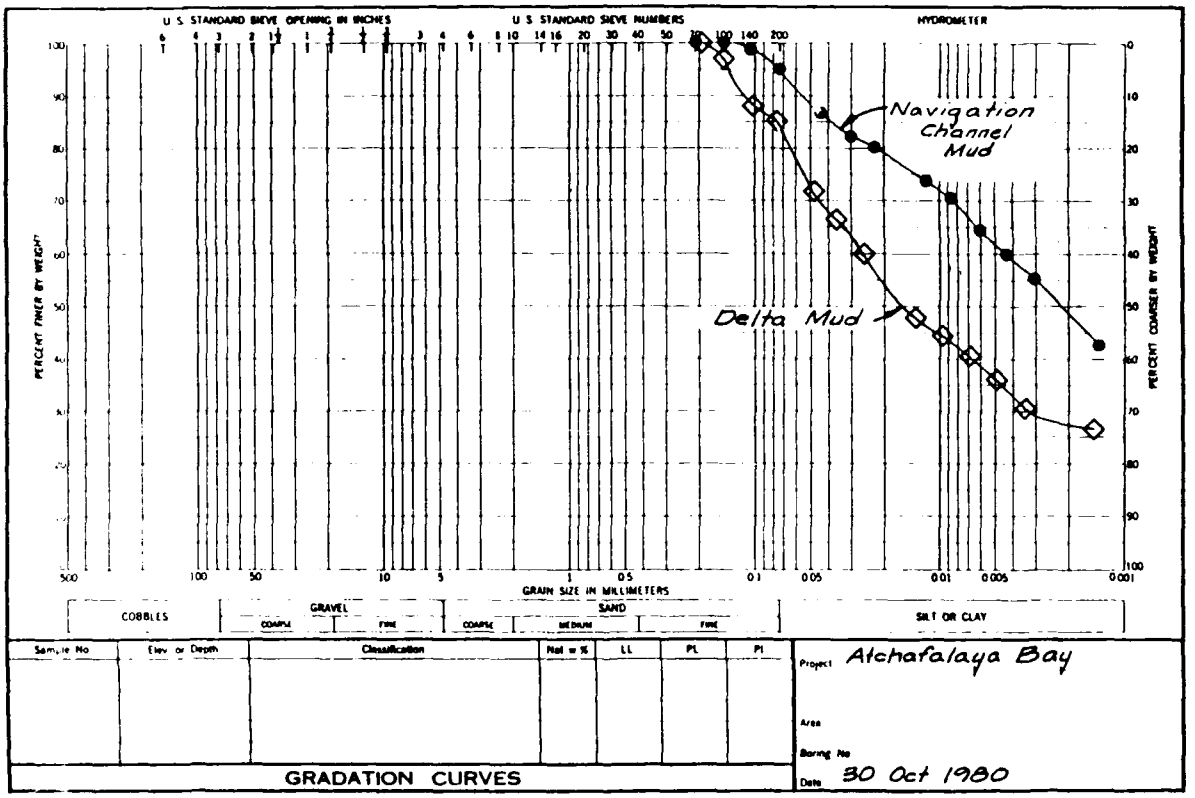

Figure 4. Dispersed grain size distribution for two sampling stations

14. To represent mathematically the vertical settling of fine sediments in the presence of turbulence, the one-dimensional transport equation with Fickian diffusion and diffusivity assumptions was used:

$$\frac{\partial C}{\partial T} - W_s \frac{\partial C}{\partial Z} = \frac{\partial}{\partial Z}\left(K_z \frac{\partial C}{\partial Z}\right) \tag{1}$$

where

C = concentration

T = time

W_s = terminal scalar settling velocity resulting from the balance of gravitational forces and viscous drag (the settling velocity in quiescent fluid)

Z = vertical dimension

K_z = effective vertical eddy diffusivity

Since fine sediments are being considered, it is assumed that K_z is the same as the combined turbulent and molecular diffusivities for momentum. The vertical dimension (Z) is measured upward from the bed. The following flux boundary conditions are imposed:

$$W_s C + K_z \frac{\partial C}{\partial Z} = 0 \quad \text{at} \quad Z = H \text{ (water surface)} \tag{2}$$

and either

$$K_z \frac{\partial C}{\partial Z} = 0 \quad \text{at} \quad Z = 0 \text{ (bed)} \quad \text{for free settling} \tag{3}$$

or

$$W_s C + K_z \frac{\partial C}{\partial Z} = 0 \quad \text{at} \quad Z = 0 \text{ (bed)} \quad \text{for no-settling} \tag{4}$$

or

$$W_s C + K_z \frac{\partial C}{\partial Z} = \dot{m} \quad \text{at} \quad Z = 0 \text{ (bed)} \quad \text{for erosion} \tag{5}$$

where $\dot{m}$ is the mass rate of erosion and H is the total depth or height. Equation 1 can be nondimensionalized by substituting

$$z = \frac{Z}{H}, \quad t = \frac{W_s T}{H}, \quad \text{and} \quad P_e = \frac{W_s H}{K_z}$$

where P_e is the particle Peclet number. Then,

$$\frac{\partial C}{\partial t} - \frac{\partial C}{\partial z} = \frac{1}{P_e} \frac{\partial^2 C}{\partial z^2} \tag{6}$$

is a nondimensional transport equation and the nondimensional flux becomes

$$C + \frac{1}{P_e} \frac{\partial C}{\partial z}$$

This implies that at steady state or equilibrium

$$P_e = - \frac{1}{C} \frac{\partial C}{\partial z} \tag{7}$$

where $\partial C/\partial z$ is normally negative. The nondimensional parameter governing stratification is, therefore, the particle Peclet number. This was confirmed by numerical simulations and the relationship of Equation 7 verified. For a given probability that a particle reaching the bottom stays there, P_e affects the rate of mass flux to the bed. Parametric tests were run on the effects of P_e and bottom boundary conditions on stratification, the effect of P_e on mass flux to the bed, and the effects of P_e on the interpretation of settling velocity analyses. Depth-averaged and parabolically distributed values of K_z were tested and compared.

Description of Settling Tests

15. Settling tube tests were performed on suspended samples taken in the field. Parametric tests were also run on suspended sediments and resuspended bottom sediments to establish the effects of certain conditions on settling velocity. Conditions tested included concentration, settling height, salinity, and turbulence.

Laboratory methods

16. Tests were performed in two clear acrylic tubes, each 2 m high by 10 cm in diameter, with sampling ports constructed in them. One tube had silicon rubber ports or diaphragms and samples were drawn using an 18-gage hypodermic needle inserted through the port into the suspension. The other tube had spigots with 0.32-cm bore diameter extending 1.5 cm into the suspension.

17. Tests were carried out by sampling from the settling tube with time. The sediment to be tested was shaken by hand in a 20-ℓ carboy for

approximately 3 min before being poured into the settling tube. A sample was taken immediately, and further sampling was spaced approximately geometrically over a 6-hr period. Between 6 and 11 samples were taken during each test. TSM was determined on samples by filtration. Nuclepore polycarbonate filters with 0.40-μm pore size were used. They were desiccated and preweighed. A vacuum system (8-psi vacuum maximum) was used to draw the sample through filters. Filters and holders were then washed with distilled water to remove salts. Filters were dried at 105° C for 1 hr and reweighed. TSM was then calculated based on the net weight retained on the filter and the volume of the sample filtered.

18. Some settling tests were made at high concentration. In addition to the samples normally taken, the height of the sediment bed layer was also measured, initially at intervals of about 2 min. After the settling velocity was computed, the density of the bed deposits could be estimated as the mass of sediment settled divided by the volume it occupied at a point in time when an arbitrary 68 percent of the sediment had settled to the bed or when the test was terminated.

Field methods

19. Field settling tests were performed much the same as laboratory experiments except that samples were drawn from a field sampler immediately after the sample was taken. Field stations are shown in Figure 2. The field sampler (and settling tube) was a Niskin type made of opaque polyvinyl chloride. The sampler is an 0.85-m-long tube that opens at both ends and is held horizontally, aligned with the flow, for sampling. The field settling sampler is shown in Figure 5. After closure, it was brought to the surface and placed vertically in a rack, and sampling continued. Normally, six samples were taken over a 4-hr period. The field method minimizes the disturbance that suspended particles and aggregates experience during the settling test. The estimates of settling velocity obtained in this way are expected to be closer to in situ values than those made using laboratory tests.

Settling data reduction

20. Several methods were used to analyze the settling tube data, depending on the purpose of the tests. The accumulation method was applied to multiple-depth tests. The accumulation method was developed by Odén (1925) in 1925 and recommended for settling velocity determinations at low concentrations (Inter-Agency River Basin Committee 1953). This method relates settling

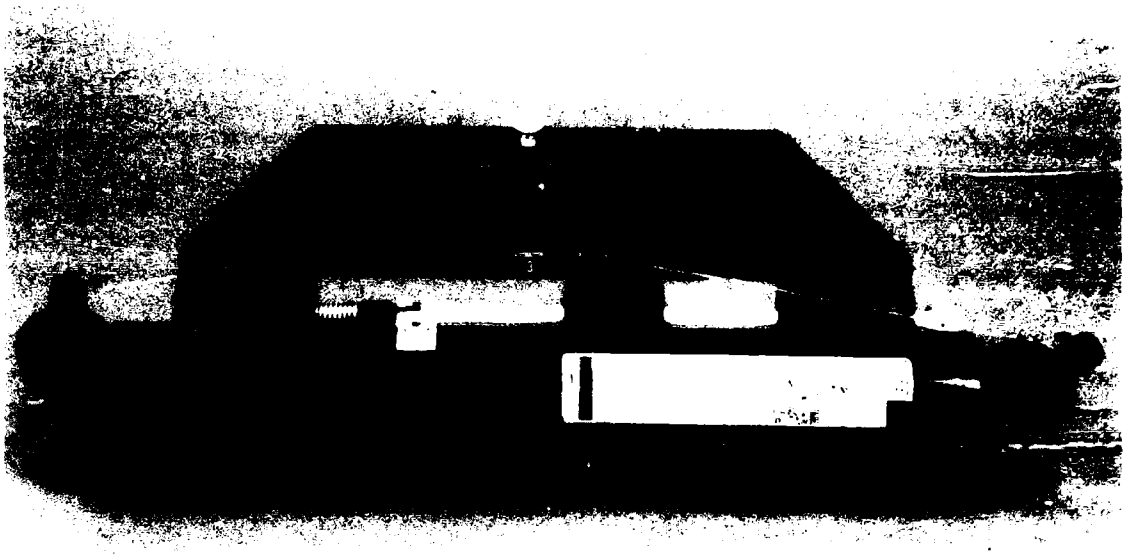

Figure 5. Settling velocity field sampling tube

velocity to the differentiation of the sedimentation curve with respect to time. Usually a bottom withdrawal tube is used in tests. However, for this study, the sedimentation curves were constructed by integrating the concentrations from several heights in a settling tube. Results from the multiple-depth tests were also used to construct concentration profile diagrams using a method proposed by McLaughlin (1959). These diagrams can be used to detect the effects of flocculation, aggregation, or hindered settling by examining the slope of the isopleths of settling height H divided by time T. Most routine settling velocity determinations used the pipette analyses, assuming that the change of concentration at H distance below the free surface represents that fraction of the suspension with settling velocity greater than H/T.

21. A computer program named SETL was developed to analyze settling test results. Data from the settling tube tests were least-squares-fit by a second-order polynomial of the form:

$$\% \text{ settled} = a_o + a_1(\ln T) + a_2 (\ln T)^2 \qquad (8)$$

where the a terms are regression constants. For the accumulation method,

settling velocity distributions were calculated by

$$\% \text{ greater than } H/T = (a_o - a_1) + (a_1 + 2a_o) \ln T + a_2(\ln T)^2 \qquad (9)$$

This technique is equivalent to older graphical methods.

22. A comparison between the regression-method computer program SETL and graphical techniques is shown in Figure 6. The data and graphical results are from Christodoulou, Leimleuhler, and Ippen (1974). For the pipette analyses, the percent greater than H/T was computed directly from Equation 8, while increments of the distribution were found by quadratic solution of that equation.

23. In addition to the cumulative distribution of settling velocity, some statistical parameters were calculated. They include geometric mean, which is more representative of the distribution than the median, and the dimensionless geometric standard deviation and skewness. The equations used are those suggested by Inman (1963) for the generally log-normal particle size distributions:

Geometric mean

$$W_{s_g} = \left(W_{s_{16}} W_{s_{84}}\right)^{1/2} \qquad (10)$$

Geometric standard deviation

$$\sigma_g = \left(\frac{W_{s_{84}}}{W_{s_{16}}}\right)^{1/2} \qquad (11)$$

Skewness

$$\frac{\log\left(\frac{W_{s_g}}{W_{s_{50}}}\right)}{\log \sigma_g} \qquad (12)$$

where W_{s_x} is the settling velocity at the x^{th} percentile. Differential settling classes were defined by a geometric series constructed by raising an

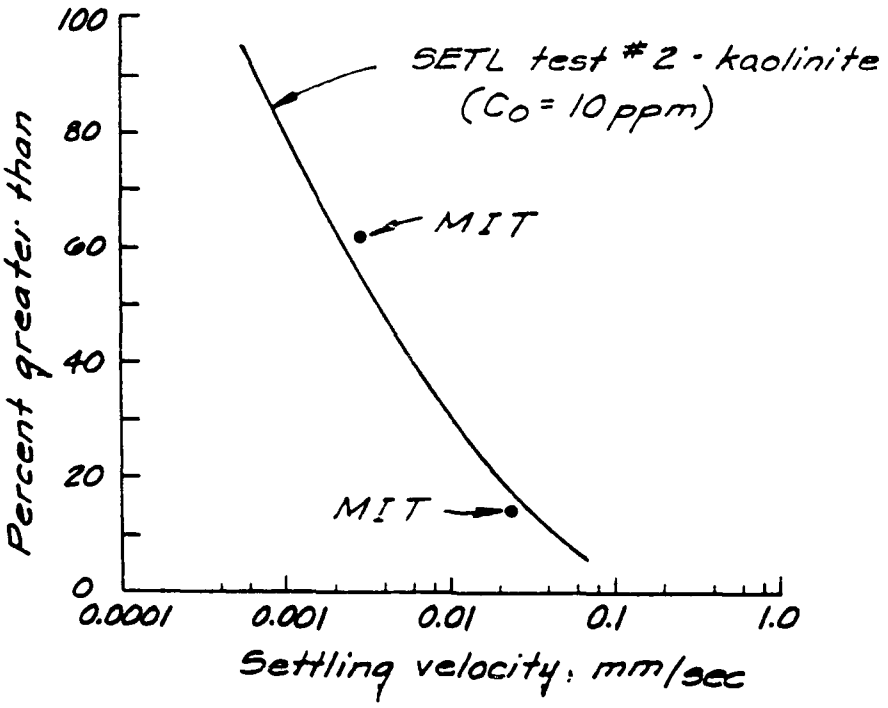

a. Computed kaolinite and field data

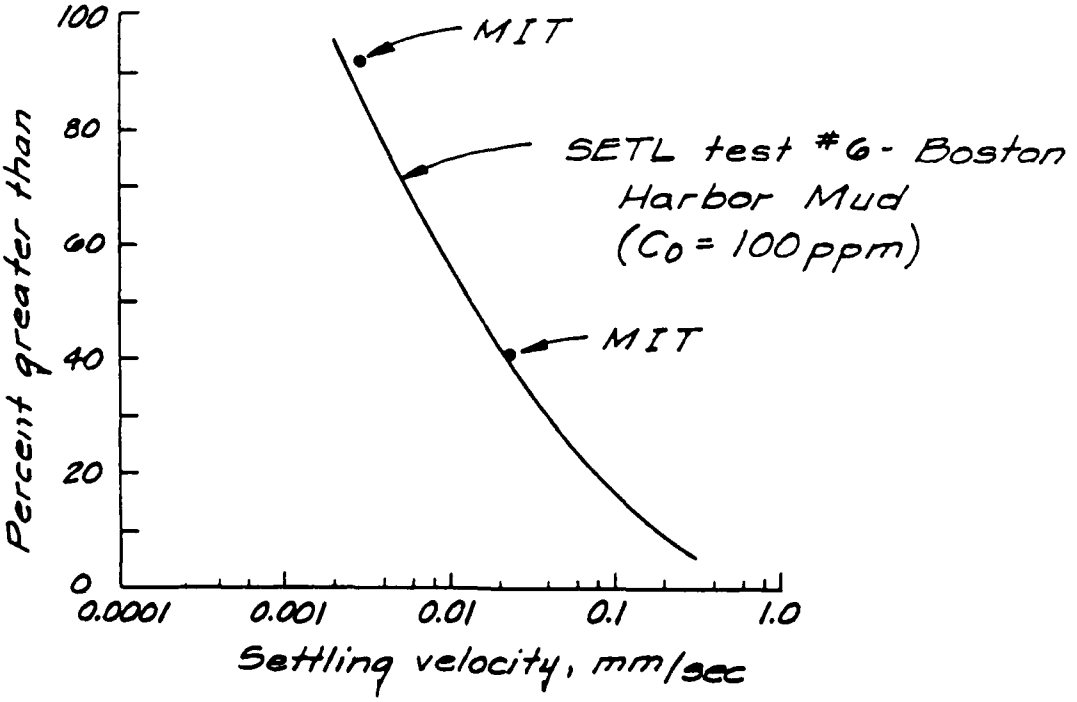

b. Boston Harbor mud and field data

Figure 6. Comparison between regression program SETL and graphical method (MIT data obtained from Christodoulou, Leimleuhler, and Ippen 1974)

arbitrary number to progressively higher powers:

$$(3 \times 10^{-7} \text{ m/sec})^{k}, \quad k = 1 \text{ to } 8$$

and the concentrations of suspended material falling within these classes were calculated by the computer program SETL. Settling velocities were also calculated at 10 percent intervals over the settling velocity distribution.

24. Several comparisons among the various settling analyses were made in addition to the comparison between graphical and regression model accumulation methods already mentioned. Figure 7 shows an example plot of a multiple-depth sedimentation test. The data were integrated and analyzed by the accumulation method as well as individually analyzed by the pipette method. Results are compared in the following tabulation:

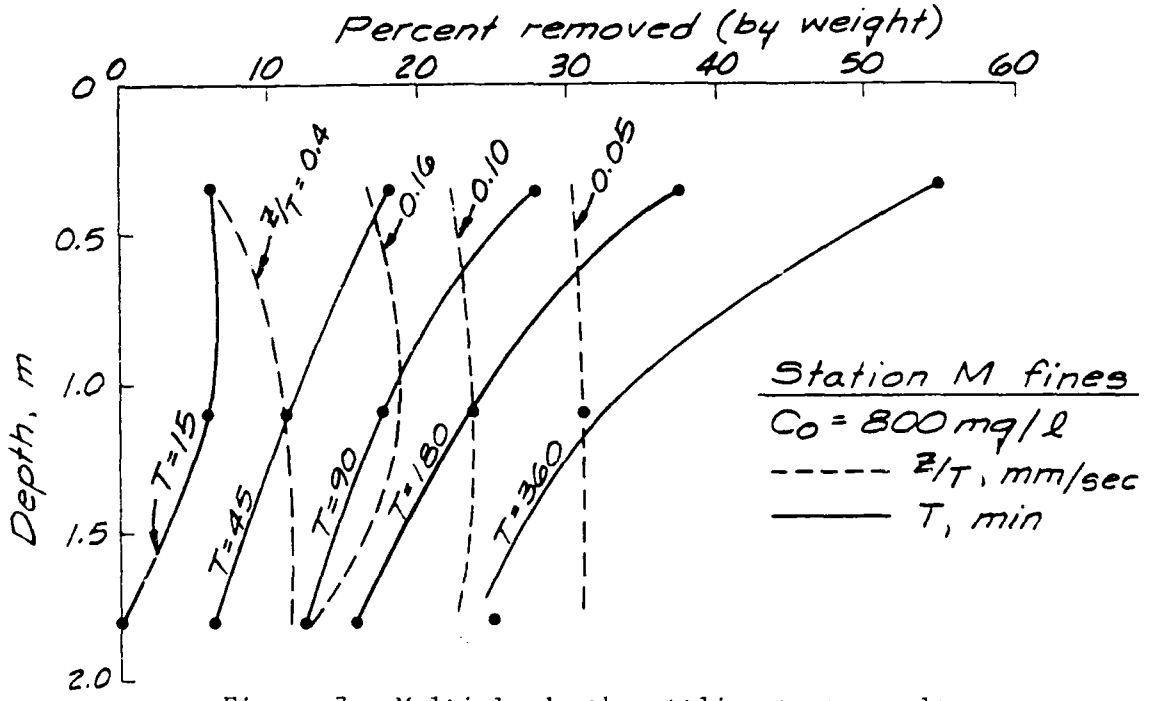

Figure 7. Multiple-depth settling test results

	Settling Velocity, mm/sec					
	Pipette			Accumulation		
Depth, m	Median	Mean	Standard Deviation	Median	Mean	Standard Deviation
0.20	0.011	0.015	5.56			
0.95	0.010	0.016	13.04			
1.65	0.012	0.018	9.47	0.012	0.018	7.66

Results showed that the accumulation and pipette methods of settling velocity analysis were equivalent, and that settling velocity results from this study should be comparable to other reliable results.

25. According to McLaughlin's interpretation of multiple-depth tests using settling depth versus time (Z/T) (McLaughlin 1959), the isopleths sloping toward the right with increased depth indicate an increase in settling velocity with depth due to aggregation or flocculation. Figure 7 therefore indicates a slight increase in W_s with depth. The same indication is given in the preceding tabulation by the pipette analyses.

26. The pipette analysis and computer program SETL were also checked by analyzing numerical settling experiments at high P_e numbers. For a specified settling velocity of 0.200 mm/sec, analysis of numerical results by the pipette method and computer program SETL recovered a mean settling velocity of 0.205 mm/sec and geometric standard deviation of 1.2 at $P_e = 100$. This test was a further indication that the pipette method and computer program SETL accurately determine settling velocity.

Field/laboratory test difference

27. Figure 8 shows a comparison between field and laboratory settling tests run on samples taken at the same location with the same sampler and as

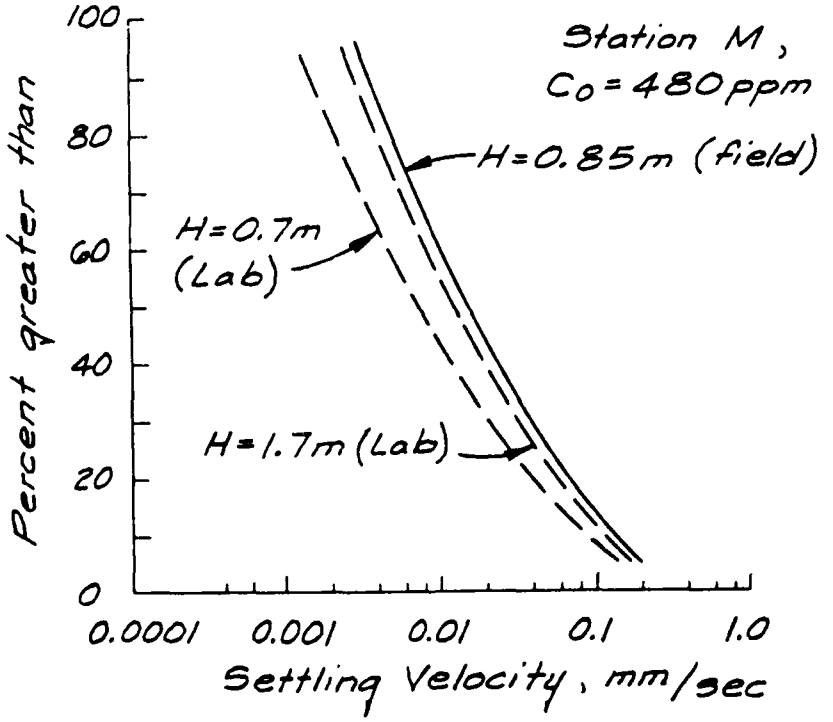

Figure 8. Comparison between field and laboratory settling tests

close in time as possible. That comparison shows that the field results were higher than those obtained with the laboratory settling tube. The laboratory tests included two different settling heights. Similar results have been reported by other investigators (Owen 1971). The explanation given was that natural turbulence brings aggregates to a state at which they will settle more quickly. As will be discussed later, settling height also increases settling velocities. When a small portion of a relatively deep suspension is collected, the field settling tests are affected by the in situ aggregation caused by both turbulence and settling height.

Numerical methods

28. The governing equation, Equation 1, along with appropriate boundary and initial conditions, was solved using a method of weighted residuals. Specifically, the method of orthogonal collocation was used where the weighting function is a Dirac delta function and the trial functions are a series of Legendre polynomials. The collocation points or nodes are located at Gauss points. Instead of breaking the domain into subelements, a single high-order element with seven nodes was used. This was easy to apply and maintained continuous first and second derivatives throughout the domain. A fourth-order Runge-Kutta method was used to integrate in time. Gaussian quadrature was used to integrate over the spatial domain. The interpolated values used to construct and plot concentration profiles were generated from nodal values using the trial functions for interpolation.

Test Results

29. Table 2 is a tabulation of the field and laboratory settling tests performed by sampling station. The table also shows other analyses performed, which will be more thoroughly discussed in Part IV. Settling velocity distributions for field settling tests are given in Table 3. Table 4 gives a summary of the turbulence settling test conditions and results. Table 5 summarizes the initial bed densities observed in high-concentration settling experiments.

Discussion of Laboratory Results

30. The field settling tests will be discussed in Part IV in the context of other field measurements.

Effect of concentration

31. Increased concentration decreases interparticle distances and generally enhances aggregation. There is an upper limit to this effect above which settling is hindered. This will be further discussed in Part III. Figure 9 shows the effect on bed samples from stations H and F. Settling velocities are plotted for 25, 50, and 75 percentiles. Figure 10 shows the effect of concentration on the settling velocity of bed sediments from station M. The greatest effect of concentration on W_s was found in the 75-percentile fraction of station H. Station F had somewhat less, and station M showed little dependence of settling velocity at low concentrations (below 1 g/ℓ), and a moderate dependence between 1 and 10 g/ℓ. Cation exchange capacities (CEC) of samples from stations H, F, and M were 32, 27, 11 meq/100 g, respectively. Therefore, CEC correlated with the concentration effects found in the settling experiments. For these samples, the higher the CEC, the greater the effect of concentration on settling velocity.

Effects of salinity

32. Suspended samples were tested with increasing salinity. Increased ionic concentration reduces electrorepulsive charges around the particles, allowing aggregation to proceed. Figure 11 shows the results of a test that consisted of a mixture of suspended samples from stations C and M. Native ocean water was used to increase the salinity. Suspended samples from stations H and F were tested and results shown in Figure 12. Their salinity was increased using a saturated brine solution made from Louisiana salt dome rock salt.

33. Composite sediments from stations C and M showed an increase in the median settling velocity by a factor of about 2.5 when the salinity was increased from about 0.25 ppt (river concentration) to between 2.3 and 2.2 ppt. Station H showed little change while station F actually showed a decrease in settling velocity between 0.25 and 2 ppt followed by a large increase in settling velocity at over 30 ppt. Experimental error is suspected in the 2-ppt test.

Effects of settling height

34. Some tests on the effects of settling height on settling velocity were made. Differential settling can lead to further aggregation and increased settling velocity. Figure 13, which shows test results for stations H and M at different settling heights, indicates increased settling velocity

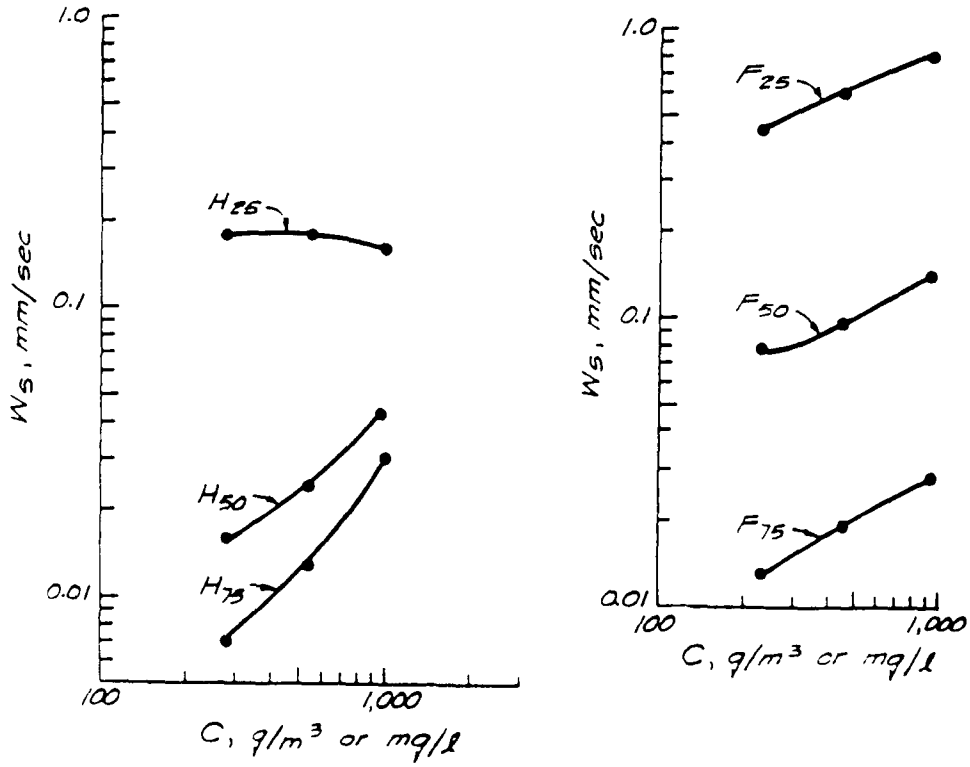

a. Station H

b. Station F

Figure 9. Effects of concentration on the settling of stations H and F sediments

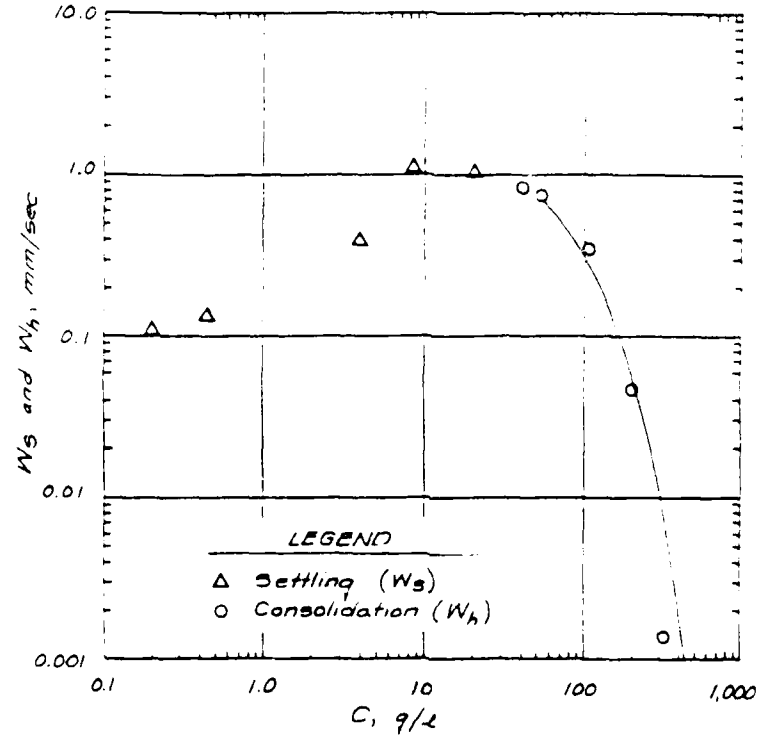

Figure 10. Effects of concentration on the settling and consolidation of station M sediments

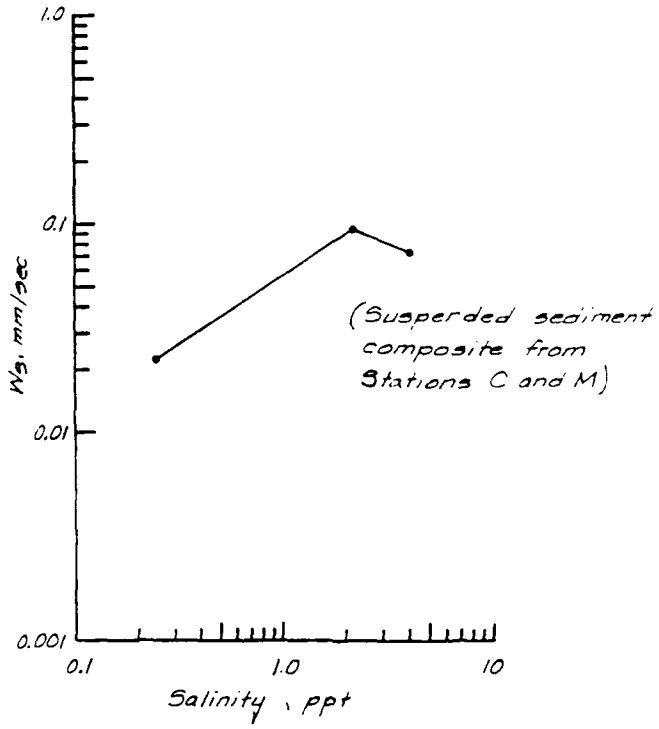

Note: River salinity assumed at 0.25ppt

Figure 11. Effects of salinity on the settling of stations C and M sediments

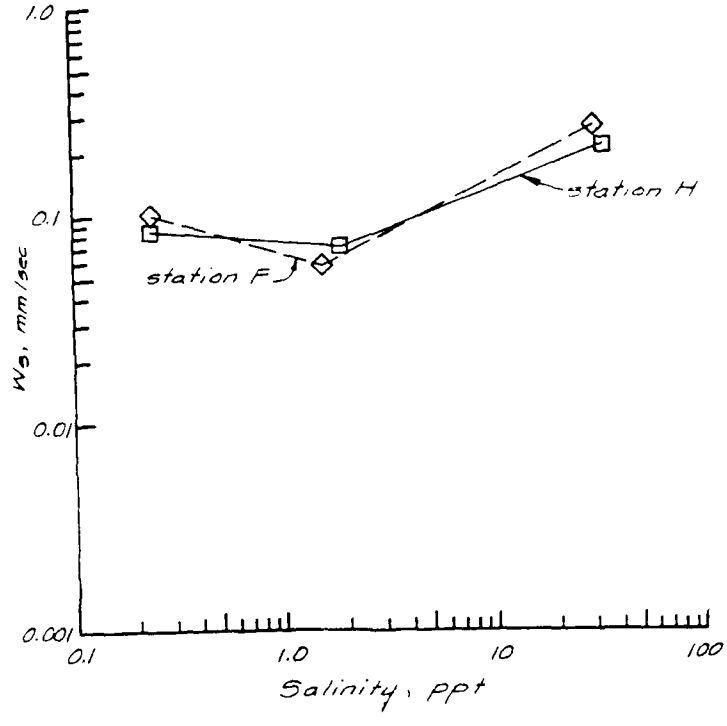

Note: River salinity assumed at 0.25ppt

Figure 12. Effects of salinity on the settling of stations F and H sediments

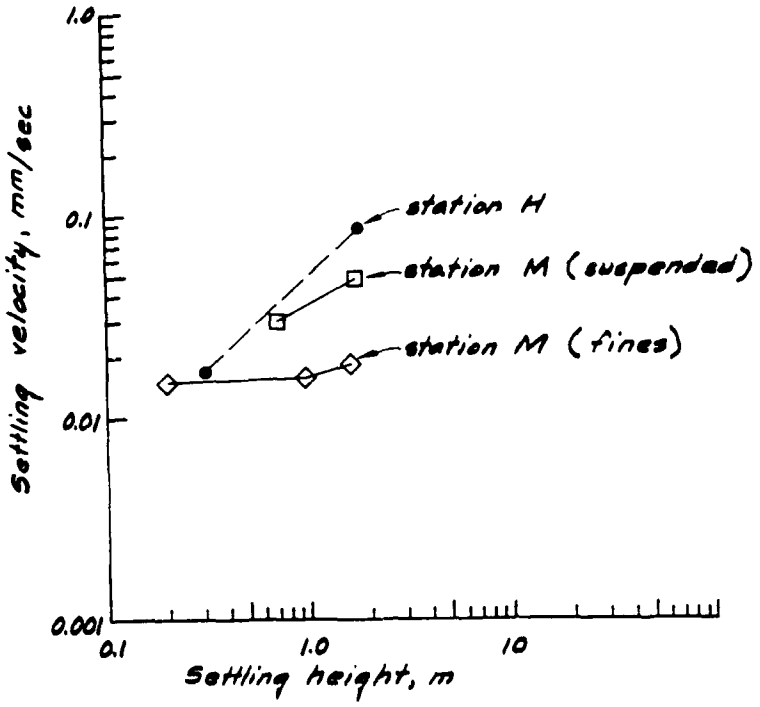

Figure 13. Effects of settling height on settling velocity

with settling height. It is generally reported that this effect ceases over about a 2.0-m height. This was not tested. Laboratory vertical clearance limited settling tests to 1.8-m settling heights. As mentioned, field tests used 0.85-m tubes.

Effects of turbulence

35. Turbulence can have different effects on sediment aggregates and their settling velocities. Turbulent shears can drive particles closer together, overcoming repulsive forces, and thus form relatively dense, strong, faster settling aggregates. Turbulence can also destroy aggregates that are too weak to withstand the imposed shear. Tests were performed to determine which of these effects dominate under natural conditions.

36. Laboratory settling tube tests were performed with an oscillating screen used to generate turbulence. A screen of 2-mm plastic mesh was attached by a long rod in the 100-mm-diameter tube and attached to a variable-speed oscillator with a 19-mm stroke mounted above the settling tube. The screen was centered between the free surface and the sampling point. A 1-m settling height was used for these tests. The sampling port was located 25 cm above the physical bottom boundary of the tube. Three oscillation speeds were

used and measured using a touchless tachometer.

37. Flow visualization tests made with the screen oscillating indicated that turbulence was most intense at the screen and decayed away from it. At the highest oscillating speed, turbulence was noticeable throughout the settling depth but decayed to very low levels near the physical bed of the tube. Resuspension of material that settled to the bottom was, therefore, unlikely.

38. Dye experiments were performed in the settling tube and the change of dye variance (σ^2) with time used to estimate diffusivities $K_z = 1/2(\partial\sigma^2/\partial T)$. For the sizes of material tested, the analogy between diffusivities of conservative dye and sediment was valid. Depth-averaged diffusivities estimated are shown in the following tabulation:

Screen Oscillation Rate, rpm	Diffusivity mm^2/sec
90	45
250	160
440	285

Except for the oscillating screen, settling tests were otherwise run normally.

39. As mentioned earlier, settling tube tests imply settling velocities from the sedimentation characteristics, specifically the time-history of concentration. Results of the turbulence tests, as shown in Table 4, indicated that sedimentation characteristics of the suspensions were generally changed. Effective values of W_s decreased with increased oscillation speeds. This does not mean that the settling velocity of the particles themselves changed, however.

40. To clarify the effect of turbulence on the particle aggregates, numerical settling experiments were performed. Using this method, the effect of turbulence on sedimentation was separated from effects on individual aggregates. The numerical methods were described earlier. Numerical settling experiments provided time-histories of suspension concentration for a fixed W_s. The same analyses were performed on the numerical results as were done on the experimental values to estimate mean effective settling velocities. Results were used to plot mean effective settling velocities normalized to the 90-rpm value versus a particle P_e calculated using the 90-rpm W_s and K_z for the test. If the actual W_s were unchanged with increased turbulence,

then the effective W_s measured in the laboratory should be reduced in the same manner as the numerical results, where W_s was held constant.

41. The numerical results are plotted in Figure 14 by normalizing the effective W_s to $P_e = 1$. Since the values of P_e for Test OE were higher than for other tests, numerical results are also plotted unnormalized for comparison to this test. Although there is scatter, the slope of the numerical results is close to Tests OB, OA, and OE. Tests OF and OD had smaller slopes, and this may indicate that mild turbulence had a positive effect on W_s. Overall, however, the range of turbulence used in these tests had no dramatic effect on the particle or aggregate settling velocities. The experimental P_e range overlaps the field measured P_e, but lower values in the field-measured P_e indicate more turbulence might be applied to future laboratory studies.

Initial bed density

42. Concentration and densities of initial bed deposits from resuspended station M sediments were similar for the range covered by the high-concentration settling tests. As noted previously, at concentrations above the settling range ($\geq$130 g/ℓ or 0.13 g/cm^3 dry weight for station M), hindered settling consolidation occurs and the sediment settles or consolidates in

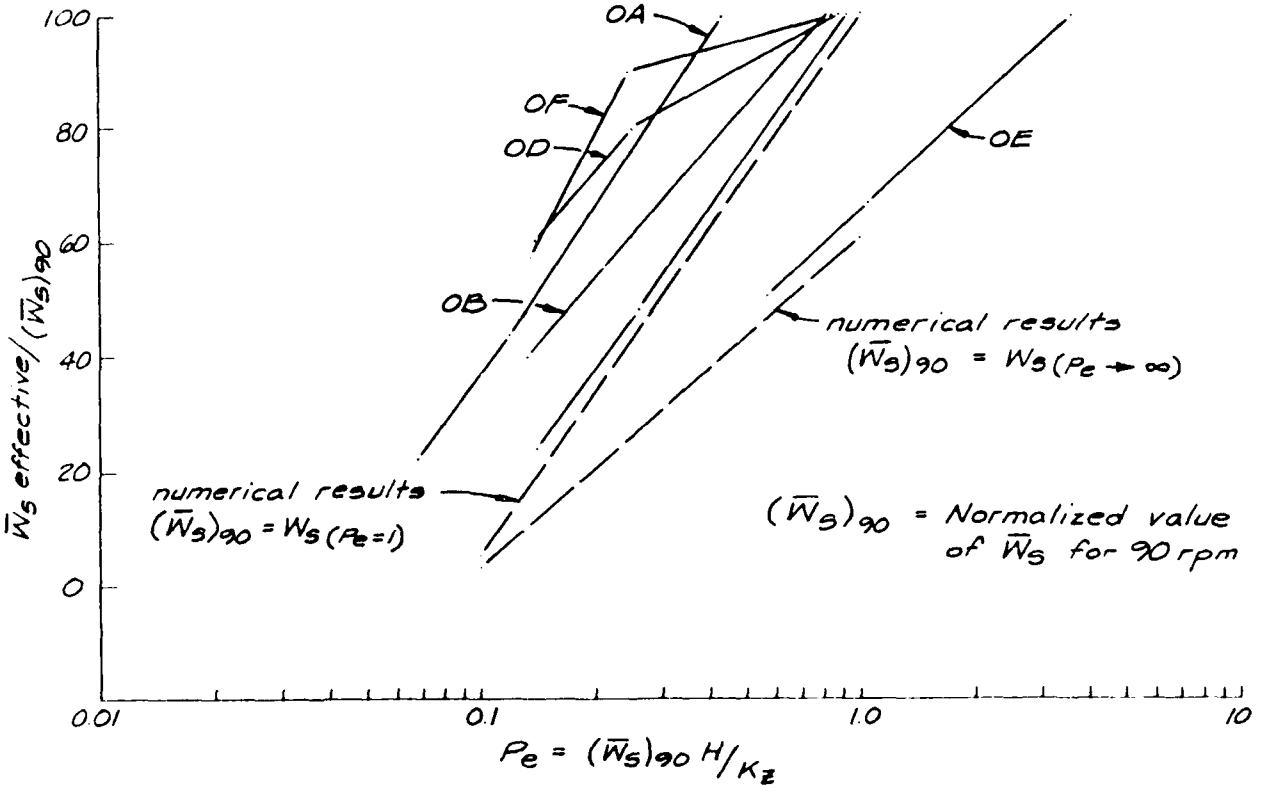

Figure 14. Effects of turbulent P_e on effective settling

mass. The experiments described here are still in the settling range of concentration so that as settling proceeds, a distinct dense layer forms below the suspension at the bottom of the settling tube. Composite sediments from station M were formed with initial bed densities of about 1.45 g/cm^3 bulk wet density (BWD) or 0.72 g/cm^3 dry weight compared with 1.8 g/cm^3 BWD or 1.27 g/cm^3 dry weight measured in field samples. Field measurements are presented in Part IV. The fine fraction of station M sediments had much lower initial bed densities than would be expected. This material is more cohesive and characteristically would be expected to have low initial densities. Still they averaged about 1.24 g/cm^3 BWD or 0.39 g/cm^3 dry weight including one low value.

Numerical stratification tests

43. Stratification was evaluated as $\delta C/\bar{C}$ where δC is the surface-to-bottom difference in concentration and $\bar{C}$ is the depth-averaged concentration. Model results with free-settling bottom boundary condition and depth-averaged K_z compared favorably to published results that used other numerical methods. Model results showed that, as indicated by Equation 7, stratification is related to P_e for a given bottom boundary condition. For a no-settling bottom boundary condition and depth-averaged K_z, $\delta C/\bar{C}$ is equal to P_e. For the same no-settling boundary condition and parabolically distributed K_z, $\delta C/\bar{C} = 1.5P_e$ over the range $0.01 \leq P_e \leq 1$ (where the particle P_e is calculated based on a depth-averaged K_z). Since the parabolic distribution is more realistic than a uniform distribution, these results were used. For free-settling bottom boundary condition, $\delta C/\bar{C} = 0.75P_e$ for $0.01 < P_e < 1$. Above $P_e = 1$, these relationships diverge slightly. Figure 15 shows the numerically generated suspension classification diagram. Figure 16 shows example equilibrium profiles with no-settling bottom boundary conditions and Figure 17 shows free-settling results at $P_e = 0.5$.

44. These results suggest that the stratification of a suspension depends on P_e and bottom boundary condition. Therefore, if stratification and particle P_e can be accurately determined, erosion or deposition that occurs over spatial scales of greater than perhaps 500 m could be estimated. Comparison to field data will be made later in Part IV.

Mass flux to the bed

45. Mass flux to the bed, or deposition D, can be described as

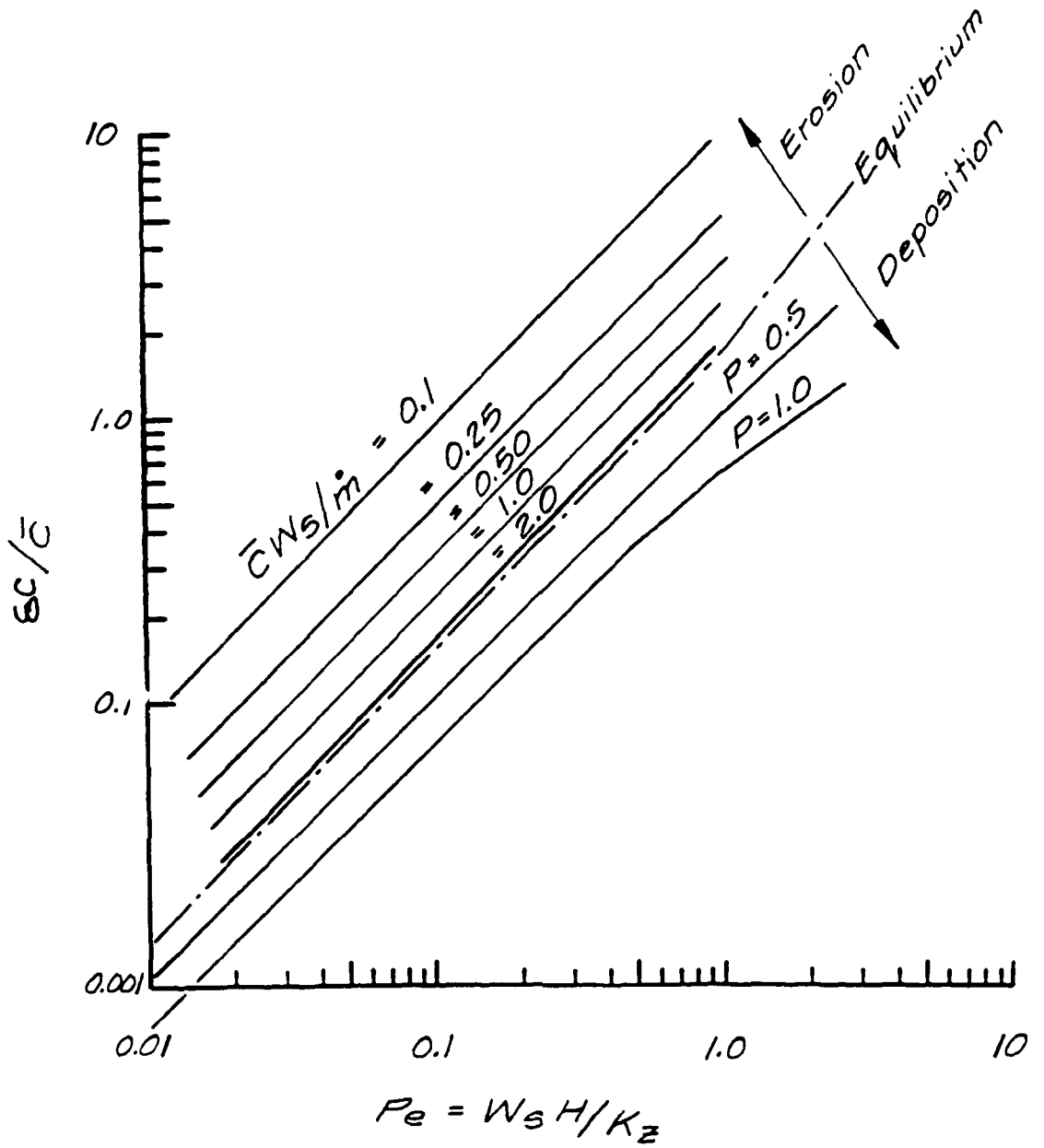

Legend

$\bar{C}$ = depth averaged concentration

δC = surface - bottom

W_s = settling velocity

H = depth

$\dot{m}$ = erosion rate

P = probability of particle sticking to bed

P_e = Peclet number

Figure 15. Suspension classification diagram

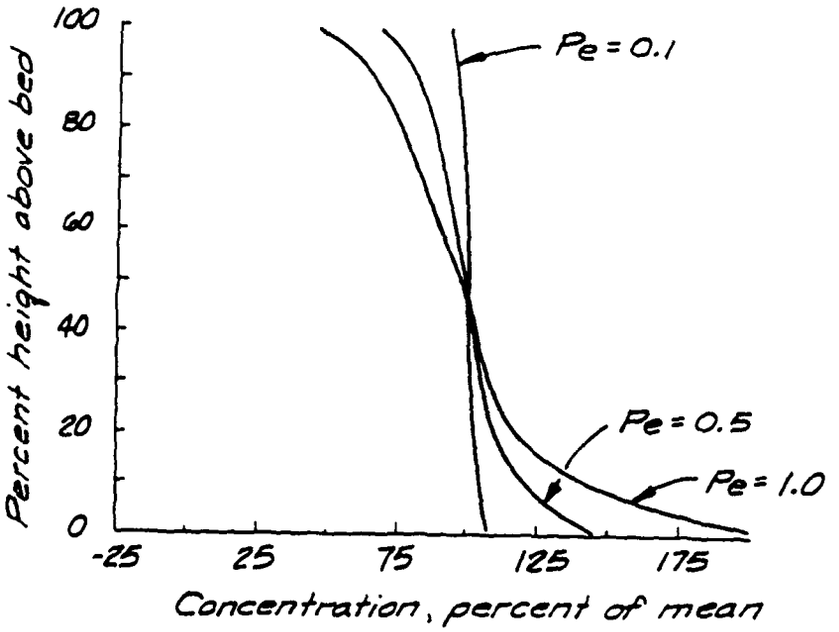

Figure 16. Numerical vertical suspended sediment profiles with no-flux bottom boundary

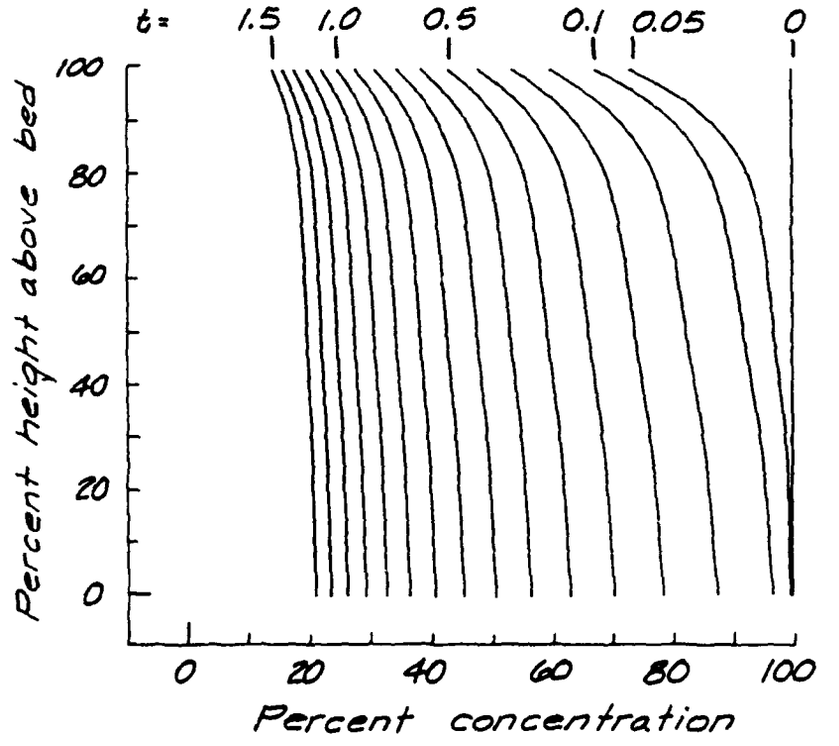

Figure 17. Numerical settling test with free-settling bottom boundary and $P_e = 0.5$

$$D = PW_s C \tag{13}$$

where P is the probability of a particle reaching the bed remaining there, and C refers to the concentration just above the bed. P has been found to vary with bed shear stress τ_b, and be 0 at some critical value τ_{cd} and 1 at $\tau_b = 0$.

46. Analytic solutions to sediment transport equations, such as Equation 1, for deposition and under certain simplifying assumptions can be made. Two such solutions were tested using numerical model results, and the effect of P_e on deposition evaluated. The two analytic solutions, assuming that $P = 1$, are

$$\frac{C}{C_o} = \exp\left(\frac{-W_s T}{H}\right) \tag{14}$$

$$\frac{C}{C_o} = 1 - \left(\frac{W_s T}{H}\right) \tag{15}$$

where C_o is the initial concentration at $T = 0$.

47. Plots of these functions and of numerical results at $P_e = 100$ and $P_e = 1$ are shown in Figure 18. The numerical results for $P_e = 1$ were obtained using a uniform initial concentration. For $P_e = 100$, the model run was made with an initial concentration varying linearly from 0 at the surface to 200 percent of the average at the bottom, a more realistic condition for this very high P_e.

48. Results showed that at values of P_e of about 1 or less, the exponential function described deposition quite well. As will be shown later, field P_e were generally in this range.

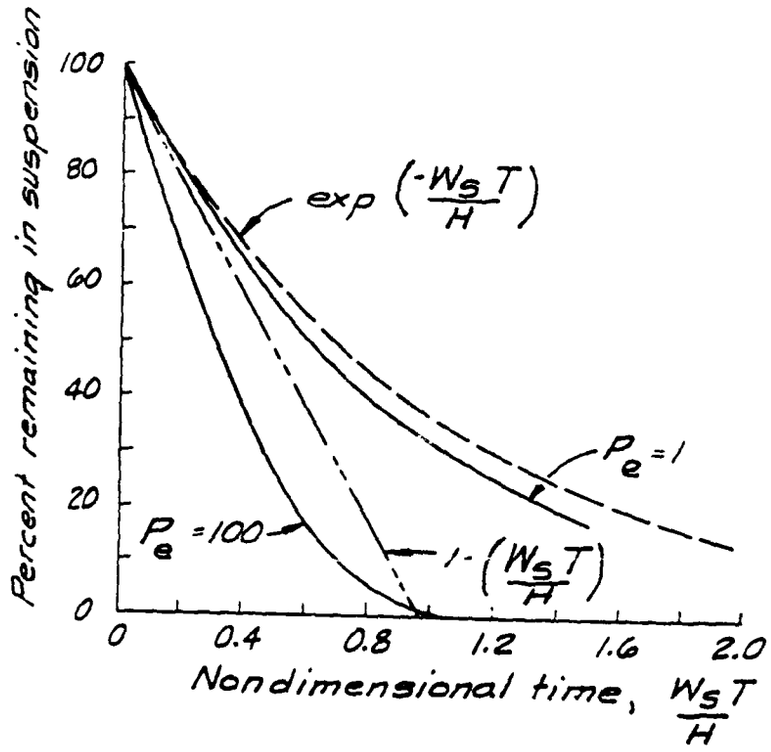

Figure 18. Analytic functions and numerical results for P_e = 1 and 100 for percent remaining in suspension with time

PART III: CONSOLIDATION TESTS

49. After sediments first settle to the bed, they undergo further settling. This is termed hindered settling consolidation because concentrations are in the hindered settling range and thus settling rates decrease with increased concentration. This is significantly different from the settling processes described in Part II.

50. Self-weight consolidation and gravity compaction were not addressed in this report. They are important to consolidation after hindered settling consolidation has taken place, especially in thick sediment layers. Important changes in density and void ratios usually occur with the first few hundred metres of burial. However, the deposits that have accumulated in Atchafalaya Bay over recent decades are on the order of 2-3 m thick or less, and in situ densities have been measured.

51. In estuaries, and Atchafalaya Bay in particular, hydrodynamic conditions are quasi-periodic or transient. Slack-water periods with low shear stresses on the bed can allow sediments to deposit. This is followed by periods of higher shear stress and possibly erosion. The critical shear stress for erosion of fine-grained sediments has been found to be strongly dependent on density. To predict this behavior, it therefore becomes important to estimate initial densities of the settled material and the increase in density of this material over periods of hours to days. This was the purpose of the consolidation tests.

Basic Concepts and Definitions

52. Hindered settling occurs when the concentration of a suspension becomes so large that interparticle distances impede settling. Hindered settling consolidation occurs at still higher concentrations when particles become immobilized in the suspension and the suspension settles as a mass. Hindered settling has been empirically described by

$$W_h = W_s(1 - KC)^5 \tag{16}$$

where

W_h = hindered settling velocity

K = an empirical coefficient, g/cm^3/dry weight

An exponent of 4.67 is sometimes used.

53. To verify this relationship and to obtain further insights on hindered settling consolidation under field conditions, a numerical model was constructed. The transport equation without diffusion was used.

$$\frac{\partial C}{\partial T} - \frac{\partial}{\partial Z}(W_h C) = 0 \tag{17}$$

Using a nondimensional depth term $z = Z/H$, the transport equation becomes

$$\frac{\partial C}{\partial T} - \frac{1}{H}\frac{\partial}{\partial z}(W_h C) = 0 \tag{18}$$

where H is the thickness or depth of the consolidating mud. The stationary lower boundary is $z = 0.0$, and $z = 1.0$ is the moving upper boundary. At the lower boundary ($z = 0.0$) the no-flux condition $W_h C = 0$ was imposed. At the upper boundary, no boundary condition was imposed and the upper boundary was allowed to settle. The thickness of the mud was calculated by

$$H = \frac{m}{\int_{z=0.0}^{1.0} C \, dz} \tag{19}$$

where m is the mass per unit surface area of the consolidating layer, a constant for a given problem.

54. A solution method similar to that presented in Part II was used for the numerical experiments. At each time-step, the variable coefficients W_h and H were calculated by Equations 18 and 19. Normally an arbitrary 301 time-steps were made. Every tenth was printed and a data file created. Plots were made of vertical profiles of concentration with nondimensional depth. Plots of thickness H were made versus time.

Description of Tests

55. Hindered settling consolidation was observed in the laboratory by

mixing bottom sediments with native water to make a dense suspension or mud, then observing its consolidation in a clear tube. Tubes 200 cm high by 10 cm in diameter of clear acrylic and 45 cm high by 22 cm in diameter of clear plastic, both equipped with 0.32-cm-bore Teflon spigots, were used. At high concentrations, suspensions settle as a mass and a very distinct clear layer forms above the consolidating sediment. Observations were made of the location of this interface with time. The rate of change in the interface height at the beginning of the tests was equal to W_h . Samples were drawn with depth through spigots and analyzed for BWD by pycnometer method during some tests.

56. BWD is the density of sediment and water mixture. BWD analyses are performed using wide-mouth, 25-cm^3, constant-volume pycnometers calibrated for tare weight and volume. To make a measurement, a pycnometer was partially filled with sediment and weighed. It was then topped off with distilled water. Care was taken to remove any bubbles from the pycnometer before it was reweighed. The BWD of the sediment was then calculated:

$$BWD = \frac{(\rho_w)(\text{sed wt} - \text{tare wt})}{(\rho_w)(\text{vol pyc}) + (\text{sed wt}) - (\text{sed + water wt})} \tag{20}$$

where

ρ_w = density of water at temperature of analysis

sed wt = weight of pycnometer with sediment

tare wt = tare weight of pycnometer

vol pyc = volume of pycnometer

sed + water wt = weight of pycnometer with sediment and water

Test Results and Discussion

57. Table 6 lists the test material sample stations, initial conditions, duration of consolidation experiments, and final average concentration for tests in which samples were drawn. Plots of these consolidation tests are given in Plates 1-6. There was no indication of a delay period before hindered settling consolidation began, as has been reported for some cohesive sediments.

58. Other tests were performed in which only the initial concentration

and interface heights were measured. Station M sediments were used for these tests, and results are shown in Figure 10. By associating W_h with C_o, the effect of C_o on settling was determined for this sediment.

59. Numerical model results indicate that the ranges of the constants W_s and K of 0.00005 to 0.00020 m/sec and 2.4 to 2.9 cm^3/g, respectively, can be used to represent the hindered settling consolidation observed in the laboratory. Values of W_s are larger and K lower near the Atchafalaya Bay river mouth where material is coarser and less cohesive.

60. Vertical concentration profiles and interface locations for a station F sediment test are plotted in Figure 19, along with numerical model results. The agreement in the interface location is excellent. The near-bottom BWD's were somewhat lower in the numerical model, but this was probably due to a coarse fraction in the prototype sediment that may have been capable of settling through finer sediments. The range of concentrations tested was not very far into the hindered settling consolidation range so that it is possible that some particles were not immobilized in the suspension at the onset of the test.

61. The inflection (curvature) in the plot of interface level was reproduced in the numerical model. It was thought that this feature signalled the onset of self-weight consolidation or compaction. The numerical model showed this to be the point when the concentration or density inflection reached the sediment surface. The consolidation process can be seen in Figure 19 as a propagation of densification that began at the bottom and propagated upward. Local gradients in W_h and C caused concentrations to increase. At the beginning of the tests the suspension was uniform and the only gradients existed at the fixed-bottom boundary. Laboratory tests also indicate that densification began at the bottom and propagated upward. The thinner the layer, the more quickly the surface density increased. Near-surface density increase corresponded to the inflection in the interface descent. For a given K and W_s, then, the increase in concentration at a point depends on its distance above the bottom stationary level, not on depth from the interface.

62. Interface heights observed in the laboratory and numerically calculated for a test using sediment from station M are shown in Figure 20. The agreement is good.

63. These results apply only to laboratory experiments. Field

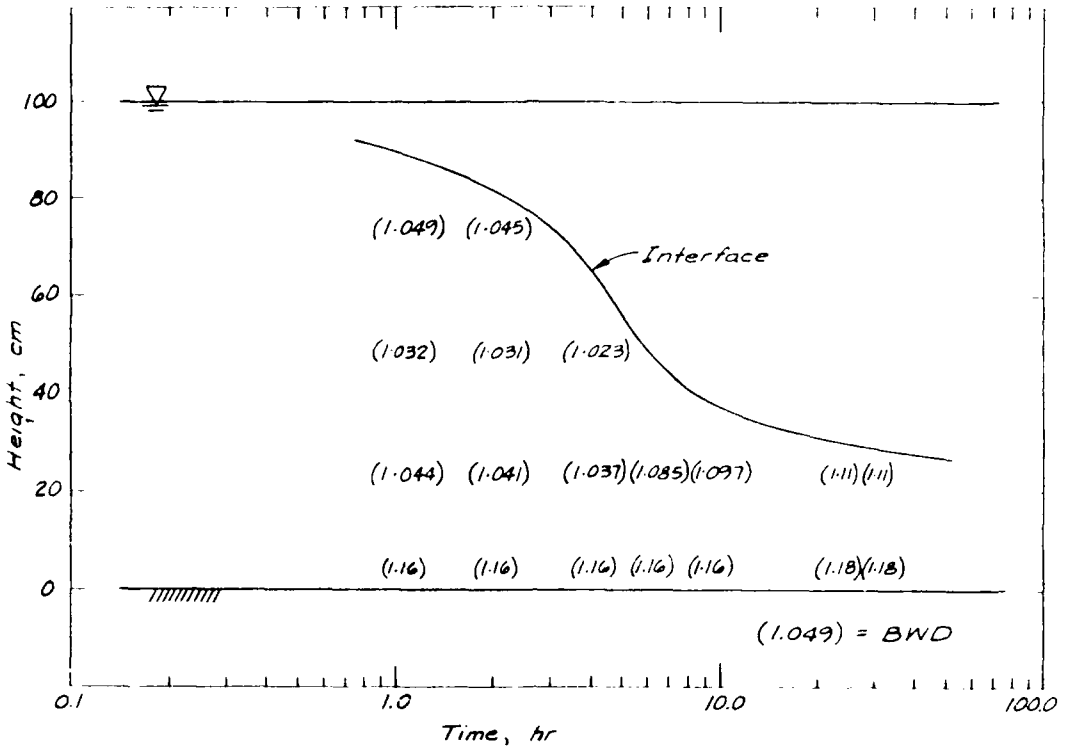

a. Experimental results

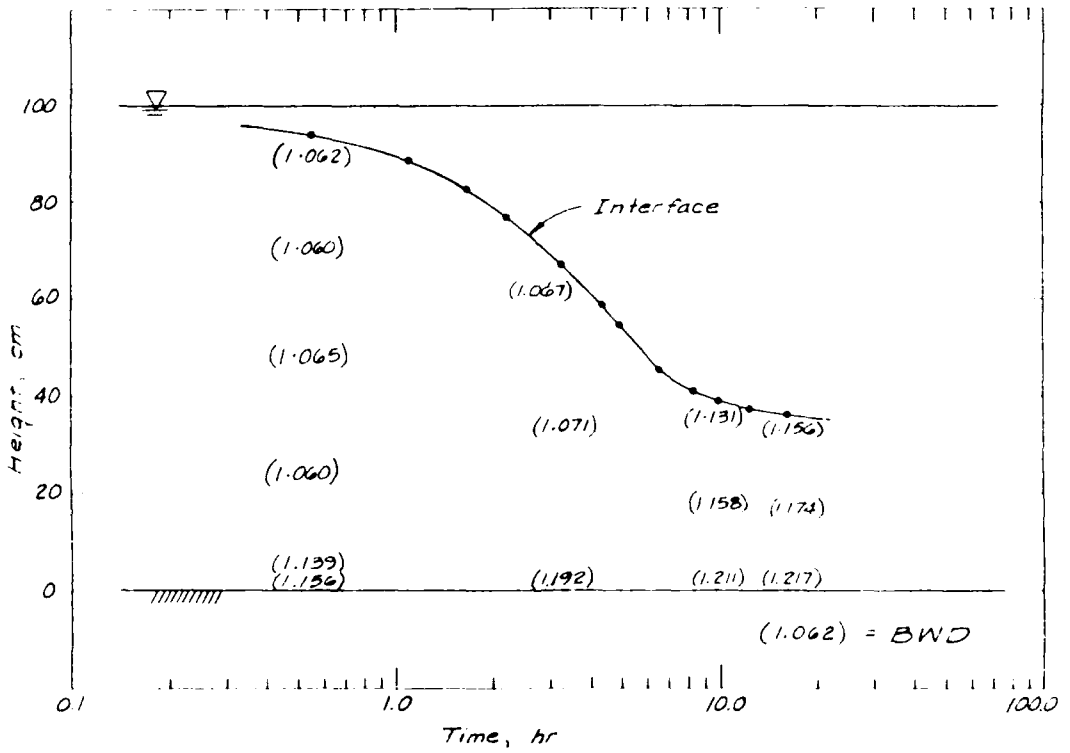

b. Numerical results

Figure 19. Experimental and numerical consolidation results for station F

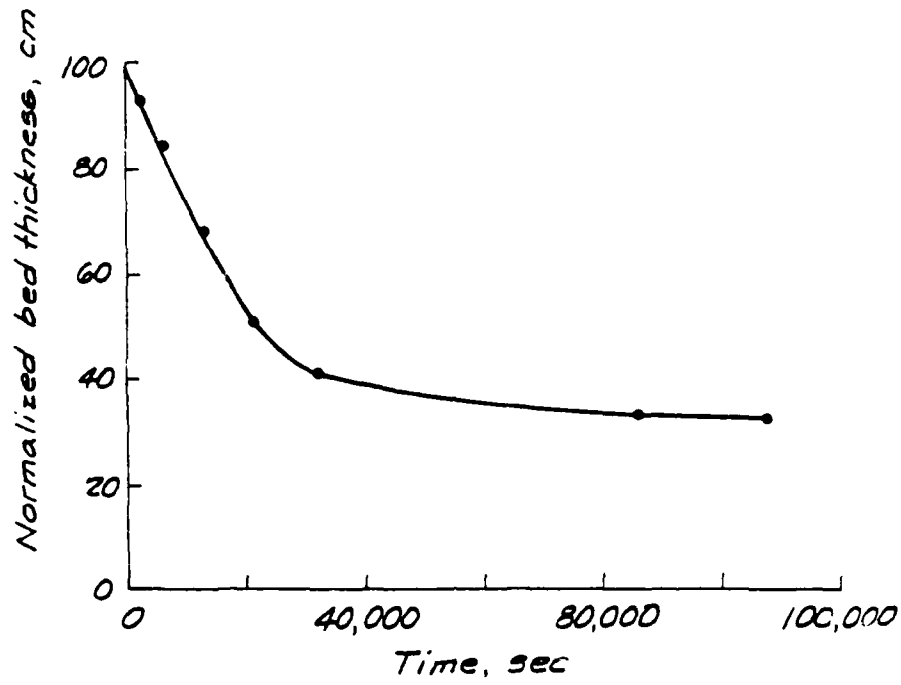

Figure 20. Experimental and numerical consolidation results for station M (Atchafalaya mud)

measurements are reported in Part IV. Experimental results presented in Part II indicate higher initial and final bed densities than those found in the laboratory tests. This is due to the difference in characteristics between deposits formed as a result of settling and those found by the hindered settling consolidation of dense suspensions. However, the hindered settling equation applies to both cases, and numerical simulations were made to represent field conditions.

PART IV: ANALYSIS OF FIELD SEDIMENTATION PROCESSES

64. The overall Atchafalaya Bay project conducted by WES, of which this work is a part, involved a large data gathering effort. Physical conditions including tide, current speed and direction, wind, and wave height were measured during a 2-year period. Complete results are given in Coleman et al. (1988), but some are summarized here in relation to suspended sediment characteristics. Field measurements of the settling velocity of suspended material were made using methods already described in Part II. Samples were also collected for TSM analysis. Often they were collected along with salinity and current measurements in vertical profiles or at select locations in the vertical. Field equipment and procedures are given in Coleman et al. (1988). CEC and BWD were measured on subsamples of sediment cores. All these data were analyzed to define and describe field processes affecting erosion, transport, and deposition of sediments.

Basic Concepts and Definitions

65. Vertical profiles of TSM concentration and velocity can be used to calculate unit sediment discharge, sediment velocity, shear velocity, sediment suspension stratification, depth-averaged sediment concentration, and depth-averaged velocity. Measurements of velocity taken in the vertical were fit to a regression equation. The following universal logarithmic profile was used:

$$\frac{U(Z)}{U^*} = \frac{1}{\kappa} \ln\left(\frac{Z}{Z_o}\right) \tag{21}$$

where

U = current velocity

U^* = bed shear velocity, $(\tau/\rho)^{1/2}$ where ρ is the mass density of the fluid

κ = assumed to be equal to 0.4

Z_o = roughness height

The regression was used to estimate the shear velocity, designated $U^*(fl)$, and to estimate current velocity at a number of points (Gauss points) in the

vertical. From the calculated depth-averaged velocity, Manning's equation was also used to estimate the shear velocity,

$$U^*(fm) = g^{1/2} n \bar{U} H^{-1/6} \tag{22}$$

where

$U^*(fm)$ = shear velocity estimated using Manning's equation

g = acceleration due to gravity

n = Manning's coefficient taken as 0.020

$\bar{U}$ = depth-averaged current velocity

Both methods of estimating shear velocity are subject to uncertainty. The logarithmic profile fit is sensitive to uncertainties in the near-bottom velocity values and value of K_o. More near-bottom measurement points would have reduced uncertainties, but could not be obtained. Manning's equation is sensitive to its assumed coefficient. For many profiles, however, reasonable agreement was found between the two methods. Where the logarithmic fit failed completely, giving a widely different or sometimes even negative shear velocity, a synthetic data point was added to the profile at the top of the laminar sublayer based on the Manning's estimated shear velocity. The depth-averaged values of velocity and concentration were calculated by

$$\bar{U} = \frac{1}{H} \int_{Z=0}^{H} U \, dZ \quad \text{and} \quad \bar{C} = \frac{1}{H} \int_{Z=0}^{H} C \, dZ \tag{23}$$

using Gaussian quadrature. The discharge of sediment per unit width of flow is

$$Q(sed) = H\bar{C} \, U(sed) = \int_{Z=0}^{H} CU \, dZ \tag{24}$$

where $U(sed)$ is the concentration-weighted sediment velocity

$$U(sed) = \frac{\int_{Z=0}^{H} CU \, dZ}{\int_{Z=0}^{H} C \, dZ} \tag{25}$$

The nondimensional stratification ($\delta C/\bar{C}$) was defined in Part II as the surface-to-bottom difference normalized by the depth-averaged concentration. To estimate this parameter, an exponential curve was used on vertical concentration data and the results used to estimate depth averages and surface-to-bottom differences. The surface-to-bottom difference was corrected by the inverse of the fraction of the water column that was sampled. This method was checked using numerical results and found to give consistent results. The depth-averaged diffusivity for homogeneous flow was estimated as

$$K_z = 0.067HU^* \tag{26}$$

66. CEC is a measure of the cations held on the surface or within the crystaline matrix of minerals. It is affected by the type and amount of clay minerals present as well as some organic material. Black's method of analysis by ammonium saturation was used because it minimizes the effects of organic material on CEC. Analyses were done by the Concrete and Materials Analysis Group of the Structures Laboratory, WES. Typical range of values for CEC found in the literature are

Mineral Fraction	CEC, meq/100 g
Kaolinite	1-15
Illite	10-40
Montmorillonite	50-150
Chlorite	10-40
Vermiculite	100-150
Organic fraction of solids	150-500

Description of Field Methods and Conditions

67. Field sampling for sediment characteristics was generally carried out in conjunction with deployment and servicing of tide, current, and meteorologic recording instruments. Sampling was, therefore, neither synoptic nor time-series in nature. Because of the size of the study area, usually more than 1 day was required to complete sampling. Even so, not every station was occupied on every survey, but repeated samplings were made at many. Sampling methods are described in Coleman et al. (1988). Suspended samples

were generally taken with a pump system or occasionally with a Kemmer-type water bottle. On one occasion, surface grabs were taken to correlate to satellite imagery. Fifteen sampling surveys were made and rated somewhat subjectively according to the transport energies imposed by diurnal tide range, wind, freshwater inflow, and TSM (Table 7). The rating covers only the range of observation for this study. For instance, high inflow in the table is considered to be that exceeding 6,400 m^3/sec (225,000 cfs) while, based on a longer historical record, this is not very high. River inflow, tidal currents, and waves contribute to differing degrees to the TSM levels of the bay complex. They represent sources of sediment by their ability to transport or erode. For comparison, Figure 21 shows a relationship between freshwater flow, Q_f and TSM at Morgan City while Figure 22 shows a plot of freshwater flow versus TSM for river mouth stations E and S. The latter stations were subject to more tidal effect than Morgan City and therefore can be expected to have greater variability in the discharge-concentration relationship.

Results and Discussion

Tidal influence on TSM

68. While the range of conditions covered by these observations was limited to inflows less than flood level, the indications are that sediment concentrations in the bay often exceed those of the inflow. This is common for estuaries in general. Plates 7-20 give areal distributions of TSM for the field survey sampling periods given in Table 7. It appears that tide was the most dominant single factor correlating to TSM, although inflow discharge certainly contributed. Wind had surprisingly little effect on the level of TSM in the bay. The most severe conditions sampled had sustained 15-knot winds accompanied by 2-ft waves. Highest concentrations were detected at times of spring tide and also on flood phase of the tide. Figures 23 and 24 show plots of TSM versus diurnal tide range at stations R and H, respectively. Flood and ebb phase samplings and river discharge are also indicated. Although samplings were not taken at exactly the same tidal phase, the data indicate that flood phase concentrations are highest and that an upward trend of concentration with increasing diurnal range exists. The correlation of TSM to river inflow is lower at these stations than at the river inflow. These stations are very much tidal at low discharges and data are scattered accordingly.

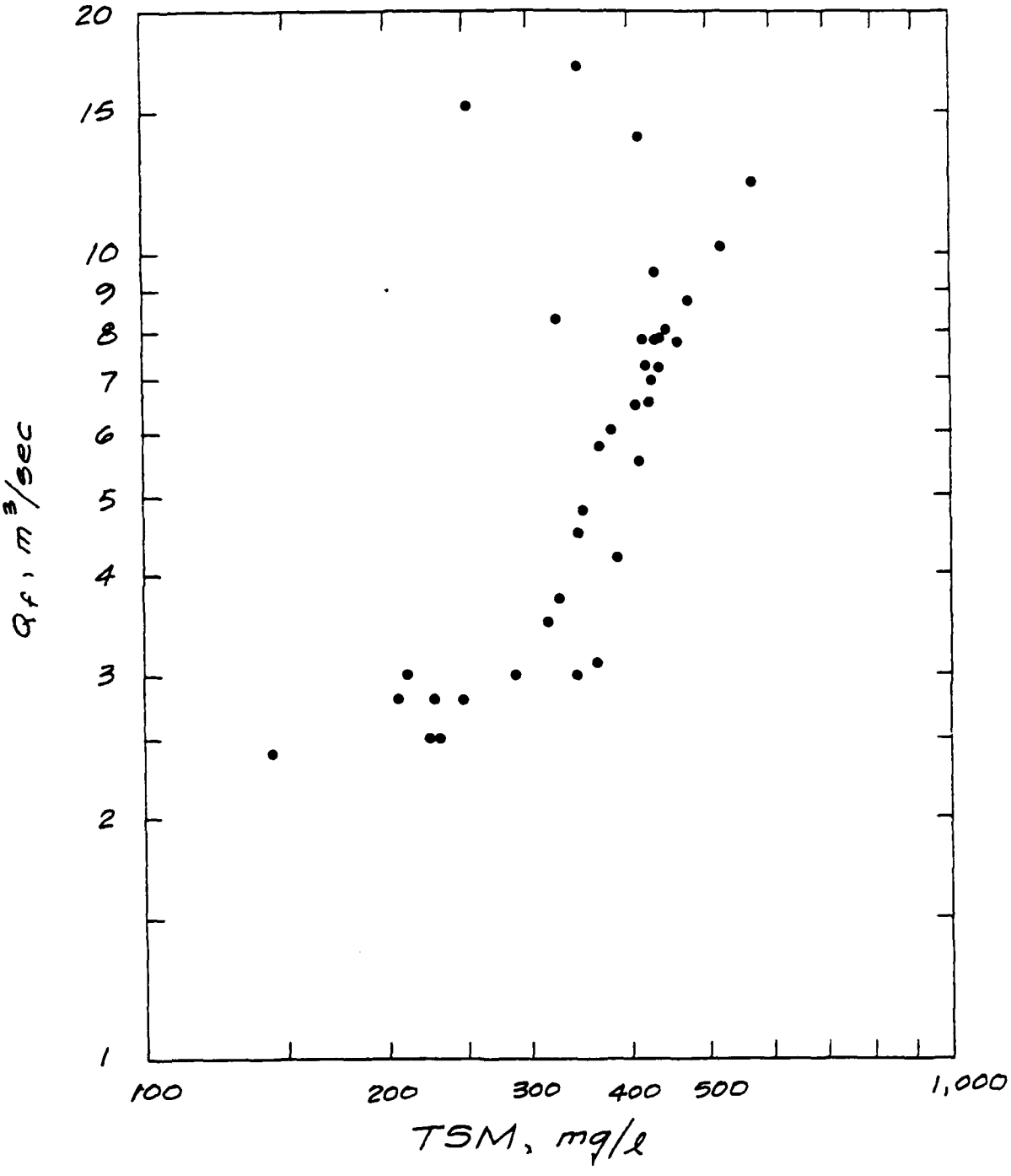

Figure 21. Freshwater flow versus TSM at Morgan City

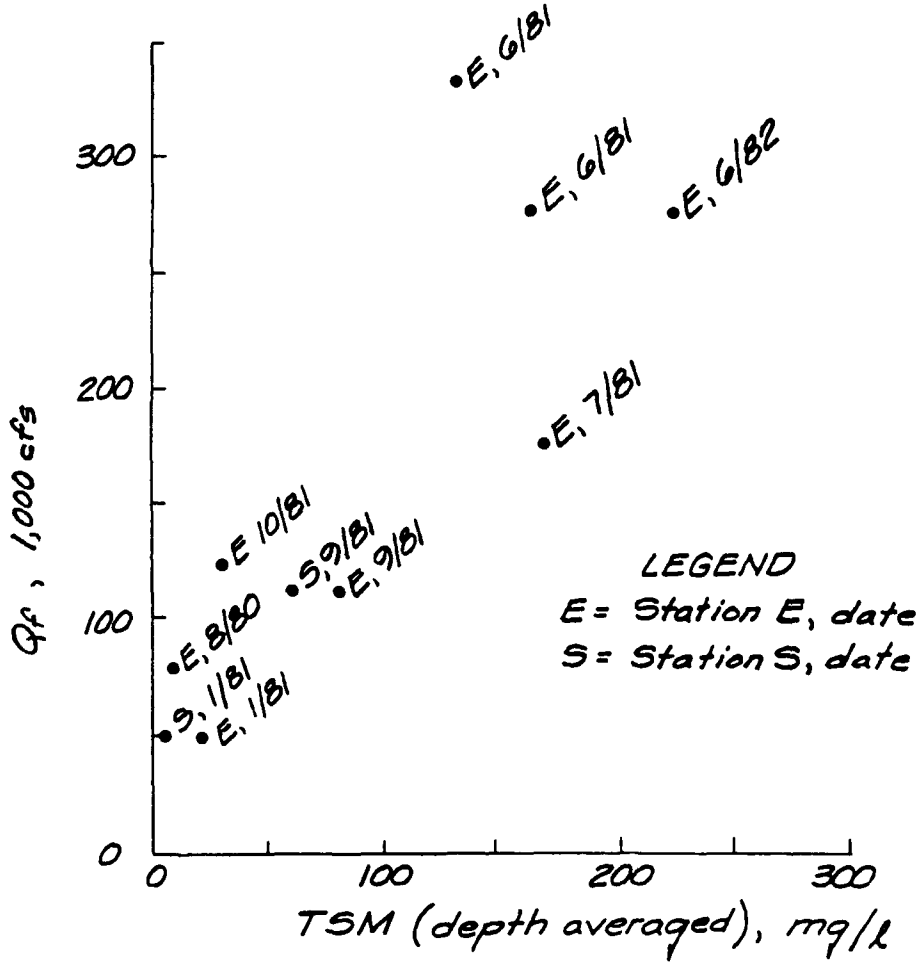

Figure 22. Freshwater flow versus TSM at river mouth stations

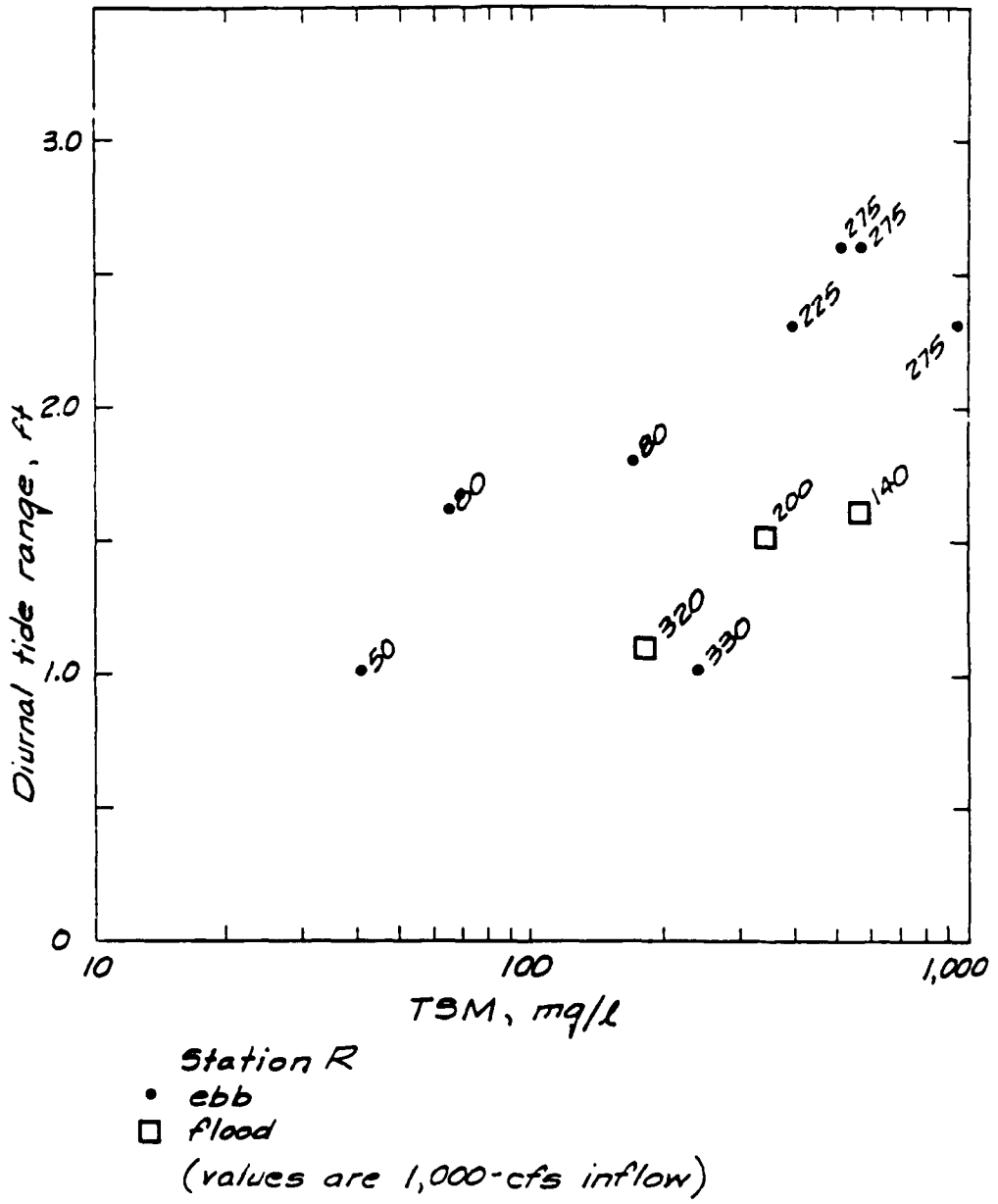

Figure 23. TSM versus tidal range for station R

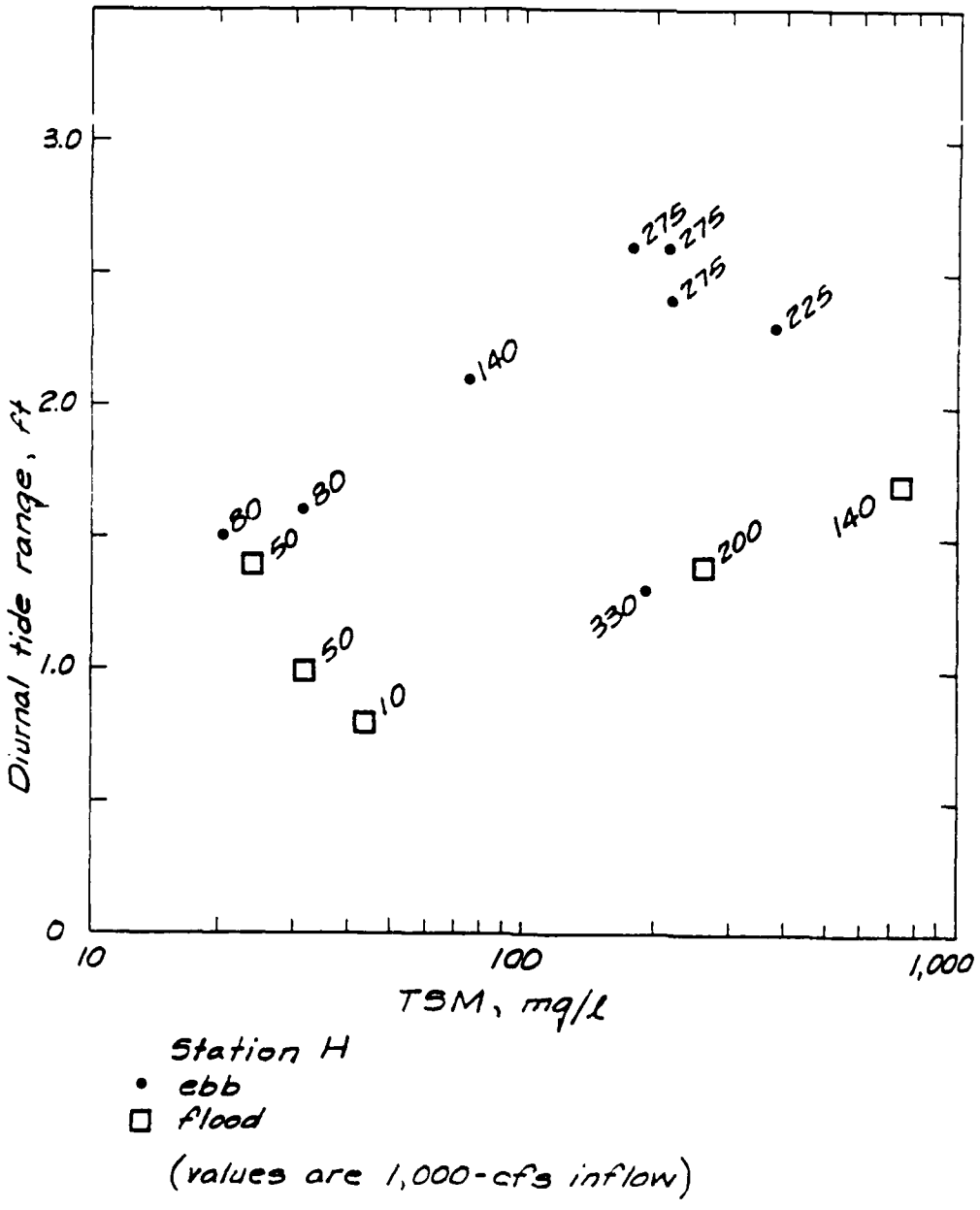

Figure 24. TSM versus tidal range for station H

Distribution of settling velocity

69. Table 8 summarizes the 30 field settling tests made in 1980-1982. Figure 25 shows the areal distribution of these field settling velocity samples. Figure 26 shows a plot of settling velocity versus TSM for all field settling data. The correlation of settling velocity to TSM for all the data is very poor; but at individual stations the correlation might be better, although not enough data are available to test this hypothesis. In general, settling velocity decreases with distance away from the river mouths. Figure 27 shows a probability plot of all field settling data. The Weibull probability distribution displayed the data in a more straight-line fashion than did normal or log-normal distributions. Figure 28 shows three station settling velocity distributions in a transect out from Wax Lake Outlet taken 16 April 1982 that demonstrate this trend. Settling velocity, especially in the coarse end of the distribution, and concentration both fall seaward of the river mouth. Settling velocities and concentration may not continue to fall into the offshore area, however. Although only one settling velocity test was done offshore (station L), sediment concentrations and stratification were observed to be high. The possibility of a local source offshore will be further discussed in the next section.

Stratification and bed shear

70. Part II presented an analysis of the stratification of suspended material in terms of the particle Peclet number and the bottom boundary condition (erosion, no flux, or deposition). Sufficient data were collected at some stations to estimate both stratification and particle Peclet number; therefore, some inferences as to the sedimentation conditions at the bed can be drawn.

71. Figure 29 shows a diagram for the classification of sediment suspensions for these stations. Data are presented in Table 9. Samplings were taken 7-9 July 1982 at midebb phase of the tide with 2.0- to 2.2-ft diurnal range, except stations U and V, which were taken near high water. Freshwater inflow was 225,000 cfs. This analysis indicated that erosion conditions were occurring at all stations. Data for station F taken 11 May 1982 are plotted for comparison and indicate a flux equilibrium bottom condition. At station F a shear stress of 0.17 N/m^2 was apparently above τ_{cd}, the critical shear stress for deposition, and a shear stress of 0.08 N/m^2 was initiating erosion

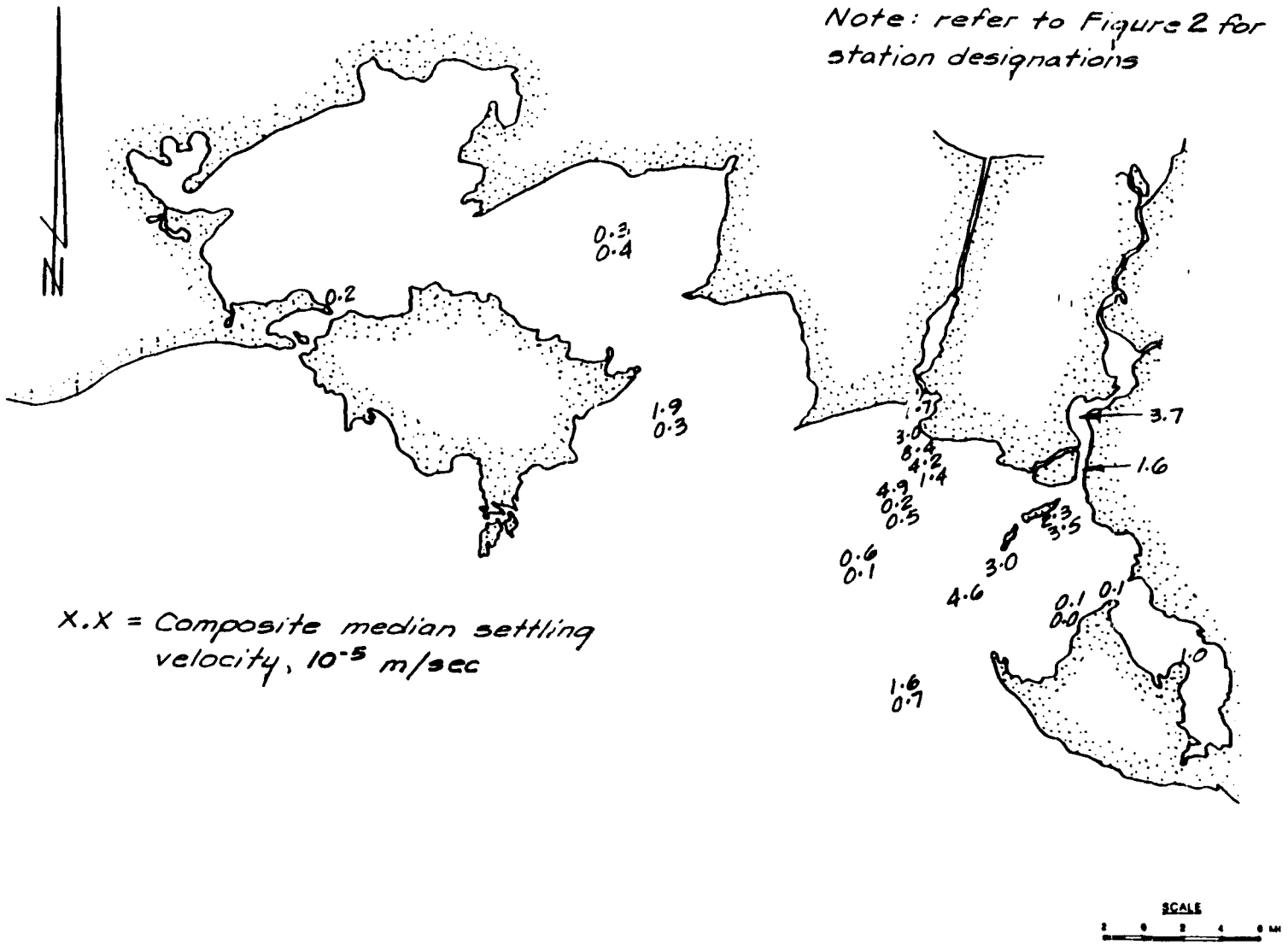

Figure 25. Areal distribution of settling velocity in Atchafalaya Bay system

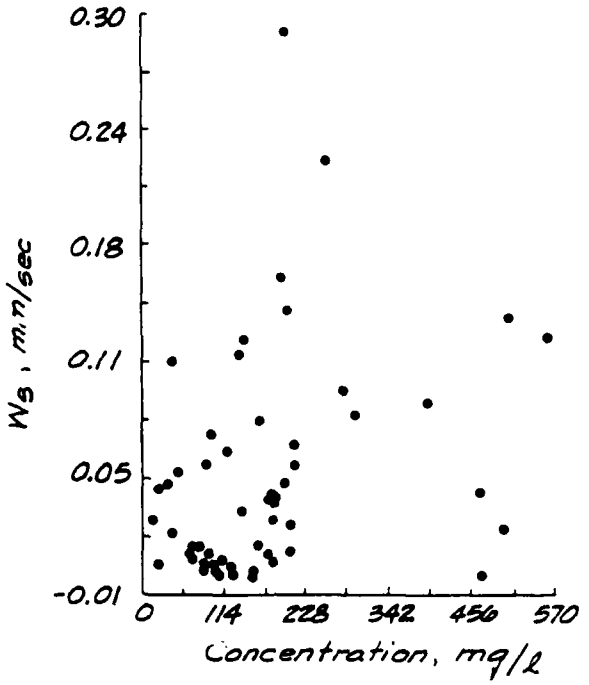

Figure 26. TSM versus settling velocity, all field tests

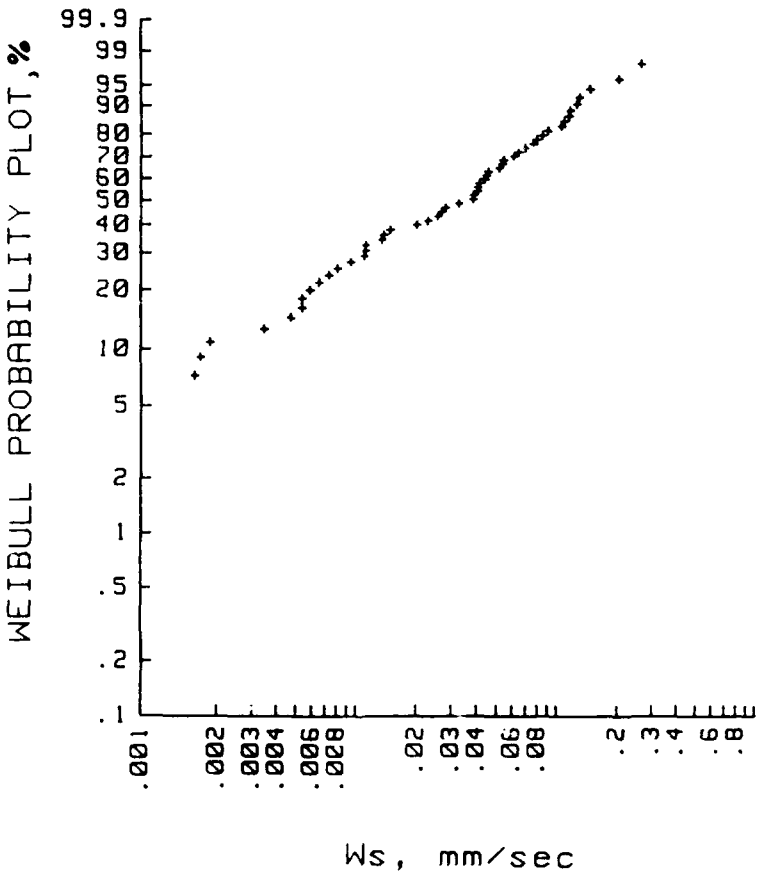

Figure 27. Probability distribution of field settling data

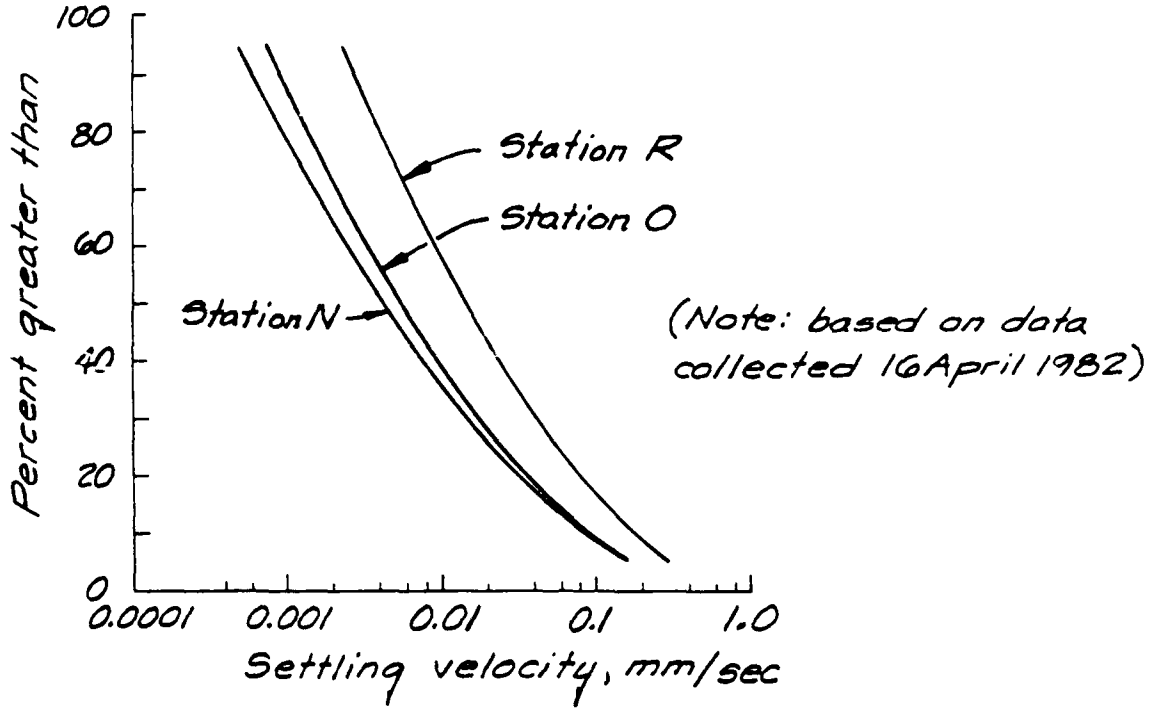

Figure 28. Settling velocity distributions for three stations across the bay

at station U. Thus sediments, at least more mobile fractions, are frequently in transport in the bay system. There are only slight differences between U and U(sed) in these data so that the assumption that sediment is moving at the depth-averaged velocity is a reasonable one. It is apparent that at least three vertical points are required to fit vertical profiles, even in shallow water.

72. Table 10 gives additional data on shear velocity and sediment stratification. Offshore stations (L, K, and tide gage 8) show a generally consistent higher sediment stratification than inshore stations. At the times these data were taken, vertical salinity stratification was small, less than 2 ppt top to bottom differences at station L and tide gage 8 in 25 ft of water and even less at station K. As noted in the last section, only one settling velocity test was run on offshore stations that indicated a high settling velocity with mean W_s of 0.357 mm/sec . If that data point is typical, offshore stations would plot on the erosional side of the suspension classification diagram, indicating an offshore sediment source. Offshore sediment beds are commonly (or easily) eroded, providing a source of sediments that may be then transported into the bays for deposition or transported downcoast and away from the site.

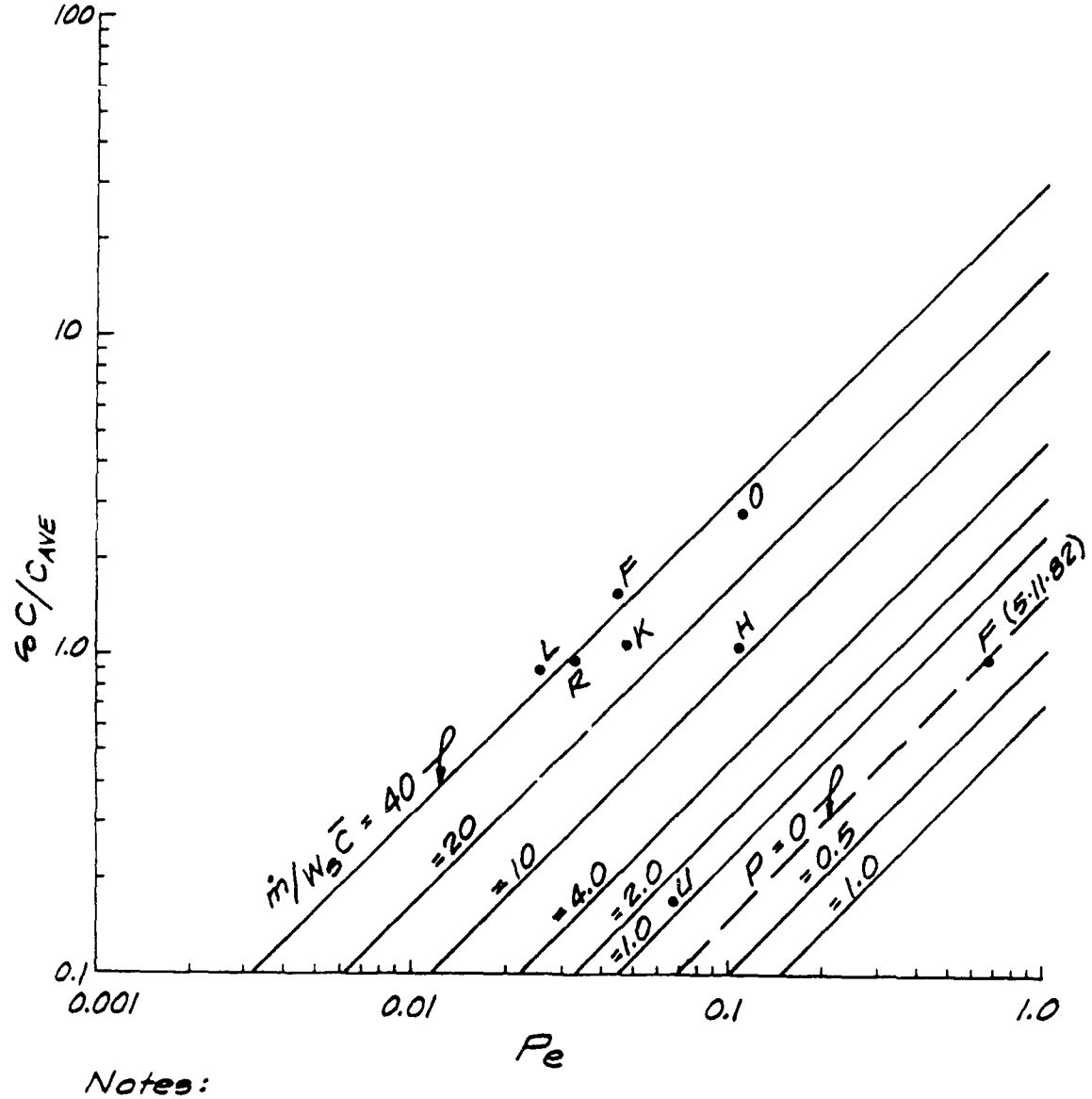

Notes:
Vertical station data collected 7-9 July 1982.
All midebb tide samples include 2.0'-2.2' range except stations U and V (taken near high water).
Freshwater flow = 225,000 cfs

Figure 29. Suspension classification diagram for a high-transport survey

Bed sediments

73. BWD analyses were performed on vertically sectioned core samples. Plates 21-28 give the vertical profiles of BWD at the stations indicated in Table 2. CEC data are given in Table 11. Figure 30 is a plot of CEC versus BWD for these samples, showing a trend for lower CEC and higher BWD near the river mouths, where sediments are also coarser. High CEC and low BWD were found further out into the bay, consistent with earlier findings that the fine fraction is most cohesive and sediments are generally fractionated with coarser material near the river mouths.

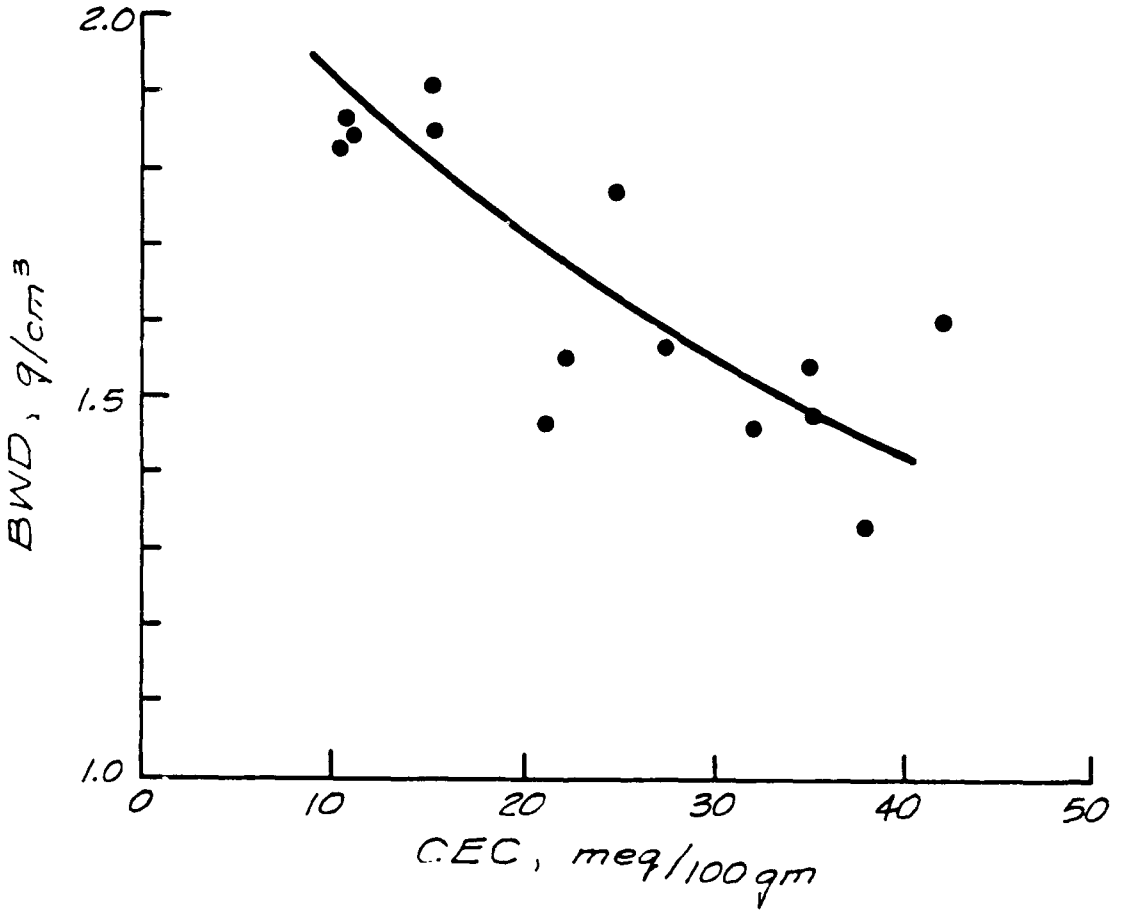

Figure 30. BWD versus CEC for Atchafalaya sediments

PART V: SUMMARY AND CONCLUSIONS

74. The settling and consolidation behavior of Atchafalaya Bay system bed and suspended sediments were observed under various conditions in laboratory and field experiments. Four ranges of concentration affecting settling were identified. The effects of settling height, salinity, and turbulence on settling were also tested. Settling with turbulence and hindered settling consolidation were also studied using numerical models. Measurements in bed sediments were made for bulk wet density, mineral size distribution, and cation exchange capacity. Total suspended material (TSM) concentrations were measured in suspended samples.

75. The following conclusions of these studies as they apply to Atchafalaya Bay were drawn:

a. Bed material is fractionated in the bay by differential settling with coarser material deposited near the river mouth and finer, more cohesive material deposited out in the bay.

b. Settling velocities of suspended material, in general, showed higher rates near river mouths but were also large off Eugene Island. Field settling velocities were not correlated to suspended concentration although laboratory tests showed that, for a given sediment, such a correlation exists.

c. Over the conditions sampled in the field, erosion and deposition are cyclic with both diurnal and spring-neap tidal cycles. Flood-tide phase sample TSM concentrations are generally higher than ebb samples, but near river mouths and at higher river flows, the reverse is true. Spring tide TSM concentrations are higher than neap. Tidal effects were found to be stronger than wind or even river discharge over the range of conditions observed.

d. Mean settling velocities of suspended material were found to vary from 0.005 to 0.3 mm/sec, while median values range from 0.001 to 0.1 mm/sec.

e. At low concentrations, settling is independent of concentration (free settling) but at higher concentrations particles interact, increasing aggregation and settling (enhanced settling). At higher concentrations, particle interactions first slow settling (hindered settling) and eventually make particles immobile in the suspension and they settle as a mass (hindered settling consolidation). Enhanced settling was found to begin at suspended concentrations about 0.1 to 0.2 g/ℓ and continue through 2 or 3 g/ℓ. Hindered settling occurs above this value and was found to follow previously established empirical laws (Equation 8). Hindered settling consolidation was not observed until concentrations of the order of 100 g/ℓ were reached. Concentration had a greater effect on settling velocity

(about a factor of 10) than did settling height (a factor of 5), salinity (a factor of 2 to 4), and turbulence.

f. Turbulence resulting in eddy diffusivities of 285 mm^2/sec had no marked effect on the equilibrium settling velocities of suspended and resuspended bed material. Laboratory and field settling tests are therefore felt to be closely related to in situ equilibrium settling, although field settling tests tended to give results about a factor of 2 greater than laboratory tests and probably are the most realistic.

g. Field estimates of the particle P_e number ($W_s H/K_z$) range from 0.6 to 0.007. Stratification in suspension for expected inflow concentration of <1 g/ℓ is expected to result in near-bottom concentrations of <1.5 g/ℓ. Since the onset of hindered settling consolidation is about 100 g/ℓ, deposition is expected to come from particle settling out of suspension.

h. For the observed range of particle P_e and suspension stratification, sediment transport velocity is very close to the vertically averaged current velocity; and the free-settling flux to the bed approaches an exponential function of depth and settling velocity. Therefore, a vertically averaged numerical modeling approach seems valid.

i. Based on laboratory tests, initial densities of newly deposited sediment are expected to be relatively high (0.7 g/cm^3) near river mouths. Out in the bay where sediments are finer and more cohesive, newly deposited sediment densities are expected to be on the order to 0.4 g/cm^3.

j. Hindered settling consolidation of thin layers of sediment with relatively high initial concentrations was found to be rapid. Numerical results showed that concentrations can double in only a few minutes.

REFERENCES

Ariathurai, R., MacArthur, R. C., and Krone, R. B. 1977 (Oct). "Mathematical Model of Estuarial Sediment Transport," Technical Report D-77-12, US Army Engineer Waterways Experiment Station, Vicksburg, MS.

Christodoulou, G. C., Leimleuhler, W. F., and Ippen, A. T. 1974. "Mathematical Models of Massachusetts Bay; Part III: A Mathematical Model for the Dispersion of Suspended Sediment in Coastal Waters," Report No. 179, Ralph M. Parsons Laboratory, Department of Civil Engineering, Massachusetts Institute of Technology, Cambridge, MA.

Coleman, C. J., Teeter, A. M., Donnell, B. P., Fisackerly, G. M., Crouse, D. A., and Parman, J. W. 1988 (Jun). "The Atchafalaya River Delta; Report 2, Field Data; Section 1: Atchafalaya Bay Program Description and Data," Technical Report HL-82-15, US Army Engineer Waterways Experiment Station, Vicksburg, MS.

Dixit, J. G., Mehta, A. J., and Partheniades, E. 1982. "Redeposition Properties of Cohesive Sediments Deposited in a Long Flume," UFL/COEL - 82/002, Coastal and Oceanographic Engineering Department, University of Florida, Gainsville, FL.

Inman, D. L. 1963. "Sediments: Physical Properties and Mechanics of Sedimentation," Submarine Geology, 2d ed., Caren Cronier, ed., Harper and Row, New York, pp 101-152.

Inter-Agency River Basin Committee. 1953. "Accuracy of Sediment Size Analyses Made by the Bottom Withdrawal Tube Method," Report No. 10, Measurement and Analysis of Sediment Loads in Streams, St. Anthony Falls Hydraulic Laboratory, Minneapolis, MN.

McAnally, W. H., Jr., and Heltzel, S. B. "A Plan for Predicting the Evolution of Atchafalaya Bay, Louisiana" (in preparation), Technical Report HL-82-15, Report 1, US Army Engineer Waterways Experiment Station, Vicksburg, MS.

McAnally, W. H., Jr., Thomas, W. A., Letter, J. V., Jr., Stewart, J. P. 1984 (Jul). "The Atchafalaya River Delta; Interim Summary Report of Growth Predictions," Technical Report HL-82-15, Report 6, US Army Engineer Waterways Experiment Station, Vicksburg, MS.

McLaughlin, R. T., Jr. 1959 (Dec). "The Settling Properties of Suspensions," Journal, Hydraulics Division, American Society of Civil Engineers, Vol 85, No. HY12, pp 9-41.

Oden, S. 1925. "The Size Distribution of Particles in Soils and the Experimental Methods of Obtaining Them," Soil Science, Vol 19, p 1.

Owen, M. V. 1971. "The Effects of Turbulence on Settling Velocities of Silt Flocs," Proceedings, International Association for Hydraulic Research, XIV Congress, Paris, 29 Aug - 3 Sept 1971, Vol 4.

Table 1

Atchafalaya River Delta Reports

Report No.	Title	Contents
1	Plan of Investigation	Investigation Methods and Approach
2	Field Data Program	Field Data Collection Methods and Presentation of Data (4 Sections)
3	Extrapolation of Delta Growth	Analytical Extrapolation of Historical Behavior
4	Generic Analysis of Delta Growth	Comparison with Similar Deltas to Identify Stage of Development and Predict Future Trends
5	Quasi-Two-Dimensional Modeling	Quasi-Two-Dimensional Hydrodynamic and Sedimentation Riverflow Modeling
6	Interim Summary of Results	Summary and Analysis of Reports 3, 4, and 5
7	Analytical Analysis of the Development of the Atchafalaya River Delta	Analytical Treatment of a Simple Jet Discharging into a Quiet Bay
8	Numerical Modeling of Hurricane-Induced Storm Surge	Two-Dimensional Modeling Hurricane-Induced Storm Surge
9	Wind Climatology	Predictions of Wind Conditions Over the Bay
10	Wave Hindcasts	Modeling of Locally Generated Wind Waves
11	Two-Dimensional Modeling	Two-Dimensional Finite Element Modeling of Hydrodynamics, Salinity, and Sedimentation
12	2-D Modeling of Alternative Plans and Impacts on the Atchafalaya Bay and Terrebonne Marshes	Employs the tools described in Report 11, and shows the effects of plans
13	Summary Report	Summary and Analysis of the Study

Table 2
Field and Laboratory Sediment Tests

Station	Source		Lab	Field			
	Suspended	Bed	Settling	Settling	BWD*	Grain Size	CEC**
A	x		x	x			
		x			x	x	
B	x			x			
C	x		x	xxxxx			
		x			xx	x	x
D	x			x			
E	x			x			
F	x		xxx	xx			
		x	xxx		x	x	x
G		x				x	x
H	x		xxx	xxxxx			
		x	xxxxxx		xx	x	x
I	x		x	x			
		x			x	x	
K	x			xxxxx			
		x			x		x
L	x			x			
M	x		xx	x			
		x	xxxxxx		x	x	x
N	x			xx			
O	x			xxxxxxxx			
		x			xx	x	
R	x		x	xxxxxxxxx			
.		x			xx		x
S	x			xx			
		x			x		
U	x			xxxxx			
		x			x		
V	x			xxxx			
X	x			x			

* BWD = Bulk wet density.
** CEC = Cation exchange capacity.

Table 3

Settling Velocity Distributions

Salinity ppt	Initial Concentration mg/ℓ	Geometric Mean Settling Velocity mm/sec	Standard Deviation	Skewness	Kurtosis	Cumulative: Percent Greater than Settling Velocity	Cumulative: Settling Velocity mm/sec	Differential: Settling Velocity Range mm/sec	Differential: Concentration mg/ℓ
				Station F; 6-3-81					
0.0	211	0.085	3.40	0.16	0.40	10	4.098E-01	≥0.6561	7.0
						20	2.356E-01	0.6561-0.2187	38.4
						30	1.490E-01	0.2187-0.0729	57.5
						40	9.999E-02	0.0729-0.0243	76.5
						50	6.986E-02	0.0243-0.0081	31.6
						60	5.030E-02	0.0081-0.0009	0.0
						70	3.709E-02	0.0009-0.0003	0.0
						80	2.788E-02	≤0.0003	0.0
						90	2.129E-02		
				Station R; 6-3-81					
0.0	500	0.341	6.88	0.16	0.40	10	4.069E+00	≥0.6561	167.1
						20	1.690E+00	0.6561-0.2187	95.0
						30	8.203E-01	0.2187-0.0729	113.5
						40	4.373E-01	0.0729-0.0243	124.4
						50	2.488E-01	0.0243-0.0081	0.0
						60	1.485E-01	0.0081-0.0009	0.0
						70	9.202E-02	0.0009-0.0003	0.0
						80	5.879E-02	≤0.0003	0.0
						90	3.852E-02		

(Continued)

Table 3 (Continued)

Salinity ppt	Initial Concentration mg/ℓ	Geometric Mean Settling Velocity mm/sec	Standard Deviation	Skewness	Kurtosis	Cumulative: Percent Greater than Settling Velocity	Cumulative: Settling Velocity mm/sec	Differential: Settling Velocity Range mm/sec	Differential: Concentration mg/ℓ
				Station S; 6-3-81					
0.0	204	0.019	10.38	0.19	0.45	10	4.141E-01	>0.6561	14.2
						20	1.282E-01	0.6561-0.2187	16.4
						30	5.172E-02	0.2187-0.0729	22.3
						40	2.401E-02	0.0729-0.0243	28.3
						50	1.220E-02	0.0243-0.0081	34.2
						60	6.608E-03	0.0081-0.0009	86.0
						70	3.759E-03	0.0009-0.0003	2.5
						80	2.223E-03	<0.0003	0.0
						90	1.357E-03		
				Station B; 10-22-81					
15.5	13	0.050	15.20	0.19	0.44	10	1.817E+00	>0.6561	2.2
						20	4.684E-01	0.6561-0.2187	1.3
						30	1.634E-01	0.2187-0.0729	1.6
						40	6.697E-02	0.0729-0.0243	1.8
						50	3.045E-02	0.0243-0.0081	2.1
						60	1.491E-02	0.0081-0.0009	4.0
						70	7.729E-03	0.0009-0.0003	0.0
						80	4.190E-03	<0.0003	0.0
						90	2.357E-03		
				Station D; 10-22-81					
0.3	39	0.155	4.54	0.20	0.48	10	1.179E+00	>0.6561	6.6
						20	5.307E-01	0.6561-0.2187	7.3
						30	2.925E-01	0.2187-0.0729	10.2
						40	1.774E-01	0.0729-0.0243	13.0
						50	1.151E-01	0.0243-0.0081	1.9
						60	7.774E-02	0.0081-0.0009	0.0
						70	5.424E-02	0.0009-0.0003	0.0
						80	3.882E-02	<0.0003	0.0
						90	2.837E-02		

(Continued)

Table 3 (Continued)

Salinity ppt	Initial Concentration mg/ℓ	Geometric Mean Settling Velocity mm/sec	Standard Deviation	Skewness	Kurtosis	Cumulative: Percent Greater than Settling Velocity	Cumulative: Settling Velocity mm/sec	Differential: Settling Velocity Range mm/sec	Differential: Concentration mg/ℓ
				Station E; 10-22-81					
0.4	33	0.060	3.65	0.16	0.40	10	3.172E-01	≥0.6561	0.3
						20	1.761E-01	0.6561-0.2187	5.0
						30	1.085E-01	0.2187-0.0729	7.7
						40	7.117E-02	0.0729-0.0243	10.4
						50	4.874E-02	0.0243-0.0081	9.6
						60	3.448E-02	0.0081-0.0009	0.0
						70	2.501E-02	0.0009-0.0003	0.0
						80	1.851E-02	≤0.0003	0.0
						90	1.394E-02		
				Station I; 10-22-81					
31.0	198	0.178	3.81	0.17	0.42	10	1.012E+00	≥0.6561	32.8
						20	5.373E-01	0.6561-0.2187	44.2
						30	3.232E-01	0.2187-0.0729	60.4
						40	2.087E-01	0.0729-0.0243	60.6
						50	1.414E-01	0.0243-0.0081	0.0
						60	9.918E-02	0.0081-0.0009	0.0
						70	7.146E-02	0.0009-0.0003	0.0
						80	5.261E-02	≤0.0003	0.0
						90	3.943E-02		
				Station K; 10-27-81					
31.0	21	0.069	6.78	0.19	0.46	10	8.671E-01	≥0.6561	2.6
						20	3.274E-01	0.6561-0.2187	2.7
						30	1.553E-01	0.2187-0.0729	3.6
						40	8.291E-02	0.0729-0.0243	4.5
						50	4.770E-02	0.0243-0.0081	5.4
						60	2.894E-02	0.0081-0.0009	2.2
						70	1.828E-02	0.0009-0.0003	0.0
						80	1.192E-02	≤0.0003	0.0
						90	7.979E-03		

(Continued)

Table 3 (Continued)

Salinity ppt	Initial Concentration mg/ℓ	Geometric Mean Settling Velocity mm/sec	Standard Deviation	Skewness	Kurtosis	Cumulative: Percent Greater than Settling Velocity	Cumulative: Settling Velocity mm/sec	Differential: Settling Velocity Range mm/sec	Differential: Concentration mg/ℓ
				Station L; 10-27-81					
19.3	198	0.386	7.40	0.14	0.38	10	4.827E+00	≥0.6561	72.1
						20	2.071E+00	0.6561-0.2187	37.1
						30	1.001E+00	0.2187-0.0729	42.9
						40	5.239E-01	0.0729-0.0243	45.9
						50	2.906E-01	0.0243-0.0081	0.0
						60	1.686E-01	0.0081-0.0009	0.0
						70	1.013E-01	0.0009-0.0003	0.0
						80	6.277E-02	≤0.0003	0.0
						90	3.986E-02		
				Station M; 10-29-81					
0.7	472	0.059	4.57	0.17	0.42	10	4.232E-01	≥0.6561	25.0
						20	2.051E-01	0.6561-0.2187	64.7
						30	1.149E-01	0.2187-0.0729	94.9
						40	6.990E-02	0.0729-0.0243	125.1
						50	4.491E-02	0.0243-0.0081	155.3
						60	3.003E-02	0.0081-0.0009	7.1
						70	2.070E-02	0.0009-0.0003	0.0
						80	1.463E-02	≤0.0003	0.0
						90	1.055E-02		
				Station R; 11-18-81					
0.3	50	0.167	4.50	0.18	0.43	10	1.196E+00	≥0.6561	100.6
						20	5.745E-01	0.6561-0.2187	110.8
						30	3.223E-01	0.2187-0.0729	148.5
						40	1.969E-01	0.0729-0.0243	186.2
						50	1.272E-01	0.0243-0.0081	13.9
						60	8.551E-02	0.0081-0.0009	1.0
						70	5.931E-02	0.0009-0.0003	0.0
						80	4.217E-02	≤0.0003	0.0
						90	3.059E-02		

(Continued)

Table 4 (Continued)

Salinity ppt	Initial Concentration mg/ℓ	Geometric Mean Settling Velocity mm/sec	Standard Deviation	Skewness	Kurtosis	Cumulative: Percent Greater than Settling Velocity	Cumulative: Settling Velocity mm/sec	Differential: Settling Velocity Range mm/sec	Differential: Concentration mg/ℓ
				Station O; 12-2-81					
0.3	100	0.009	11.41	0.18	0.44	10	2.251E-01	≥0.6561	3.8
						20	6.751E-02	0.6561-0.2187	6.4
						30	2.637E-02	0.2187-0.0729	9.1
						40	1.188E-02	0.0729-0.0243	11.7
						50	5.865E-03	0.0243-0.0081	14.3
						60	3.094E-03	0.0081-0.0009	36.5
						70	1.717E-03	0.0009-0.0003	18.2
						80	9.916E-04	≤0.0003	0.0
						90	5.919E-04		
				Station S; 12-2-81					
0.3	123	0.067	4.62	0.17	0.42	10	4.932E-01	≥0.6561	8.4
						20	2.377E-01	0.6561-0.2187	17.8
						30	1.326E-01	0.2187-0.0729	25.6
						40	8.039E-02	0.0729-0.0243	33.4
						50	5.150E-02	0.0243-0.0081	37.9
						60	3.435E-02	0.0081-0.0009	0.0
						70	2.362E-02	0.0009-0.0003	0.0
						80	1.666E-02	≤0.0003	0.0
						90	1.199E-02		
				Station U; 12-2-81					
9.4	49	0.074	4.54	0.18	0.43	10	5.364E-01	≥0.6561	3.8
						20	2.570E-01	0.6561-0.2187	7.3
						30	1.437E-01	0.2187-0.0729	10.5
						40	8.755E-02	0.0729-0.0243	13.8
						50	5.641E-02	0.0243-0.0081	13.7
						60	3.784E-02	0.0081-0.0009	0.0
						70	2.619E-02	0.0009-0.0003	0.0
						80	1.857E-02	≤0.0003	0.0
						90	1.345E-02		

(Continued)

Table 3 (Continued)

Salinity ppt	Initial Concentration mg/ℓ	Geometric Mean Settling Velocity mm/sec	Standard Deviation	Skewness	Kurtosis	Cumulative: Percent Greater than Settling Velocity	Cumulative: Settling Velocity mm/sec	Differential: Settling Velocity Range mm/sec	Differential: Concentration mg/ℓ
				Station V; 12-2-81					
5.9	69	0.016	72.27	0.14	0.37	10	3.462E+00	≥0.6561	13.3
						20	5.817E-01	0.6561-0.2187	4.8
						30	1.241E-01	0.2187-0.0729	5.2
						40	3.113E-02	0.0729-0.0243	5.6
						50	8.809E-03	0.0243-0.0081	6.1
						60	2.736E-03	0.0081-0.0009	13.4
						70	9.164E-04	0.0009-0.0003	7.4
						80	3.267E-04	≤0.0003	13.2
						90	1.227E-04		
				Station X; 12-2-81					
15.0	19	0.007	134.97	0.04	0.33	10	2.408E+00	≥0.6561	3.5
						20	5.079E-01	0.6561-0.2187	1.4
						30	1.111E-01	0.2187-0.0729	1.4
						40	2.513E-02	0.0729-0.0243	1.4
						50	5.870E-03	0.0243-0.0081	1.4
						60	1.413E-03	0.0081-0.0009	2.9
						70	3.496E-04	0.0009-0.0003	1.5
						80	8.883E-05	≤0.0003	5.5
						90	2.315E-05		
				Station N; 4-16-82					
12.2	93	0.018	8.02	0.18	0.43	10	2.728E-01	≥0.6561	3.6
						20	9.844E-02	0.6561-0.2187	7.5
						30	4.420E-02	0.2187-0.0729	10.8
						40	2.235E-02	0.0729-0.0243	14.1
						50	1.222E-02	0.0243-0.0081	17.4
						60	7.063E-03	0.0081-0.0009	39.6
						70	4.262E-03	0.0009-0.0003	0.0
						80	2.661E-03	≤0.0003	0.0
						90	1.709E-03		

(Continued)

Table 3 (Continued)

Salinity ppt	Initial Concentration mg/ℓ	Geometric Mean Settling Velocity mm/sec	Standard Deviation	Skewness	Kurtosis	Cumulative: Percent Greater than Settling Velocity	Cumulative: Settling Velocity mm/sec	Differential: Settling Velocity Range mm/sec	Differential: Concentration mg/ℓ
				Station O; 4-16-82					
0.1	159	0.023	6.99	0.18	0.43	10	2.941E-01	≥0.6561	6.1
						20	1.141E-01	0.6561-0.2187	14.2
						30	5.407E-02	0.2187-0.0729	20.6
						40	2.860E-02	0.0729-0.0243	27.0
						50	1.626E-02	0.0243-0.0081	33.4
						60	9.739E-03	0.0081-0.0009	57.5
						70	6.070E-03	0.0009-0.0003	0.0
						80	3.906E-03	≤0.0003	0.0
						90	2.580E-03		
				Station R; 4-16-82					
0.1	180	0.057	5.77	0.18	0.43	10	5.702E-01	≥0.6561	15.6
						20	2.425E-01	0.6561-0.2187	23.0
						30	1.237E-01	0.2187-0.0729	31.9
						40	6.964E-02	0.0729-0.0243	40.9
						50	4.186E-02	0.0243-0.0081	49.8
						60	2.637E-02	0.0081-0.0009	18.8
						70	1.723E-02	0.0009-0.0003	0.0
						80	1.158E-02	≤0.0003	0.0
						90	7.969E-03		
				Station A; 5-11-82					
0.2	105	0.003	15.88	0.18	0.44	10	1.064E-01	≥0.6561	1.5
						20	2.779E-02	0.6561-0.2187	4.7
						30	9.730E-03	0.2187-0.0729	6.9
						40	3.990E-03	0.0729-0.0243	9.1
						50	1.813E-03	0.0243-0.0081	11.3
						60	8.872E-04	0.0081-0.0009	29.2
						70	4.592E-04	0.0009-0.0003	17.9
						80	2.485E-04	≤0.0003	24.3
						90	1.396E-04		

(Continued)

Table 3 (Continued)

Salinity ppt	Initial Concentration mg/ℓ	Geometric Mean Settling Velocity mm/sec	Standard Deviation	Skewness	Kurtosis	Cumulative: Percent Greater than Settling Velocity	Cumulative: Settling Velocity mm/sec	Differential: Settling Velocity Range mm/sec	Differential: Concentration mg/ℓ
				Station C; 5-11-82					
0.2	126	0.003	15.16	0.18	0.44	10	9.884E-02	≥0.6561	1.5
						20	2.585E-02	0.6561-0.2187	5.5
						30	9.057E-03	0.2187-0.0729	8.1
						40	3.716E-03	0.0729-0.0243	10.8
						50	1.689E-03	0.0243-0.0081	13.4
						60	8.265E-04	0.0081-0.0009	34.8
						70	4.278E-04	0.0009-0.0003	21.3
						80	2.316E-04	≤0.0003	30.6
						90	1.301E-04		
				Station K; 7-7-82					
1.3	40	0.030	5.85	0.18	0.43	10	3.080E-01	≥0.6561	1.5
						20	1.297E-01	0.6561-0.2187	3.9
						30	6.569E-02	0.2187-0.0729	5.9
						40	3.682E-02	0.0729-0.0243	7.9
						50	2.205E-02	0.0243-0.0081	9.8
						60	1.385E-02	0.0081-0.0009	11.0
						70	9.019E-03	0.0009-0.0003	0.0
						80	6.047E-03	≤0.0003	0.0
						90	4.152E-03		
				Station N; 7-7-82					
0.0	154	0.006	18.67	0.18	0.44	10	3.065E-01	≥0.6561	9.3
						20	7.140E-02	0.6561-0.2187	9.2
						30	2.301E-02	0.2187-0.0729	12.0
						40	8.816E-03	0.0729-0.0243	14.8
						50	3.776E-03	0.0243-0.0081	17.7
						60	1.752E-03	0.0081-0.0009	43.8
						70	8.640E-04	0.0009-0.0003	26.1
						80	4.472E-04	≤0.0003	21.0
						90	2.408E-04		

(Continued)

Table 3 (Continued)

Salinity ppt	Initial Concentration mg/	Geometric Mean Settling Velocity mm/sec	Standard Deviation	Skewness	Kurtosis	Cumulative: Percent Greater than Settling Velocity	Cumulative: Settling Velocity mm/sec	Differential: Settling Velocity Range mm/sec	Differential: Concentration mg/
				Station O; 7-7-82					
0.0	508	0.183	4.93	0.18	0.43	10	1.481E+00	≥0.6561	104.2
						20	6.789E-01	0.6561-0.2187	98.7
						30	3.677E-01	0.2187-0.0729	129.4
						40	2.181E-01	0.0729-0.0243	160.0
						50	1.373E-01	0.0243-0.0081	15.7
						60	9.020E-02	0.0081-0.0009	0.0
						70	6.125E-02	0.0009-0.0003	0.0
						80	4.269E-02	≤0.0003	0.0
						90	3.040E-02		
				Station R; 7-7-82					
0.0	392	0.119	4.24	0.18	0.42	10	7.834E-01	≥0.6561	48.2
						20	3.915E-01	0.6561-0.2187	71.8
						30	2.254E-01	0.2187-0.0729	99.9
						40	1.405E-01	0.0729-0.0243	128.0
						50	9.233E-02	0.0243-0.0081	44.1
						60	6.303E-02	0.0081-0.0009	0.0
						70	4.431E-02	0.0009-0.0003	0.0
						80	3.189E-02	≤0.0003	0.0
						90	2.339E-02		
				Station C; 7-8-82					
0.0	154	0.001	24.07	0.18	0.44	10	5.022E-02	≥0.6561	0.8
						20	1.038E-02	0.6561-0.2187	4.6
						30	3.036E-03	0.2187-0.0729	7.0
						40	1.070E-03	0.0729-0.0243	9.4
						50	4.257E-04	0.0243-0.0081	11.8
						60	1.847E-04	0.0081-0.0009	30.7
						70	8.557E-05	0.0009-0.0003	18.9
						80	4.178E-05	≤0.0003	70.7
						90	2.130E-05		

(Continued)

Table 3 (Continued)

Salinity ppt	Initial Concentration mg/ℓ	Geometric Mean Settling Velocity mm/sec	Standard Deviation	Skewness	Kurtosis	Cumulative: Percent Greater than Settling Velocity	Cumulative: Settling Velocity mm/sec	Differential: Settling Velocity Range mm/sec	Differential: Concentration mg/ℓ
				Station U; 7-9-82					
0.0	111	0.015	29.15	0.18	0.43	10	1.190E+00	≥0.6561	14.8
						20	2.330E-01	0.6561-0.2187	7.9
						30	6.400E-02	0.2187-0.0729	9.4
						40	2.122E-02	0.0729-0.0243	10.9
						50	7.962E-03	0.0243-0.0081	12.3
						60	3.269E-03	0.0081-0.0009	29.1
						70	1.438E-03	0.0009-0.0003	16.8
						80	6.679E-04	≤0.0003	9.8
						90	3.247E-04		
				Station V; 7-9-82					
0.0	66	0.018	8.27	0.19	0.45	10	2.908E-01	≥0.6561	3.0
						20	1.003E-01	0.6561-0.2187	5.1
						30	4.416E-02	0.2187-0.0729	7.5
						40	2.208E-02	0.0729-0.0243	9.8
						50	1.198E-02	0.0243-0.0081	12.2
						60	6.892E-03	0.0081-0.0009	28.4
						70	4.143E-03	0.0009-0.0003	0.0
						80	2.580E-03	≤0.0003	0.0
						90	1.653E-03		
				Station C; 1-24-83					
0.1	211	0.085	7.83	0.18	0.44	10	1.270E+00	≥0.6561	34.1
						20	4.620E-01	0.6561-0.2187	27.9
						30	2.091E-01	0.2187-0.0729	35.5
						40	1.065E-01	0.0729-0.0243	43.2
						50	5.865E-02	0.0243-0.0081	50.9
						60	3.413E-02	0.0081-0.0009	19.3
						70	2.072E-02	0.0009-0.0003	0.0
						80	1.301E-02	≤0.0003	0.0
						90	8.401E-03		

(Continued)

Table 3 (Continued)

Salinity ppt	Initial Concentration mg/ℓ	Geometric Mean Settling Velocity mm/sec	Standard Deviation	Skewness	Kurtosis	Cumulative: Percent Greater than Settling Velocity	Cumulative: Settling Velocity mm/sec	Differential: Settling Velocity Range mm/sec	Differential: Concentration mg/ℓ
				Station K; 1-24-83					
11.5	67	0.022	8.11	0.19	0.44	10	3.518E-01	≥0.6561	3.7
						20	1.238E-01	0.6561-0.2187	5.7
						30	5.508E-02	0.2187-0.0729	8.2
						40	2.773E-02	0.0729-0.0243	10.6
						50	1.512E-02	0.0243-0.0081	13.0
						60	8.735E-03	0.0081-0.0009	25.8
						70	5.270E-03	0.0009-0.0003	0.0
						80	3.291E-03	≤0.0003	0.0
						90	2.115E-03		
				Station O; 1-24-83					
0.1	84	0.000	-	0.17	0.41	10	2.241E-04	≥0.6561	2.1
						20	8.050E-08	0.6561-0.2187	0.7
						30	1.263E-10	0.2187-0.0729	0.8
						40	4.725E-13	0.0729-0.0243	0.8
						50	3.193E-15	0.0243-0.0081	0.9
						60	3.337E-17	0.0081-0.0009	1.9
						70	4.890E-19	0.0009-0.0003	1.0
						80	9.414E-21	≤0.0003	75.9
						90	2.272E-22		
				Station R; 1-24-83					
1.2	196	0.074	17.93	0.14	0.37	10	2.826E+00	≥0.6561	43.7
						20	8.424E-01	0.6561-0.2187	21.3
						30	2.963E-01	0.2187-0.0729	24.0
						40	1.165E-01	0.0729-0.0243	26.8
						50	4.976E-02	0.0243-0.0081	29.5
						60	2.265E-02	0.0081-0.0009	50.7
						70	1.085E-02	0.0009-0.0003	0.0
						80	5.421E-03	≤0.0003	0.0
						90	2.808E-03		

(Continued)

Table 3 (Continued)

[illegible]	Initial Concentration mg/ℓ	Geometric Mean Settling Velocity mm/sec	Standard Deviation	Skewness	Kurtosis	Cumulative: Percent Greater than Settling Velocity	Cumulative: Settling Velocity mm/sec	Differential: Settling Velocity Range mm/sec	Differential: Concentration mg/ℓ
				Station U; 1-25-83					
.5	192	0.221	5.73	0.19	0.45	10	2.214E+00	≥0.6561	47.6
						20	9.237E-01	0.6561-0.2187	36.2
						30	4.695E-01	0.2187-0.0729	46.1
						40	2.648E-01	0.0729-0.0243	56.1
						50	1.597E-01	0.0243-0.0081	5.9
						60	1.011E-01	0.0081-0.0009	0.0
						70	6.632E-02	0.0009-0.0003	0.0
						80	4.480E-02	≤0.0003	0.0
						90	3.099E-02		
				Station F; 1-26-83					
[illegible]	183	0.065	8.84	0.18	0.43	10	1.114E+00	≥0.6561	26.9
						20	3.900E-01	0.6561-0.2187	22.1
						30	1.694E-01	0.2187-0.0729	27.9
						40	8.303E-02	0.0729-0.0243	33.6
						50	4.407E-02	0.0243-0.0081	39.4
						60	2.478E-02	0.0081-0.0009	33.1
						70	1.456E-02	0.0009-0.0003	0.0
						80	8.870E-03	≤0.0003	0.0
						90	5.562E-03		
				Station H; 1-26-83					
[illegible]	506	0.046	25.82	0.15	0.39	10	2.861E+00	≥0.6561	42.0
						20	6.900E-01	0.6561-0.2187	18.9
						30	2.081E-01	0.2187-0.0729	21.4
						40	7.237E-02	0.0729-0.0243	23.9
						50	2.785E-02	0.0243-0.0081	26.3
						60	1.158E-02	0.0081-0.0009	60.1
						70	5.114E-03	0.0009-0.0003	13.4
						80	2.374E-03	≤0.0003	0.0
						90	1.149E-03		

(Continued)

Table 3 (Continued)

Salinity ppt	Initial Concentration mg/ℓ	Geometric Mean Settling Velocity mm/sec	Standard Deviation	Skewness	Kurtosis	Cumulative: Percent Greater than Settling Velocity	Cumulative: Settling Velocity mm/sec	Differential: Settling Velocity Range mm/sec	Differential: Concentration mg/ℓ
				Station U; 2-23-83					
0.2	472	0.001	39.77	0.19	0.46	10	1.139E-01	>0.6561	18.6
						20	1.714E-02	0.6561-0.2187	16.2
						30	4.063E-03	0.2187-0.0729	21.9
						40	1.213E-03	0.0729-0.0243	27.6
						50	4.189E-04	0.0243-0.0081	33.3
						60	1.604E-04	0.0081-0.0009	83.7
						70	6.641E-05	0.0009-0.0003	50.4
						80	2.924E-05	<0.0003	220.1
						90	1.354E-05		
				Station K; 2-24-83					
9.8	180	0.059	6.0	0.16	0.40	10	5.821E-01	>0.6561	15.7
						20	2.606E-01	0.6561-0.2187	24.8
						30	1.336E-01	0.2187-0.0729	32.3
						40	7.453E-02	0.0729-0.0243	39.7
						50	4.408E-02	0.0243-0.0081	47.2
						60	2.723E-02	0.0081-0.0009	20.3
						70	1.741E-02	0.0009-0.0003	0.0
						80	1.145E-02	<0.0003	0.0
						90	7.706E-03		
				Station O; 2-24-83					
0.1	116	0.081	2.6	0.20	0.49	10	2.967E-01	>0.6561	2.9
						20	1.770E-01	0.6561-0.2187	15.0
						30	1.208E-01	0.2187-0.0729	36.1
						40	8.784E-02	0.0729-0.0243	57.2
						50	6.650E-02	0.0243-0.0081	4.7
						60	5.176E-02	0.0081-0.0009	0.0
						70	4.113E-02	0.0009-0.0003	0.0
						80	3.323E-02	<0.0003	0.0
						90	2.721E-02		

(Continued)

Table 3 (Continued)

Salinity ppt	Initial Concentration mg/ℓ	Geometric Mean Settling Velocity mm/sec	Standard Deviation	Skewness	Kurtosis	Cumulative: Percent Greater than Settling Velocity	Cumulative: Settling Velocity mm/sec	Differential: Settling Velocity Range mm/sec	Differential: Concentration mg/ℓ
				Station R; 2-24-83					
0.1	186	0.016	172.1	-0.18	0.43	10	5.404E+00	≥0.6561	53.4
						20	1.806E+00	0.6561-0.2187	16.6
						30	5.632E-01	0.2187-0.0729	15.5
						40	1.614E-01	0.0729-0.0243	14.4
						50	4.161E-02	0.0243-0.0081	13.3
						60	9.340E-03	0.0081-0.0009	23.5
						70	1.729E-03	0.0009-0.0003	10.1
						80	2.387E-04	≤0.0003	39.2
						90	1.922E-05		
				Station H; 3-29-83					
0.2	162	0.128	17.2	0.15	0.39	10	4.780E+00	≥0.6561	43.6
						20	1.378E+00	0.6561-0.2187	18.7
						30	4.827E-01	0.2187-0.0729	21.3
						40	1.915E-01	0.0729-0.0243	23.8
						50	8.297E-02	0.0243-0.0081	26.4
						60	3.845E-02	0.0081-0.0009	28.2
						70	1.879E-02	0.0009-0.0003	0.0
						80	9.592E-03	≤0.0003	0.0
						90	5.077E-03		
				Station K; 3-29-83					
15.9	94	0.109	6.4	0.20	0.49	10	1.319E+00	≥0.6561	15.7
						20	4.934E-01	0.6561-0.2187	13.7
						30	2.374E-01	0.2187-0.0729	18.3
						40	1.291E-01	0.0729-0.0243	22.9
						50	7.569E-02	0.0243-0.0081	23.3
						60	4.681E-02	0.0081-0.0009	0.0
						70	3.012E-02	0.0009-0.0003	0.0
						80	2.000E-02	≤0.0003	0.0
						90	1.362E-02		

(Continued)

Table 3 (Continued)

Salinity ppt	Initial Concentration mg/ℓ	Geometric Mean Settling Velocity mm/sec	Standard Deviation	Skewness	Kurtosis	Cumulative: Percent Greater than Settling Velocity	Cumulative: Settling Velocity mm/sec	Differential: Settling Velocity Range mm/sec	Differential: Concentration mg/ℓ
				Station O; 3-29-83					
0.2	84	0.010	14.6	0.16	0.40	10	3.035E-01	≥0.6561	4.0
						20	9.140E-02	0.6561-0.2187	6.5
						30	3.371E-02	0.2187-0.0729	8.1
						40	1.409E-02	0.0729-0.0243	9.6
						50	6.428E-03	0.0243-0.0081	11.2
						60	3.130E-03	0.0081-0.0009	27.1
						70	1.605E-03	0.0009-0.0003	15.9
						80	8.578E-04	≤0.0003	1.6
						90	4.747E-04		
				Station H; 4-26-83					
0.2	253	0.133	32.8	-0.15	0.38	10	6.963E+00	≥0.6561	97.4
						20	3.175E+00	0.6561-0.2187	29.5
						30	1.385E+00	0.2187-0.0729	26.9
						40	5.733E-01	0.0729-0.0243	24.4
						50	2.226E-01	0.0243-0.0081	21.8
						60	7.972E-02	0.0081-0.0009	35.9
						70	2.570E-02	0.0009-0.0003	14.1
						80	7.155E-03	≤0.0003	2.8
						90	1.591E-03		
				Station O; 4-26-83					
0.2	85	0.004	25.9	0.19	0.46	10	2.841E-01	≥0.6561	5.4
						20	5.341E-02	0.6561-0.2187	4.2
						30	1.498E-02	0.2187-0.0729	5.6
						40	5.149E-03	0.0729-0.0243	6 9
						50	2.013E-03	0.0243-0.0081	8.2
						60	8.622E-04	0.0081-0.0009	20.3
						70	3.955E-04	0.0009-0.0003	12.1
						80	1.916E-04	≤0.0003	22.3
						90	9.702E-05		

(Continued)

Table 3 (Continued)

Salinity ppt	Initial Concentration mg/ℓ	Geometric Mean Settling Velocity mm/sec	Standard Deviation	Skewness	Kurtosis	Cumulative: Percent Greater than Settling Velocity	Cumulative: Settling Velocity mm/sec	Differential: Settling Velocity Range mm/sec	Differential: Concentration mg/ℓ
				Station R; 4-26-83					
0.2	180	0.019	105.9	-0.09	0.34	10	4.066E+00	≥0.6561	46.0
						20	1.276E+00	0.6561-0.2187	16.1
						30	3.823E-01	0.2187-0.0729	15.5
						40	1.087E-01	0.0729-0.0243	14.9
						50	2.913E-02	0.0243-0.0081	14.2
						60	7.282E-03	0.0081-0.0009	26.7
						70	1.678E-03	0.0009-0.0003	12.4
						80	3.509E-04	≤0.0003	34.3
						90	6.507E-05		
				Station U; 4-27-83					
0.2	176	0.014	5.1	0.19	0.45	10	1.217E-01	≥0.6561	0.4
						20	5.316E-02	0.6561-0.2187	8.4
						30	2.814E-02	0.2187-0.0729	19.0
						40	1.646E-02	0.0729-0.0243	29.6
						50	1.026E-02	0.0243-0.0081	40.2
						60	6.689E-03	0.0081-0.0009	78.5
						70	4.514E-03	0.0009-0.0003	0.0
						80	3.131E-03	≤0.0003	0.0
						90	2.220E-03		
				Station V; 4-27-83					
0.2	136	0.041	2.2	0.18	0.44	10	1.126E-01	≥0.6561	6.6
						20	7.681E-02	0.6561-0.2187	-6.4
						30	5.699E-02	0.2187-0.0729	29.2
						40	4.424E-02	0.0729-0.0243	64.7
						50	3.536E-02	0.0243-0.0081	41.9
						60	2.887E-02	0.0081-0.0009	0.0
						70	2.395E-02	0.0009-0.0003	0.0
						80	2.012E-02	≤0.0003	0.0
						90	1.708E-02		

(Continued)

Table 3 (Continued)

Salinity ppt	Initial Concentration mg/ℓ	Geometric Mean Settling Velocity mm/sec	Standard Deviation	Skewness	Kurtosis	Cumulative: Percent Greater than Settling Velocity	Cumulative: Settling Velocity mm/sec	Differential: Settling Velocity Range mm/sec	Differential: Concentration mg/ℓ
				Station J; 5-24-83					
0.1	180	0.013	21.4	0.19	0.45	10	7.362E-01	≥0.6561	19.1
						20	1.556E-01	0.6561-0.2187	12.4
						30	4.719E-02	0.2187-0.0729	15.5
						40	1.726E-02	0.0729-0.0243	18.6
						50	7.118E-03	0.0243-0.0081	21.7
						60	3.195E-03	0.0081-0.0009	52.6
						70	1.530E-03	0.0009-0.0003	30.9
						80	7.707E-04	≤0.0003	9.3
						90	4.048E-04		
				Station H; 5-24-83					
0.1	292	0.127	9.0	0.17	0.42	10	2.212E+00	≥0.6561	63.8
						20	7.760E-01	0.6561-0.2187	40.7
						30	3.359E-01	0.2187-0.0729	49.7
						40	1.637E-01	0.0729-0.0243	58.6
						50	8.638E-02	0.0243-0.0081	67.6
						60	4.829E-02	0.0081-0.0009	11.5
						70	2.822E-02	0.0009-0.0003	0.0
						80	1.709E-02	≤0.0003	0.0
						90	1.065E-02		
				Station O; 5-24-83					
0.1	168	0.000	151.5	0.19	0.45	10	8.878E-02	≥0.6561	4.7
						20	7.200E-03	0.6561-0.2187	3.1
						30	1.029E-03	0.2187-0.0729	3.7
						40	1.983E-04	0.0729-0.0243	4.4
						50	4.635E-05	0.0243-0.0081	5.1
						60	1.243E-05	0.0081-0.0009	12.2
						70	3.704E-06	0.0009-0.0003	7.1
						80	1.199E-06	≤0.0003	67.7
						90	4.153E-07		

(Continued)

Table 3 (Continued)

Salinity ppt	Initial Concentration mg/ℓ	Geometric Mean Settling Velocity mm/sec	Standard Deviation	Skewness	Kurtosis	Cumulative: Percent Greater than Settling Velocity	Cumulative: Settling Velocity mm/sec	Differential: Settling Velocity Range mm/sec	Differential: Concentration mg/ℓ
				Station R; 5-24-83					
0.1	278	0.142	12.4	0.14	0.38	10	3.406E+00	>0.6561	72.6
						20	1.167E+00	0.6561-0.2187	36.5
						30	4.667E-01	0.2187-0.0729	41.8
						40	2.066E-01	0.0729-0.0243	47.1
						50	9.855E-02	0.0243-0.0081	52.4
						60	4.975E-02	0.0081-0.0009	27.4
						70	2.628E-02	0.0009-0.0003	0.0
						80	1.442E-02	≤0.0003	0.0
						90	8.162E-03		
				Station C; 6-22-83					
0.2	86	0.079	4.8	0.18	0.44	10	6.150E-01	>0.6561	8.0
						20	2.830E-01	0.6561-0.2187	12.7
						30	1.548E-01	0.2187-0.0729	18.2
						40	9.288E-02	0.0729-0.0243	23.8
						50	5.913E-02	0.0243-0.0081	23.2
						60	3.928E-02	0.0081-0.0009	0.0
						70	2.696E-02	0.0009-0.0003	0.0
						80	1.898E-02	≤0.0003	0.0
						90	1.365E-02		
				Station H; 6-22-83					
0.2	140	0.175	6.5	0.18	0.43	10	2.003E+00	>0.6561	31.9
						20	8.129E-01	0.6561-0.2187	23.7
						30	3.976E-01	0.2187-0.0729	29.8
						40	2.157E-01	0.0729-0.0243	35.8
						50	1.254E-01	0.0243-0.0081	18.7
						60	7.656E-02	0.0081-0.0009	0.0
						70	4.857E-02	0.0009-0.0003	0.0
						80	3.176E-02	≤0.0003	0.0
						90	2.130E-02		

(Continued)

Table 3 (Concluded)

Salinity ppt	Initial Concentration mg/ℓ	Geometric Mean Settling Velocity mm/sec	Standard Deviation	Skewness	Kurtosis	Cumulative: Percent Greater than Settling Velocity	Cumulative: Settling Velocity mm/sec	Differential: Settling Velocity Range mm/sec	Differential: Concentration mg/ℓ
				Station R; 6-22-83					
0.2	135	0.164	11.0	0.13	0.37	10	3.332E+00	>0.6561	36.8
						20	1.237E+00	0.6561-0.2187	19.0
						30	5.218E-01	0.2187-0.0729	21.6
						40	2.406E-01	0.0729-0.0243	24.3
						50	1.185E-01	0.0243-0.0081	26.9
						60	6.142E-02	0.0081-0.0009	6.4
						70	3.319E-02	0.0009-0.0003	0.0
						80	1.857E-02	≤0.0003	0.0
						90	1.070E-02		
				Station V2; 6-22-83					
0.2	80	0.024	17.2	0.18	0.43	10	9.995E-01	>0.6561	10.2
						20	2.539E-01	0.6561-0.2187	6.8
						30	8.554E-02	0.2187-0.0729	8.3
						40	3.373E-02	0.0729-0.0243	9.8
						50	1.476E-02	0.0243-0.0081	11.3
						60	6.964E-03	0.0081-0.0009	27.0
						70	3.482E-03	0.0009-0.0003	6.7
						80	1.823E-03	≤0.0003	0.0
						90	9.917E-04		

Table 4

Turbulence Settling Tests

Test	Initial Concentration mg/ℓ	Salinity ppt	Sta	Source	Screen Oscillation Rate rpm	Effective Settling Velocity, mm/sec Median	Mean
OA	310	0.2	C,M	Suspended	90	0.0085	0.0196
					250	0.0018	0.0086
					440	0.0016	0.0045
OB	254	4.3	C,M	Suspended	90	0.019	0.0367
					250	0.020	0.0379
					440	0.0049	0.0152
OC	298	3.8	C,M,N	Suspended	90	0.20	0.0418
					250	0.0078	0.0204
					440	0.0032	0.0102
OD	177	2.3	C,M,N	Suspended	90	0.0138	0.0401
					250	0.0073	0.0315
					440	0.0061	0.0233
OE	198	4.2	M	Bed	90	0.0369	0.1652
					250	0.0249	0.1108
					440	0.0170	0.0847
OF	183	0.2	R	Suspended	0*	0.0151	0.0437
					90	0.0080	0.0389
					250	0.0078	0.0353
					440	0.0047	0.0224

* Performed in the field with H = 0.85 m .

Table 5

Initial Densities of Beds Settled from Suspension

Initial Concentration g/ℓ	Settling Height cm	Time hr	Bed Thickness cm	Bulk Wet Density g/cm^3	Concentration g/cm^3 dry wt.
		Station M Composite			
78.8	180	2	14	1.52	0.82
39.5	180	4	9	1.45	0.71
78.8	30.2	0.2	2.3	1.45	0.71
39.5	30.2	0.1	1.2	1.42	0.67
8.2	180	0.5	1.6	1.46	0.73
41.1	180	0.5	10.1	1.41	0.65
		Station M Fine Fraction			
3.8	180	0.5	1.8	1.13	0.20
3.4	180	0.5	0.9	1.31	0.49
27.8	180	0.5	9.2	1.30	0.48

Table 6

Hindered Settling Consolidation Tests

	Initial Values				Average Concentration
Station	BWD g/cm^3	C_o g/ℓ	H cm	Duration hr	$\bar{C}$ g/ℓ
F	1.0980	159	160.0	45	277
F	1.0887	144	100.0	45	533
F	1.0887	144	30.5	50	558
H	1.1100	178	160.0	26	380
M	1.1213	202	100.0	28	803
M	1.0864	141	100.0	28	742
C	1.0852	139	100.0	54	556
C	1.0852	139	30.5	45	695

Table 7

Rating of Field Survey Conditions

	Survey Dates														
	8/19-21 1980	1/27-29 1981	9/3 1981	8/5-7 1980	6/2-3 1981	10/22 1981	12/2-3 1981	4/18 1982	5/11 1982	6/23-26 1981	7/21-23 1981	10/27-29 1981	11/18 1981	6/8-9 1982	7/7-9 1982
High Transport Energy															
Tide Range >2 ft				x	x									x	x
Wind >9 mph				x					x	x					
Inflow > 6,400 m^3/sec (225 × 10^3 cfs)				x				x		x				x	x
TSM > 250 mg/ℓ										x	x	x	x	x	x
Medium Transport Energy															
Tide Range 1.3 to 2 ft	x					x	x		x	x	x	x	x		
Wind 5-9 mph					x							x			
Inflow 2,800-6,400 m^3/sec (100-225 × 10^3 cfs)			x			x	x		x		x	x	x		
TSM 80-250 mg/ℓ				x	x	x	x	x	x						
Low Transport Energy															
Tide Range < 1.3 ft		x	x					x							
Wind <5 mph	x	x	x			x	x			x			x	x	x
Inflow <2,800 m^3/sec (100 × 10^3 cfs)	x	x		x											
TSM <80 mg/ℓ	x	x	x												

Table 8

Field Settling Test Conditions and Results for 1980-1982

Sta	TSM mg/ℓ	W_s	C1	C2	C3	Sal	SPD	Dir	Wind	Sea
A	108	0.1	3	17	85	0.2	1.0	090	SE 12	--
B	13	1.0	3	3	7	15.5	0.0	344	00	00
C	154	0.0	0	20	134	0.0	0.2	323	00	0.2
C	126	0.1	5	18	103	0.2	0.4	022	SE 15	2.0
D	39	3.7	11	23	5	0.3	0.5	330	NE 3	0.3
E	33	1.6	3	18	12	0.4	1.0	015	N 2	0.0
F	145	3.5	61	33	61	0.2	0.7	040	SE 15	2.0
F	211	2.3	27	138	46	0.0	--	--	SE 10	1.2
H	754	3.0	158	453	143	0.3	0.8	042	E 2	00
I	198	4.6	59	133	6	31.0	0.2	243	00	00
K	21	1.6	4	8	9	31.0	0.3	170	NE 4	00
K	40	0.7	4	14	22	1.3	0.7	252	SW 2	0.8
L	198	10.0	99	91	8	19.3	0.2	314	NW 6	0.3
M	472	1.5	61	222	189	0.7	0.3	098	E 3	0.3
N	154	0.1	15	28	111	0.0	0.4	064	SW 3	0.8
N	93	0.6	7	26	60	12.2	--	--	E 15	2.0
O	508	4.9	173	310	25	0.0	0.9	052	N 5	0.8
O	159	0.5	14	50	95	0.1	--	--	SE 10	1.0
O	100	0.2	8	21	71	0.3	0.2	012	NW 4	0.7
R	392	3.0	90	239	63	0.0	1.8	330	N 2	00
R	560	4.2	168	364	28	0.3	0.7	314	SE 2	0.2
R	500	8.4	235	240	25	0.0	--	--	SE 10	1.2
R	180	1.4	29	75	76	0.1	--	--	W 10	1.0
S	123	1.7	18	59	46	0.3	0.5	008	00	00
S	204	0.4	24	51	129	0.0	--	--	SE 10	--
U	49	1.9	8	24	17	9.4	0.3	014	NW 3	0.7
V	111	0.3	20	22	69	0.0	0.4	190	W 1	0.2
V	66	0.4	5	23	38	0.0	0.6	118	N 1	0.5
V	69	0.3	17	11	41	5.9	0.4	303	NW 3	0.7
X	19	0.2	5	3	11	15.0	0.6	290	SE 10	1.0

Note: C1 = TSM with settling velocity greater than 10^{-1} mm/sec (equivalent Stokes diameter > 12 μm);
C2 = TSM with settling velocity between 10^{-1} and 10^{-2} mm/sec (equivalent Stokes diameter between 12 and 3.5 μm);
C3 = TSM with settling velocity less than 10^{-2} mm/sec (equivalent Stokes diameter < 3.5 μm);
Sal = salinity, ppt;
SPD = current speed, fps;
Dir = current direction, deg;
Wind direction and speed in knots;
Sea = wind waves, ft.

Table 9

Suspension Classification Data for Stations Diagrammed in Figure 29

Station	Date	Depth m	$\bar{U}$ m/sec	$\bar{C}$ mg/ℓ	U*(fm) m/sec	Stratification	P_e
F	7/07/82	5.34	0.448	322	0.021	1.53	0.072
R	7/07/82	1.89	0.561	371	0.032	0.94	0.056
O	7/07/82	1.98	0.282	433	0.016	2.80	0.171
H	7/07/82	2.93	0.254	379	0.013	1.07	0.101
V	7/09/82	2.29	0.206	55	0.011	0.90	0.024
U	7/09/82	2.90	0.163	112	0.009	0.17	0.025
U	1/25/83	2.29	0.270	202	0.015	0.51	0.220
U	2/23/83	2.59	0.035	536	0.002	0.64	0.007
R	2/24/83	1.83	0.426	183	0.024	0.48	0.010
O	2/24/83	2.44	0.090	162	0.005	1.25	0.242
H	3/29/83	2.44	0.304	185	0.016	1.00	0.119
H	4/26/83	2.44	0.419	277	0.023	0.68	0.086
O	4/26/83	1.83	0.093	93	0.005	0.27	0.012
R	5/24/83	1.98	0.874	255	0.049	0.43	0.043
H	5/24/83	2.44	0.487	314	0.026	0.16	0.073
C	5/24/83	1.22	0.206	180	0.012	0.71	0.016
H	6/22/83	3.66	0.516	167	0.026	0.76	0.100
R	6/22/83	2.44	0.615	141	0.033	0.42	0.074
C	6/22/83	1.83	0.244	76	0.014	0.27	0.084

Table 10

Shear Velocity and Suspension Stratification Data

Station	Date	Depth m	$\bar{U}$ m/sec	U*(fm) m/sec	$\bar{C}$ g/ℓ	$\delta C/\bar{C}$
A	05/11/82	2.0	0.336	0.019	0.103	0.0
C	01/24/83	2.3	0.248	0.014	0.210	0.701
C	05/24/83	1.2	0.206	0.022	0.180	0.712
C	06/22/83	1.8	0.244	0.014	0.076	0.265
F	05/11/82	5.3	0.266	0.018	0.109	0.972
F	06/08/82	4.9	0.223	0.013	0.326	1.064
F	07/07/82	5.3	0.448	0.021	0.322	1.530
H	08/05/80	2.4	0.417	0.023	0.033	0.28
H	05/11/82	2.7	0.473	0.025	0.077	0.32
H	06/08/82	2.9	0.224	0.012	0.221	0.13
H	07/07/82	2.9	0.254	0.013	0.379	1.070
H	02/24/83	2.4	0.270	0.015	0.194	0.229
H	03/29/83	2.4	0.304	0.016	0.185	1.004
H	04/26/83	2.4	0.419	0.034	0.277	0.677
H	05/24/83	2.4	0.487	0.024	0.314	0.158
H	06/22/83	3.7	0.516	0.043	0.167	0.764
I	05/11/82	1.7	0.183	0.011	0.072	0.18
I	06/09/82	1.7	0.137	0.008	0.312	0.06
K	06/09/82	3.4	0.112	0.005	0.130	1.38
K	07/07/82	3.1	0.143	0.007	0.061	1.06
K	04/26/83	2.0	0.286	0.016	0.104	0.151
L	08/05/80	6.4	0.447	0.021	0.042	2.51
L	08/19/80	7.0	0.168	0.008	0.028	1.71
L	06/09/82	6.9	0.163	0.009	0.015	2.59
L	07/07/82	7.0	0.203	0.009	0.010	3.54
M	06/08/82	1.7	0.107	0.006	0.151	0.36
M	07/08/82	1.6	0.092	0.005	0.159	NA
N	06/09/82	2.0	0.102	0.005	0.244	0.397
O	08/05/80	1.5	0.488	0.029	0.095	0.66
O	08/19/80	1.5	0.229	0.013	0.022	0.36
O	06/10/82	1.8	0.163	0.009	0.345	1.82

(Continued)

Table 10 (Concluded)

Station	Date	Depth m	$\bar{U}$ m/sec	U*(fm) m/sec	$\bar{C}$ g/ℓ	$\delta C/\bar{C}$
O	07/07/82	2.0	0.282	0.016	0.433	2.801
O	01/24/83	2.8	0.122	0.006	0.085	0.710
O	02/24/83	2.4	0.090	0.005	0.162	1.252
O	04/26/83	1.8	0.093	0.005	0.093	0.268
O	05/24/83	2.4	0.284	0.015	0.102	0.936
R	08/05/80	1.5	0.549	0.032	0.171	0.30
R	08/19/80	1.6	0.336	0.020	0.062	0.98
R	06/09/82	1.8	0.254	0.015	0.903	0.71
R	07/07/82	1.9	0.561	0.032	0.371	0.943
R	02/24/83	1.8	0.426	0.024	0.183	0.482
R	05/24/83	2.0	0.874	0.049	0.255	0.432
R	06/22/83	2.4	0.615	0.033	0.141	0.416
U	08/06/80	2.9	0.203	0.011	0.042	0.49
U	06/09/82	3.1	0.112	0.005	0.059	0.27
U	07/09/82	2.9	0.163	0.009	0.112	0.171
U	01/25/83	2.3	0.270	0.015	0.202	0.505
U	02/23/83	2.6	0.035	0.002	0.536	0.636
V	08/06/80	2.9	0.163	0.008	0.045	0.12
V	07/09/82	2.3	0.206	0.011	0.055	0.902
V	01/25/83	2.13	0.094	0.005	0.225	1.455
V	04/27/83	2.3	0.132	0.007	0.147	0.002
X	08/06/80	2.9	0.427	0.022	0.053	0.20
Tide Gage 8	08/08/80	8.8	0.366	0.016	0.055	2.39
Y	08/06/80	1.8	0.671	0.[illegible]	0.033	0.32

Table 11

Test Results for Cation Exchange Capacity

Sample Station	Depth in Sediment ft	CEC meq/100 g
F	Composite	27.4
F	0.1	35.7
F	0.6	21.9
R	0.1	14.9
R	0.6	15.0
G	0.1	17.2
G	0.6	10.0
X	0.75	5.8
K	Composite	35.4
K	0.1	38.7
K	0.6	24.7
M	Composite	11.2
M	0.1	10.5
M	0.6	8.0
H	Composite	31.6
C	Composite	42.4
C	0.1	20.7
C	0.6	32.2
Commercial (Kaolinite)	--	13.1

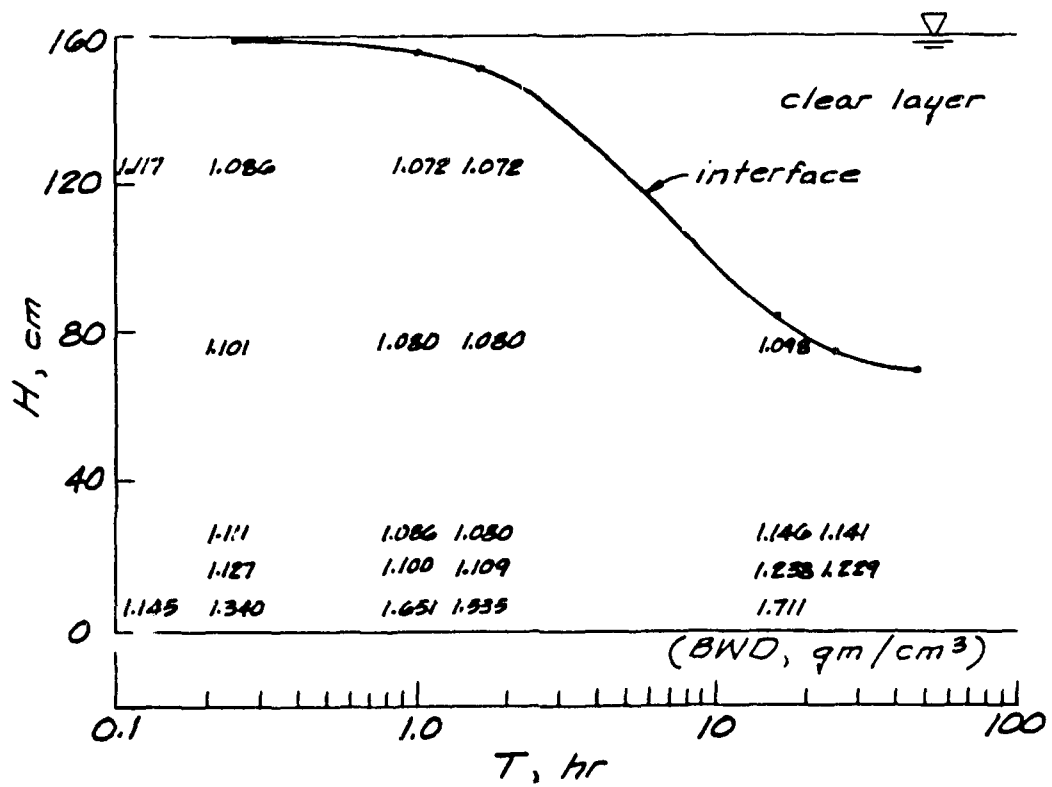

TEST B-1
Navigation Channel Mud
Station H

PLATE 1

PLATE 2

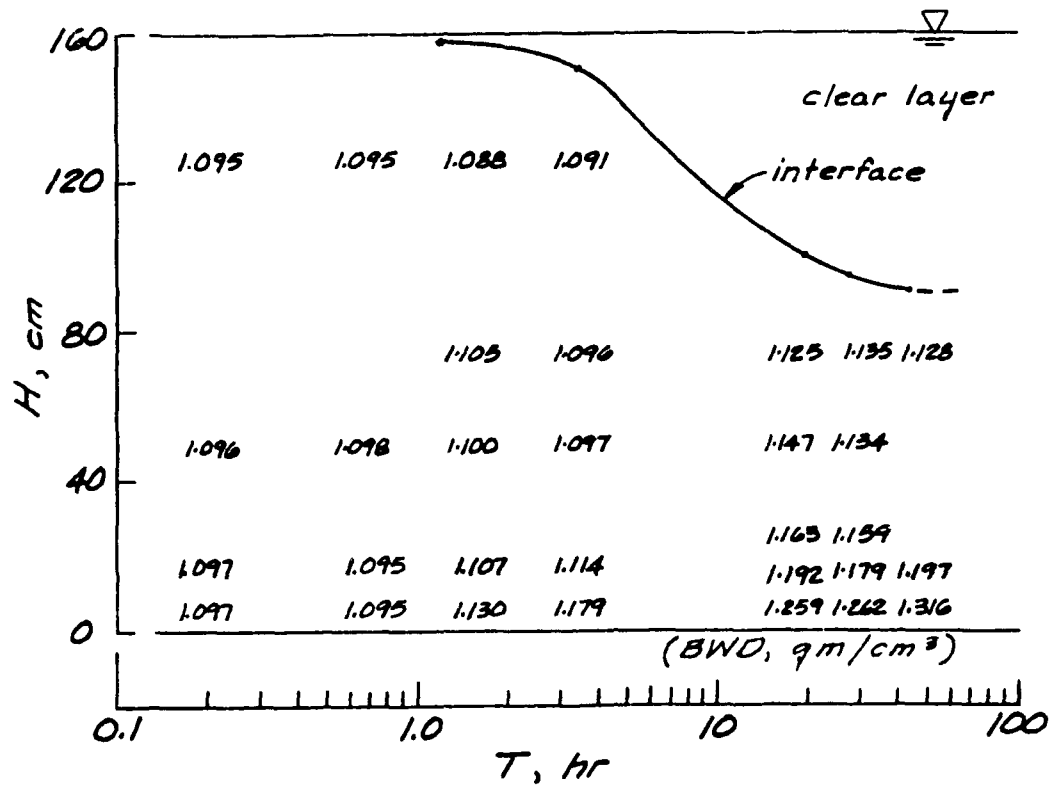

TEST B-2
Delta Mud
Station F

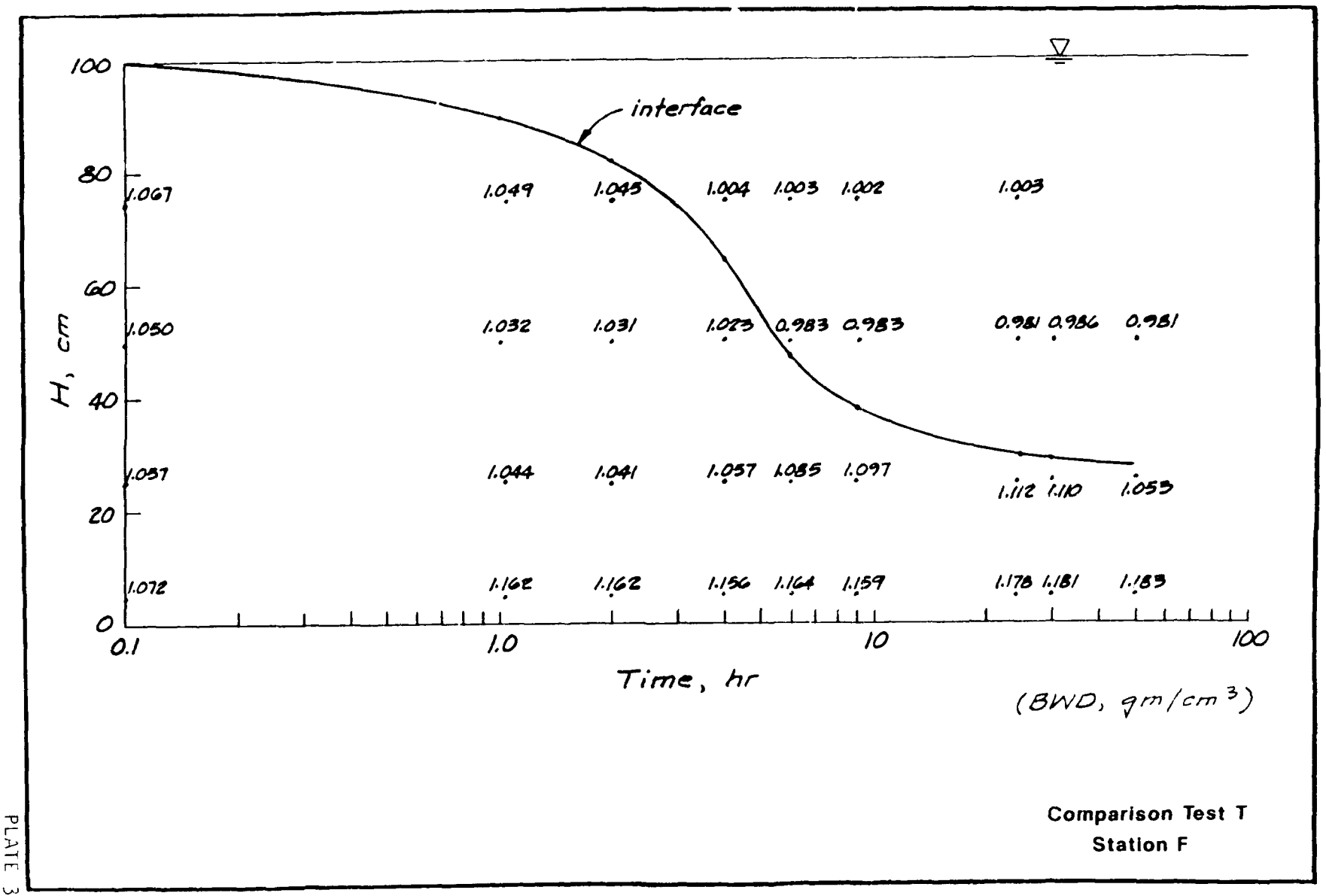

Comparison Test T
Station F

PLATE 3

PLATE 4

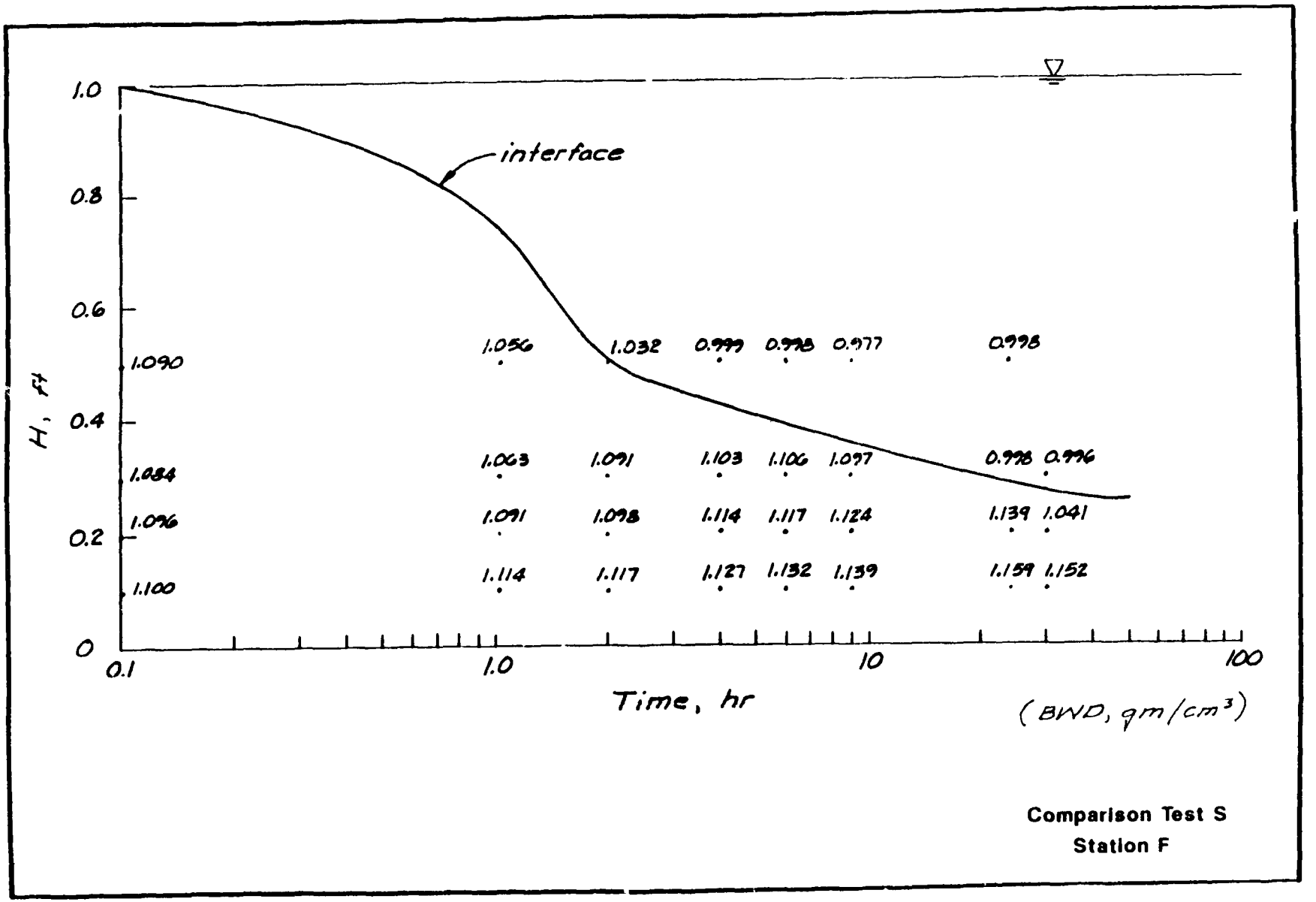

Comparison Test S
Station F

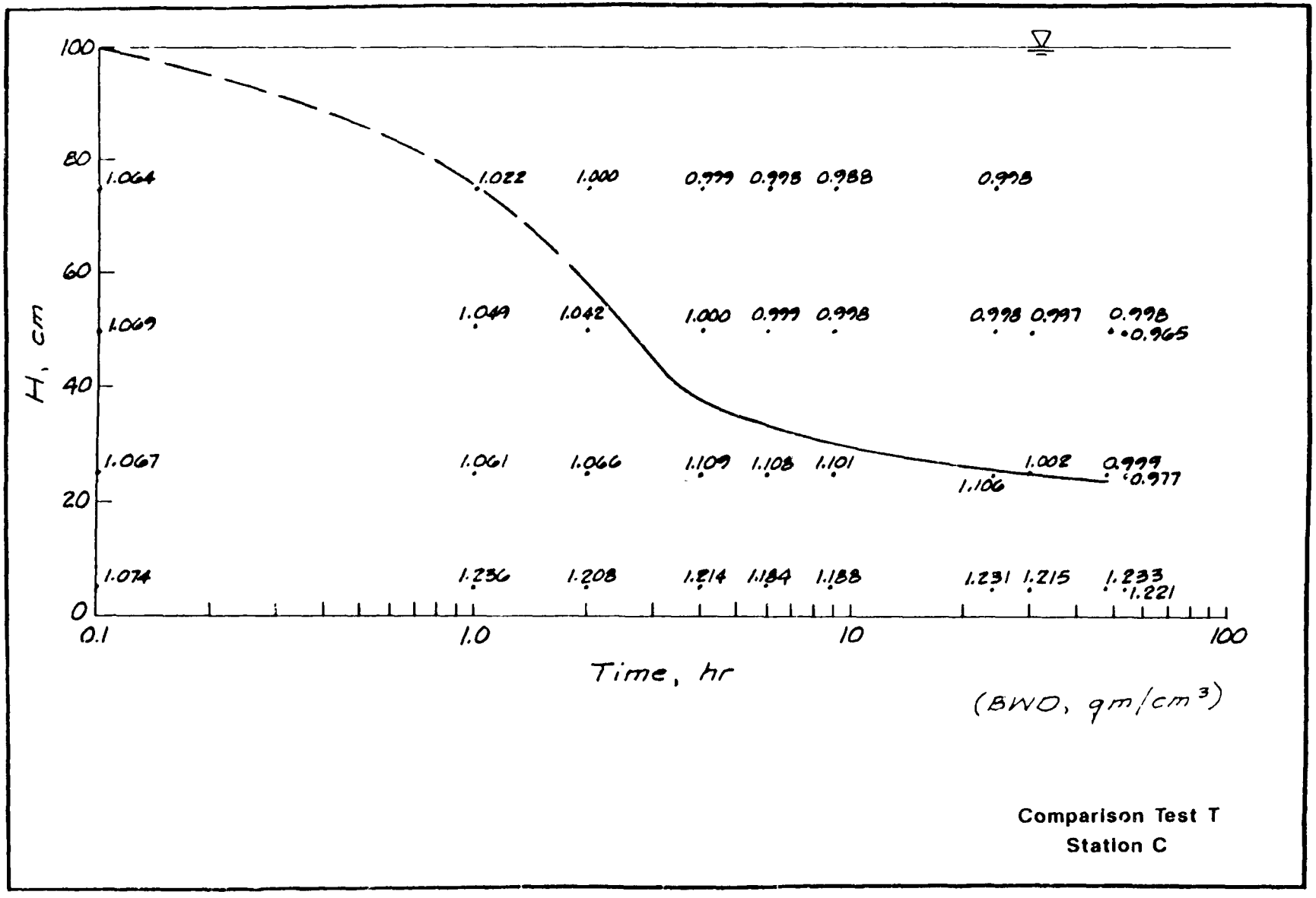
100
80
60
40
20
0
H, cm
1.064
1.069
1.067
1.074
1.022
1.049
1.061
1.236
1.000
1.042
1.066
1.208
0.979
0.978
0.988
1.000
0.999
0.998
1.109
1.108
1.101
1.214
1.184
1.188
0.998
0.998
0.997
0.998
*0.965
1.106
1.002
0.999
*0.977
1.231
1.215
1.233
*1.221
0.1
1.0
10
100
Time, hr
(BWO, gm/cm³)
Comparison Test T
Station C

PLATE 5

PLATE 6

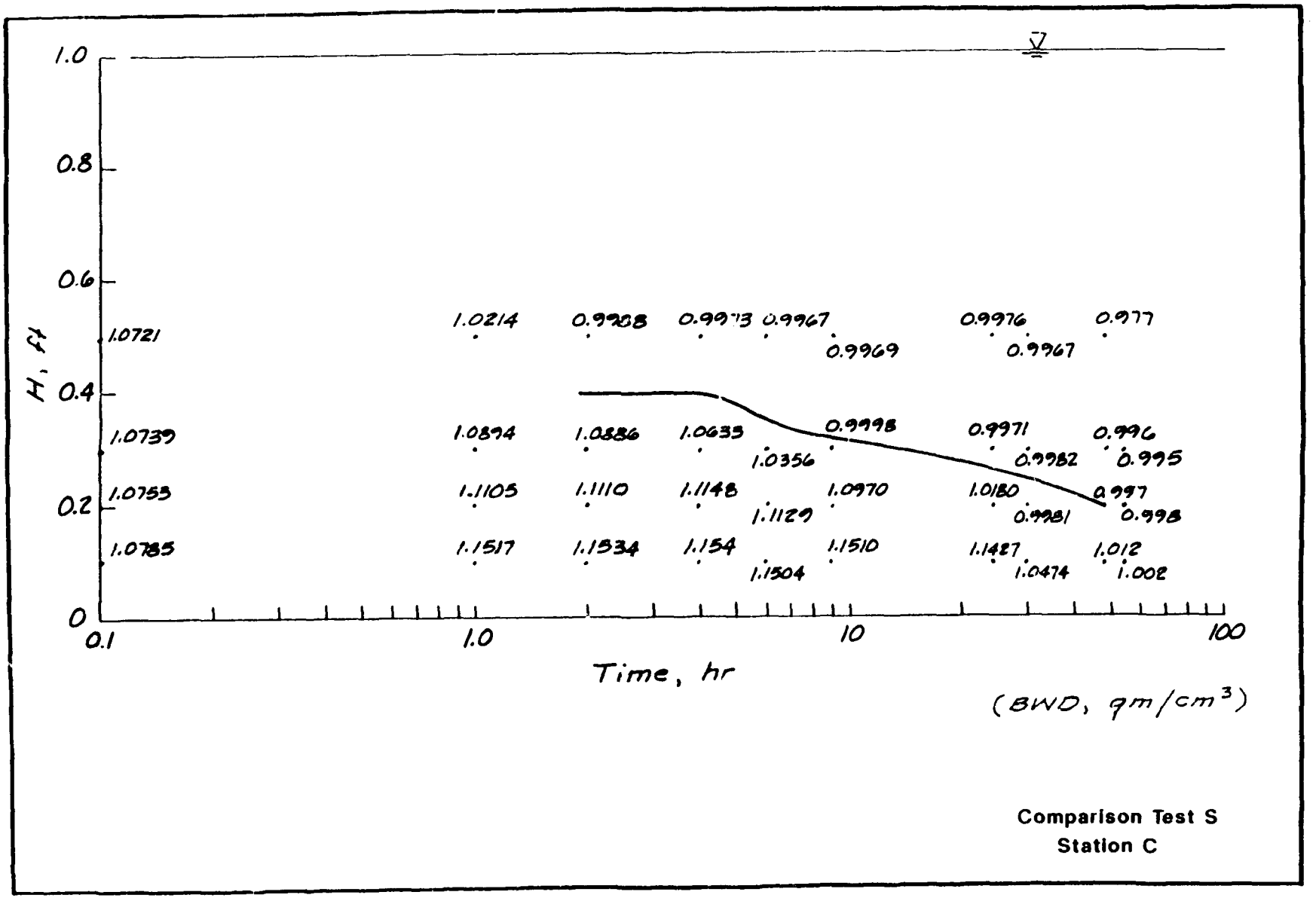
1.0
0.8
0.6
0.4
0.2
0
H, ft
1.0721
1.0739
1.0755
1.0785
1.0214
1.0894
1.1105
1.1517
0.9988
1.0886
1.1110
1.1534
0.9973
1.0635
1.1148
1.154
0.9967
1.0356
1.1129
1.1504
0.9969
0.9998
1.0970
1.1510
0.9976
0.9971
1.0180
1.1427
0.9967
0.9982
0.9981
1.0474
0.977
0.996
0.997
1.012
0.995
0.998
1.002
0.1
1.0
10
100
Time, hr
(BWD, gm/cm³)
Comparison Test S
Station C

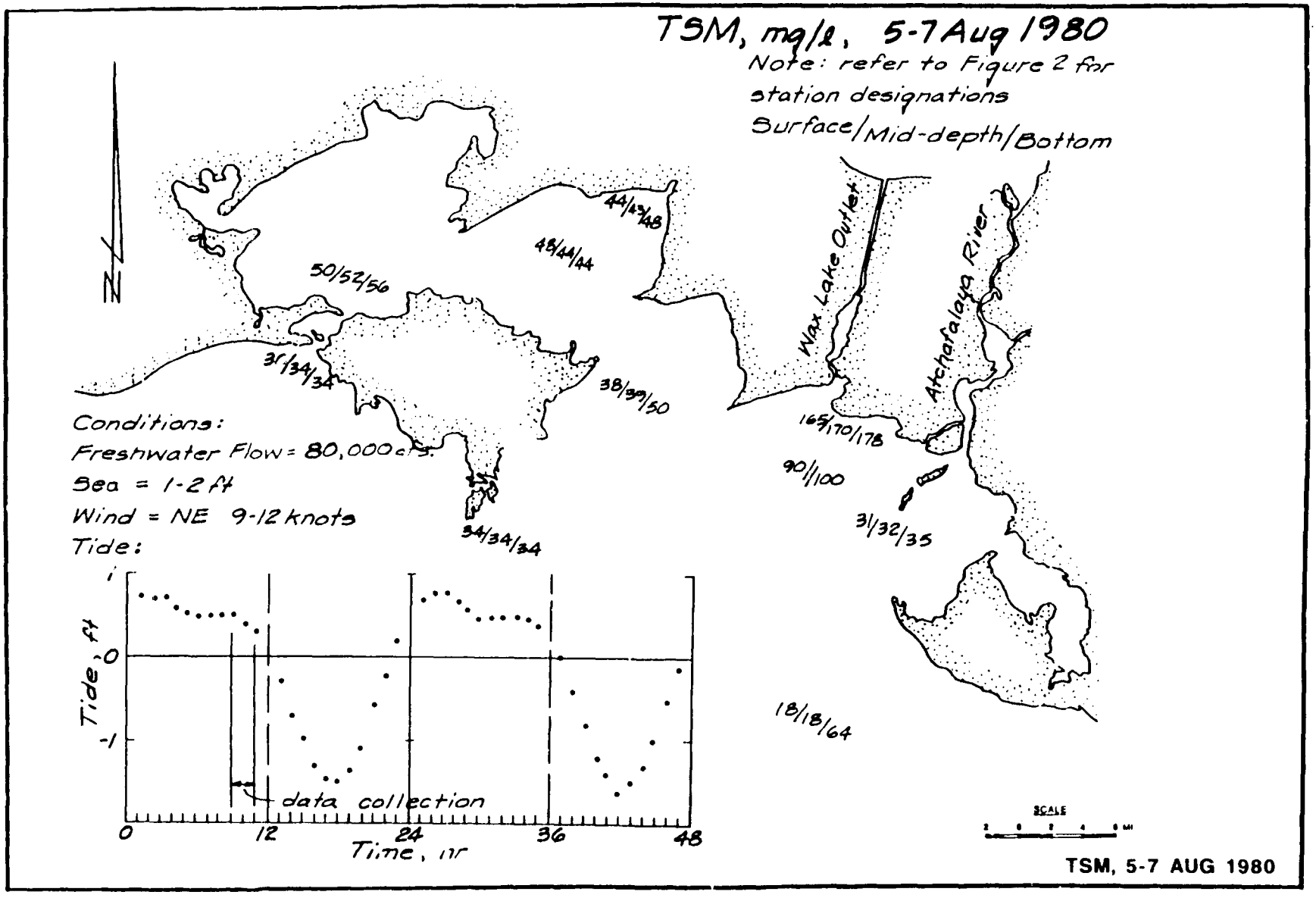
TSM, mg/l, 5-7 Aug 1980
Note: refer to Figure 2 for station designations
Surface/Mid-depth/Bottom
N
Wax Lake Outlet
Atchafalaya River
44/43/48
48/44/44
50/52/56
38/39/50
31/34/34
34/34/34
165/170/178
90/1/100
31/32/35
18/18/64
Conditions:
Freshwater Flow = 80,000 cfs.
Sea = 1-2 ft
Wind = NE 9-12 knots
Tide:
Tide, ft
1
0
-1
data collection
0
12
24
36
48
Time, hr
SCALE
TSM, 5-7 AUG 1980

PLATE 7

PLATE 8

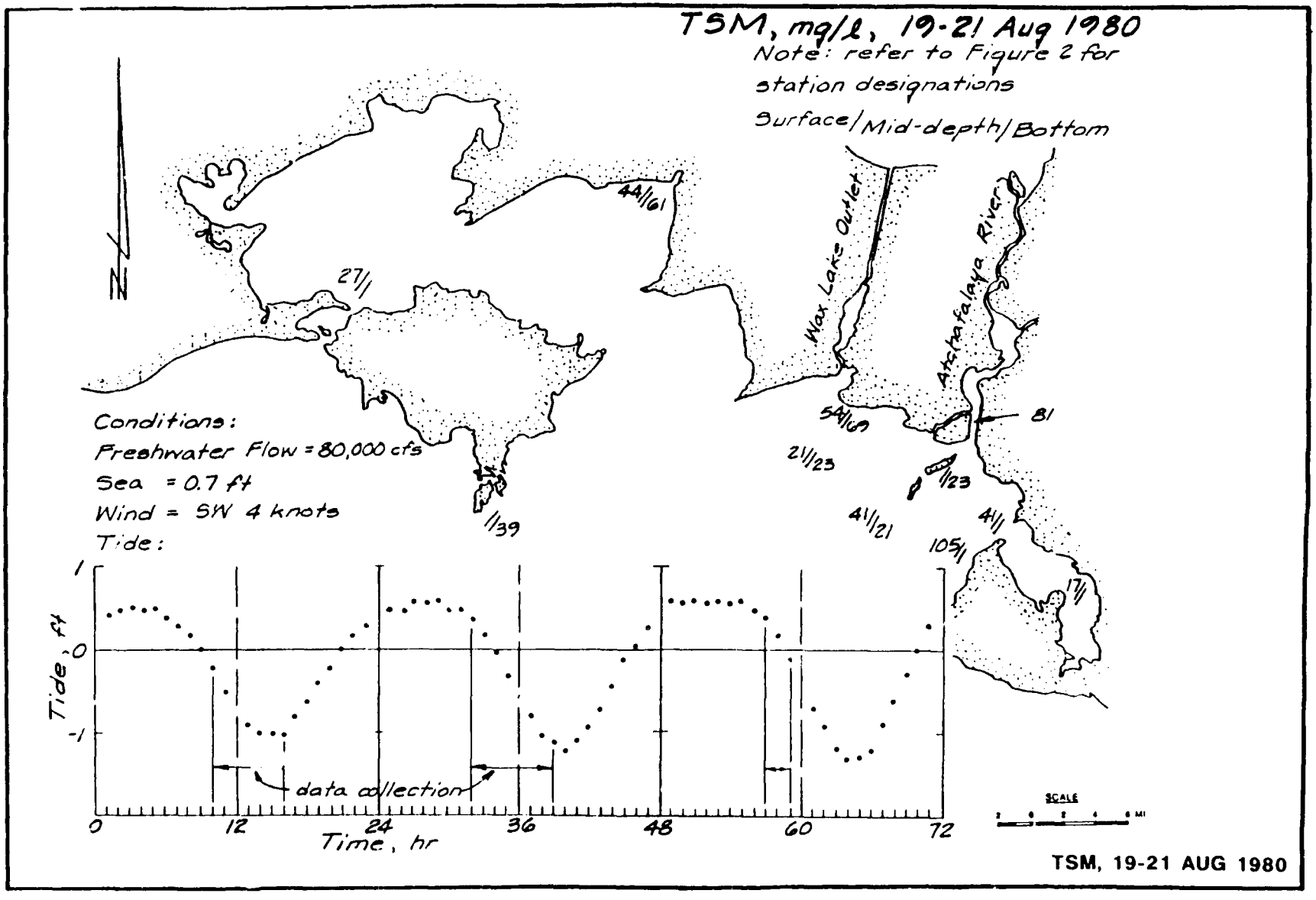
TSM, mg/l, 19-21 Aug 1980
Note: refer to Figure 2 for station designations
Surface/Mid-depth/Bottom
Wax Lake Outlet
Atchafalaya River
44//61
27//
54//69
81
21//23
//23
41//21
41//
105//
17//
//39
Conditions:
Freshwater Flow = 80,000 cfs
Sea = 0.7 ft
Wind = SW 4 knots
Tide:
Tide, ft
1
0
-1
data collection
0
12
24
36
48
60
72
Time, hr
SCALE
TSM, 19-21 AUG 1980

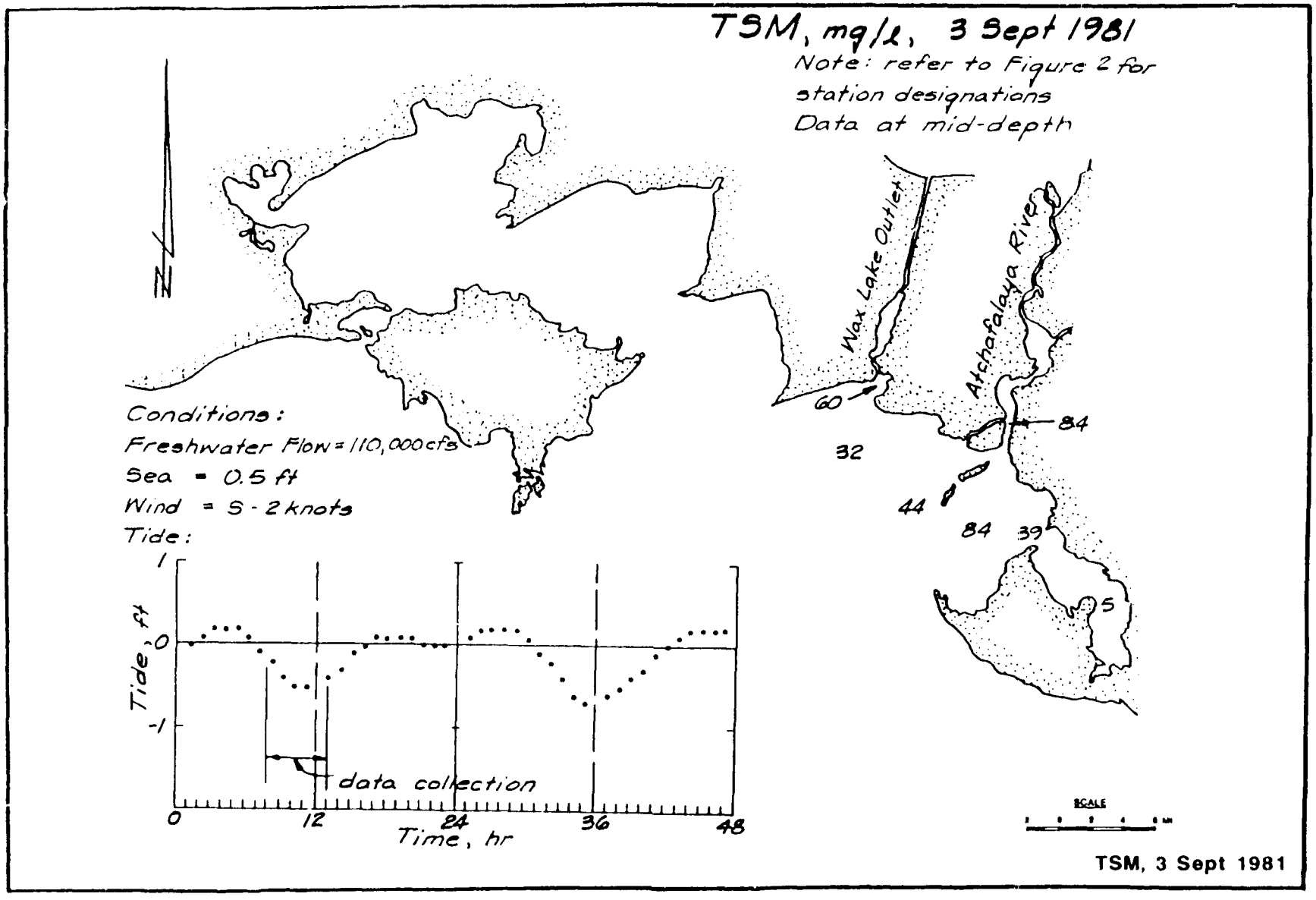
TSM, mg/l, 3 Sept 1981
Note: refer to Figure 2 for station designations
Data at mid-depth
Wax Lake Outlet
Atchafalaya River
60
84
32
44
84
39
5
Conditions:
Freshwater Flow = 110,000 cfs
Sea = 0.5 ft
Wind = S - 2 knots
Tide:
Tide, ft
1
0
-1
data collection
0
12
24
36
48
Time, hr
SCALE
TSM, 3 Sept 1981

PLATE 9

PLATE 10

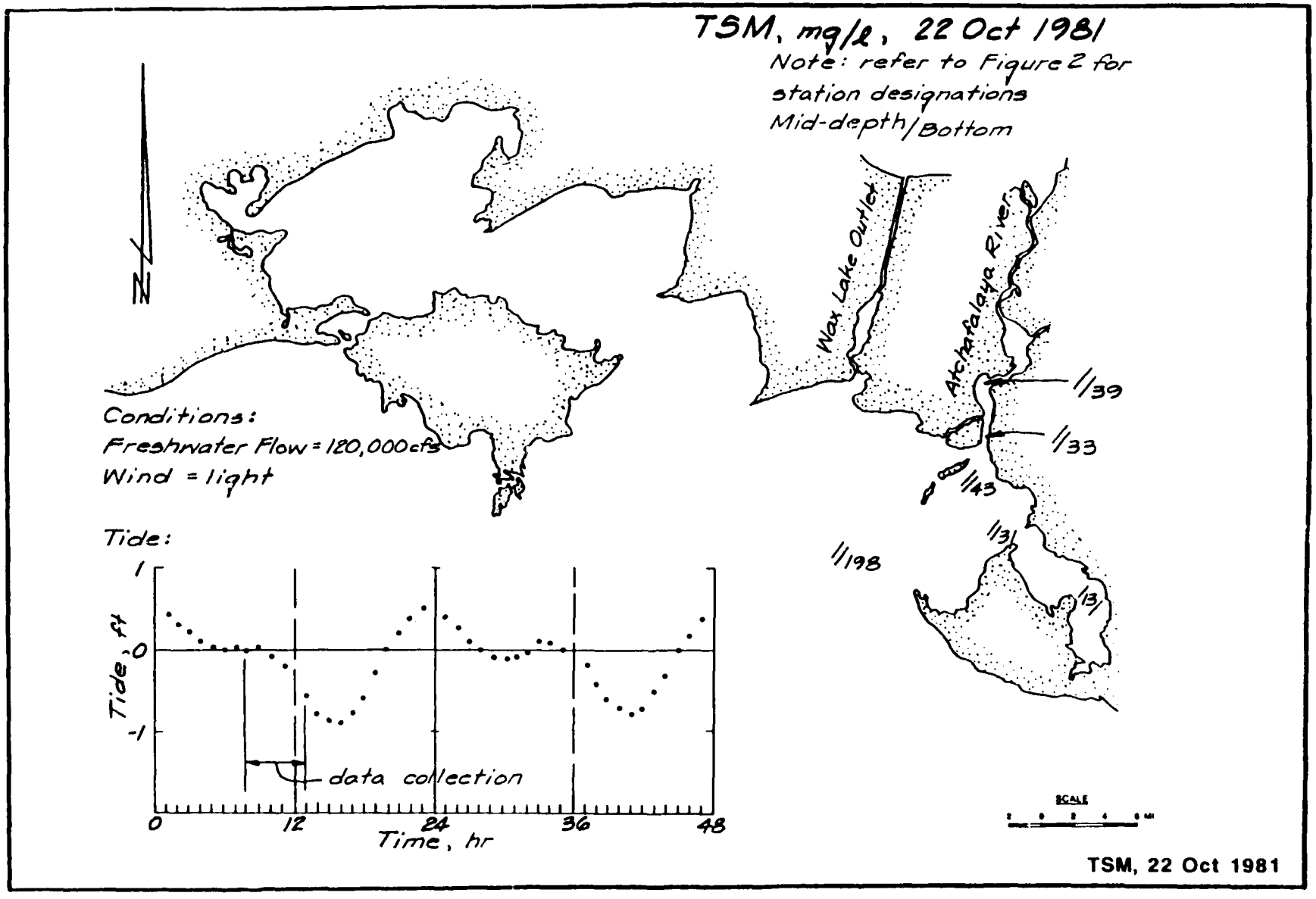
TSM, mg/l, 22 Oct 1981
Note: refer to Figure 2 for station designations
Mid-depth/Bottom
Wax Lake Outlet
Atchafalaya River
1/39
1/33
1/43
1/31
1/198
13
Conditions:
Freshwater Flow = 120,000 cfs
Wind = light
Tide:
Tide, ft
1
0
-1
data collection
0
12
24
36
48
Time, hr
SCALE
TSM, 22 Oct 1981

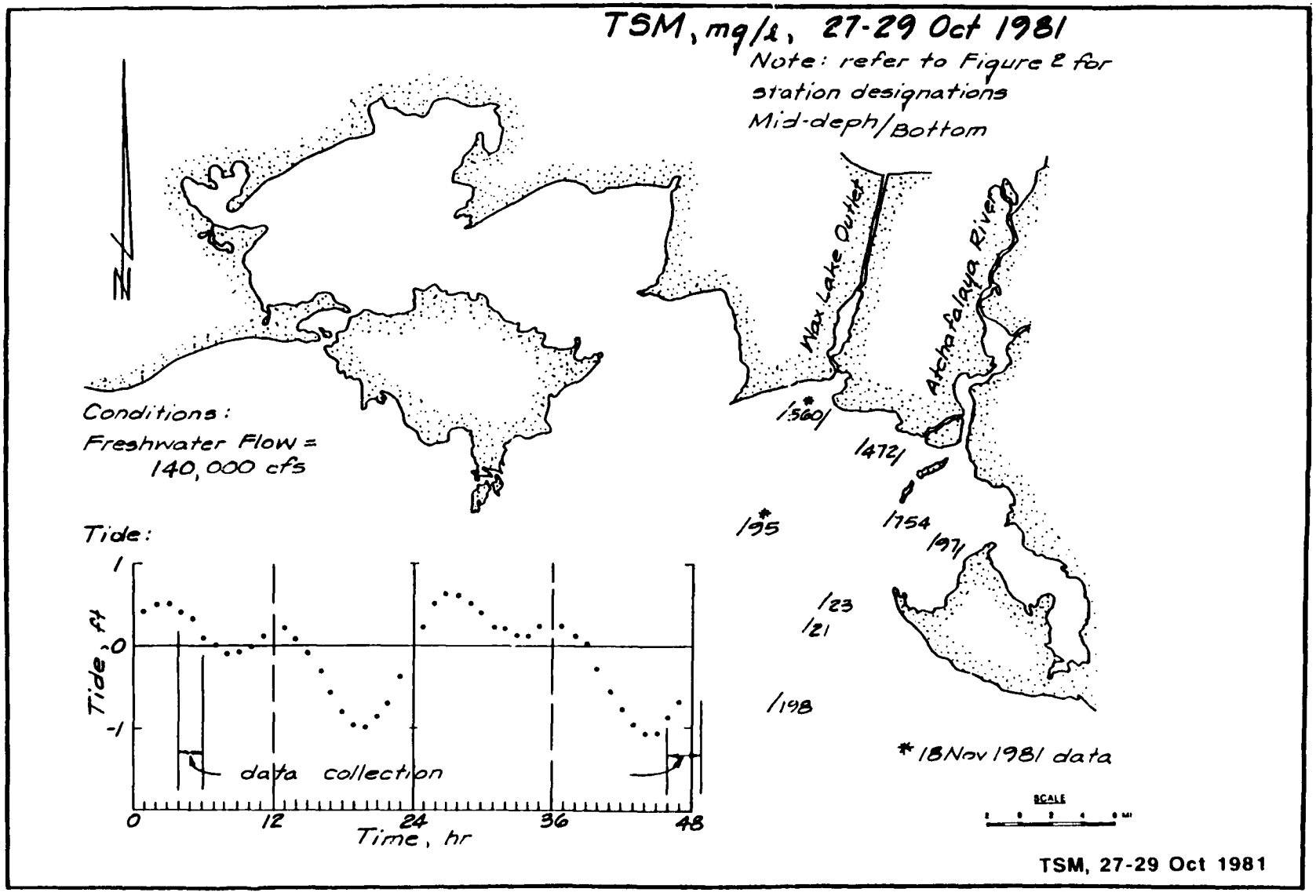
TSM, mg/ℓ, 27-29 Oct 1981
Note: refer to Figure 2 for station designations
Mid-depth/Bottom
Wax Lake Outlet
Atchafalaya River
Conditions:
Freshwater Flow = 140,000 cfs
Tide:
Tide, ft
1
0
-1
data collection
0
12
24
36
48
Time, hr
/560/
/472/
/754
/195*
/197
/23
/21
/198
*18Nov1981 data
SCALE
TSM, 27-29 Oct 1981

PLATE 11

PLATE 12

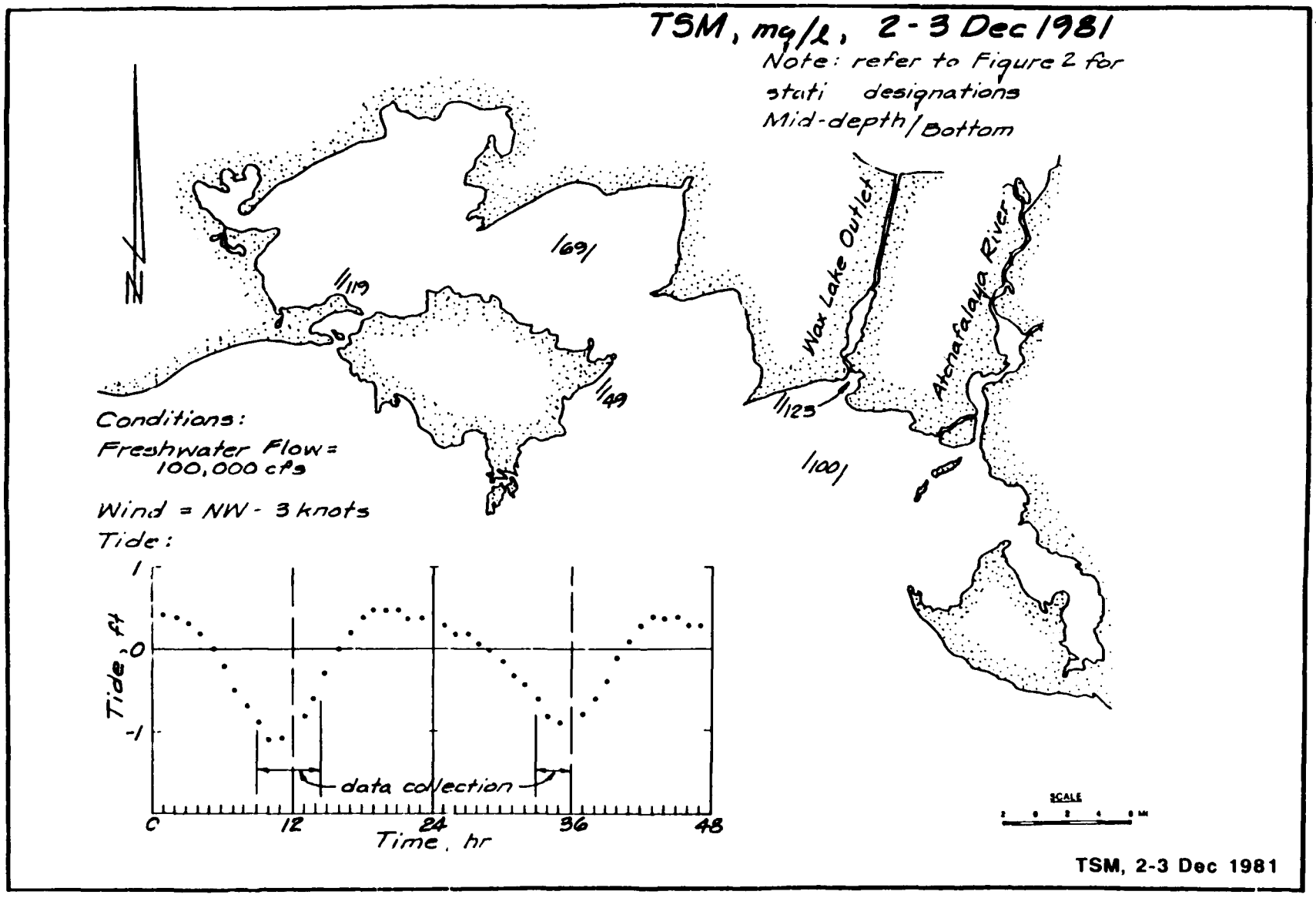
TSM, mg/l, 2-3 Dec 1981
Note: refer to Figure 2 for
stati designations
Mid-depth/Bottom
N
1119
1691
1149
Wax Lake Outlet
Atchafalaya River
1125
1100
Conditions:
Freshwater Flow =
100,000 cfs
Wind = NW - 3 knots
Tide:
Tide, ft
1
0
-1
data collection
0
12
24
36
48
Time, hr
SCALE
TSM, 2-3 Dec 1981

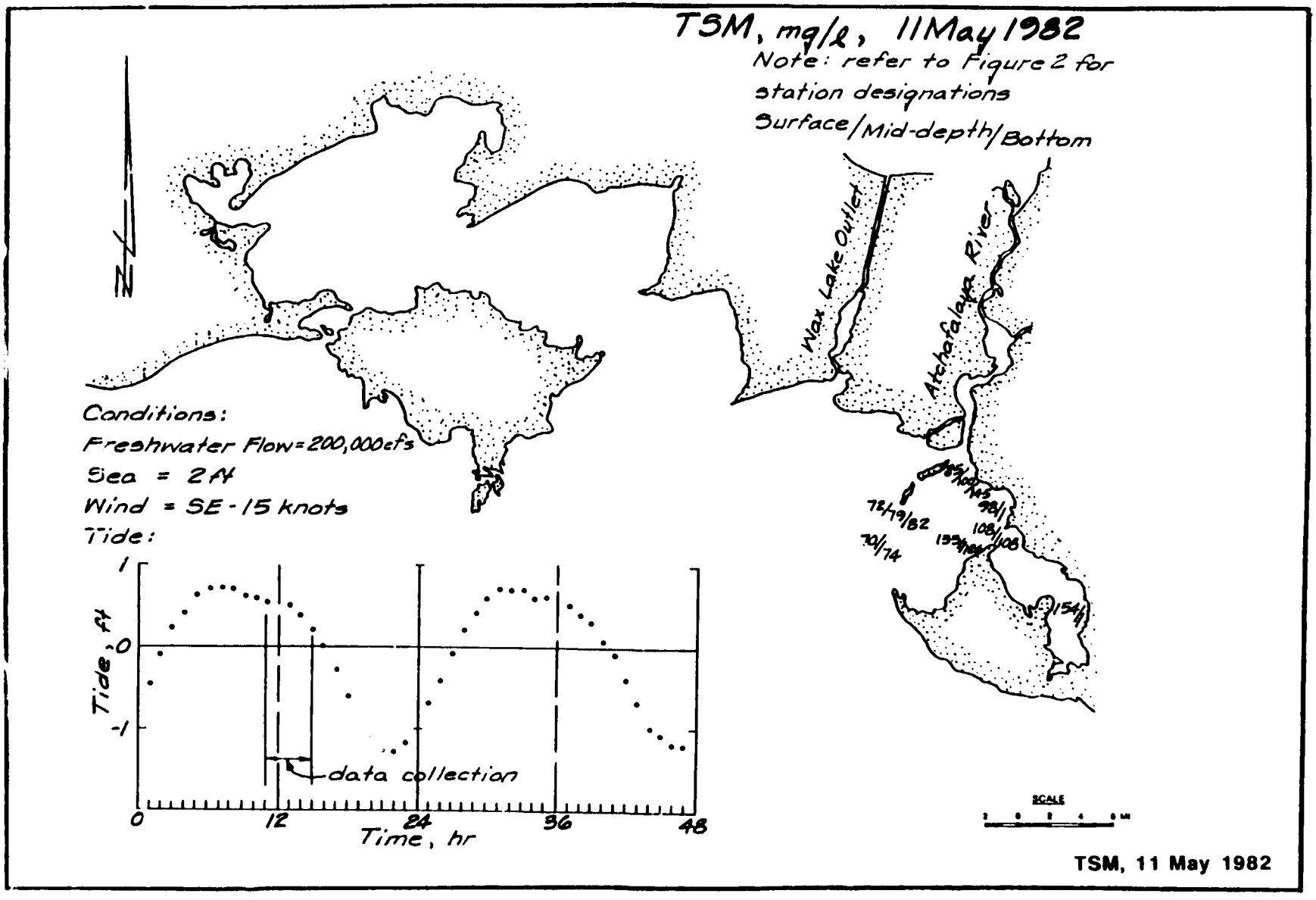
TSM, mg/ℓ, 11 May 1982
Note: refer to Figure 2 for station designations
Surface/Mid-depth/Bottom
Wax Lake Outlet
Atchafalaya River
Conditions:
Freshwater Flow = 200,000 cfs
Sea = 2 ft
Wind = SE - 15 knots
Tide:
Tide, ft
1
0
-1
data collection
0
12
24
36
48
Time, hr
72/79/82
70/74
98/
108/108
154/
SCALE
TSM, 11 May 1982

PLATE 13

PLATE 14

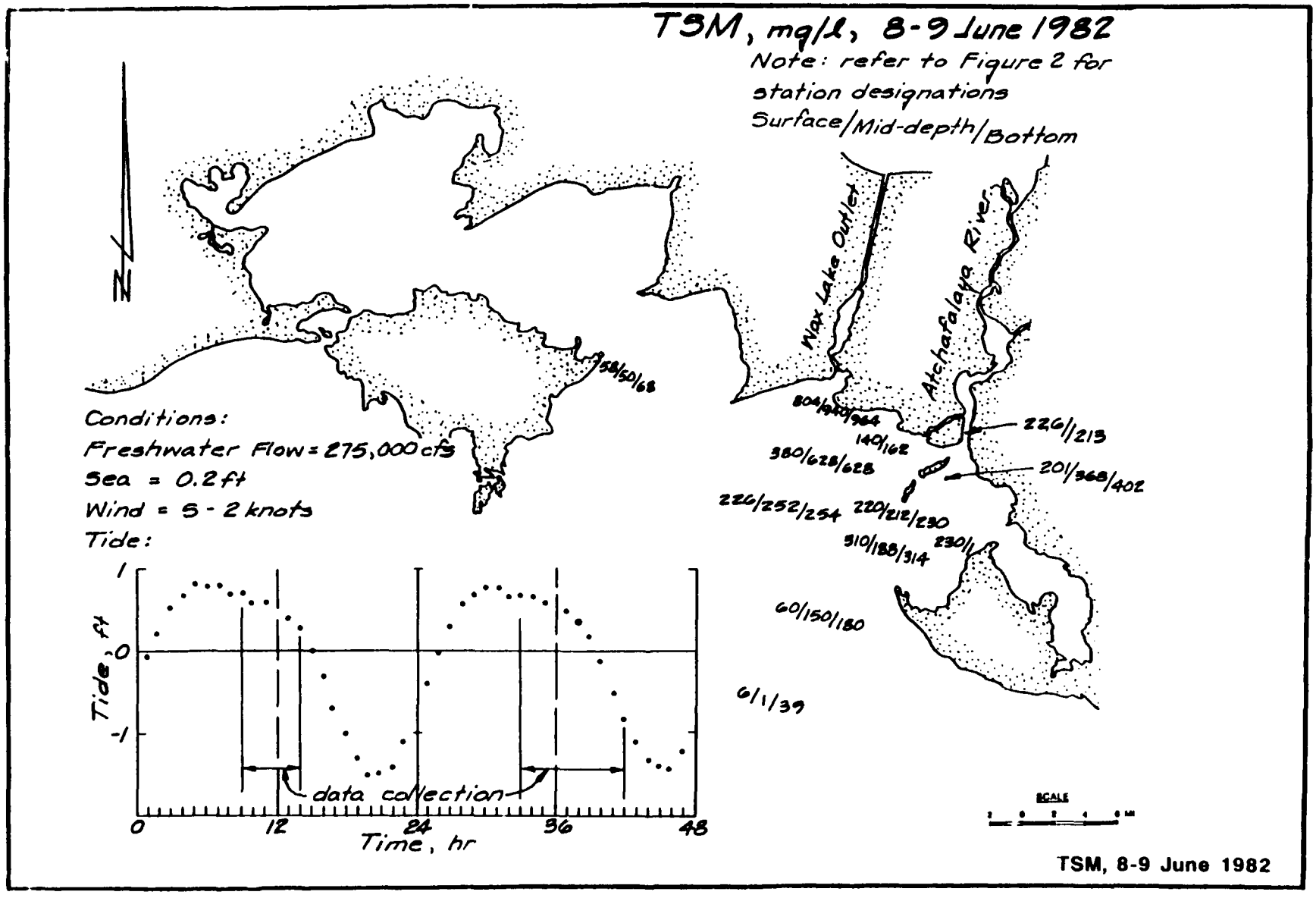
TSM, mg/l, 8-9 June 1982
Note: refer to Figure 2 for station designations
Surface/Mid-depth/Bottom
Wax Lake Outlet
Atchafalaya River
58/50/68
804/920/964
140/162
226/213
380/628/628
201/368/402
226/252/254
220/212/230
310/188/314
230/
60/150/180
6/1/39
Conditions:
Freshwater Flow = 275,000 cfs
Sea = 0.2 ft
Wind = 5 - 2 knots
Tide:
Tide, ft
1
0
-1
data collection
0
12
24
36
48
Time, hr
SCALE
TSM, 8-9 June 1982

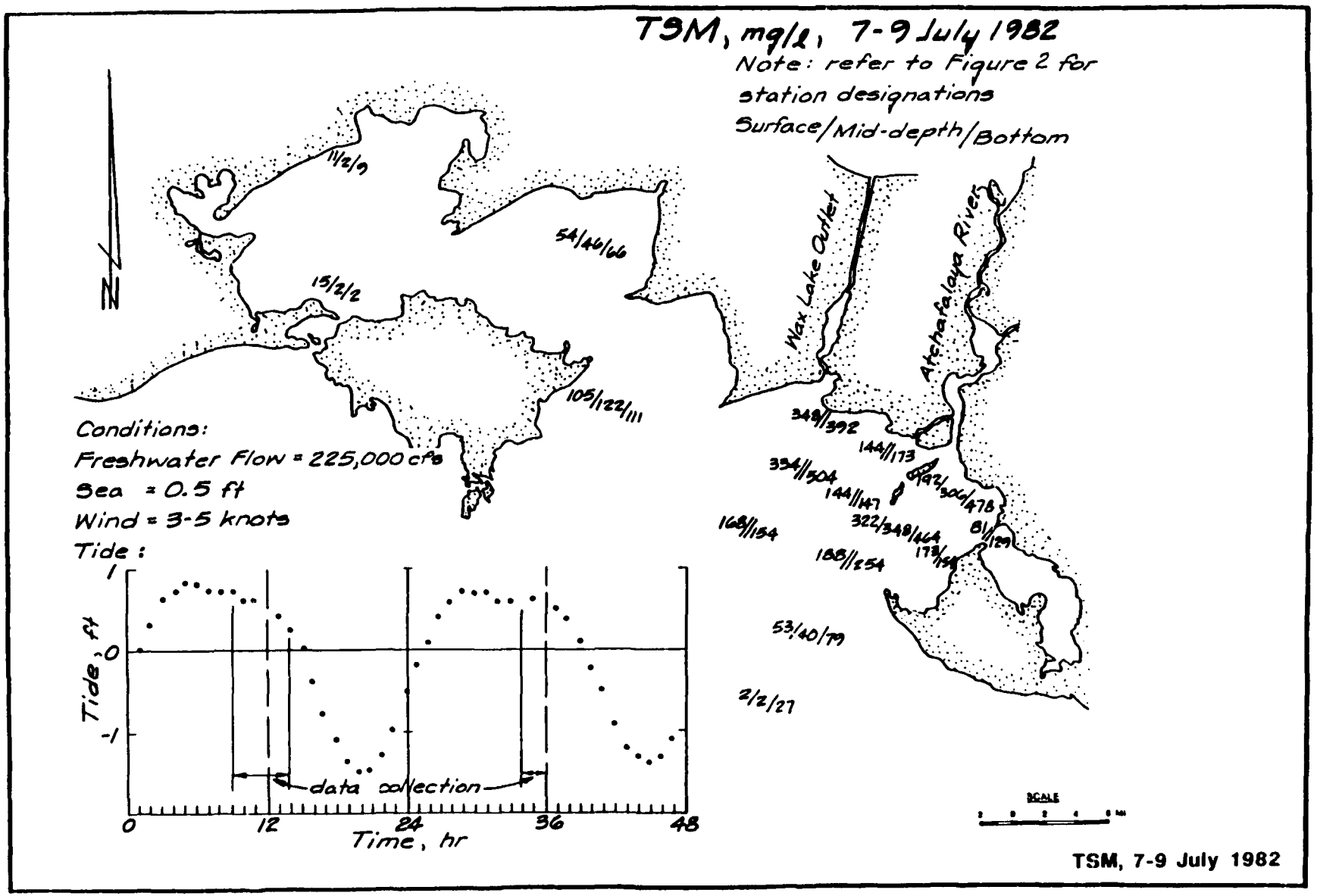
TSM, mg/l, 7-9 July 1982
Note: refer to Figure 2 for station designations
Surface/Mid-depth/Bottom
11/2/9
54/46/66
15/2/2
105/122/111
Wax Lake Outlet
Atchafalaya River
348/392
144/173
354/504
144/147
492/506/478
168/154
322/348/464
81/129
188/254
173/159
53/40/79
2/2/27
Conditions:
Freshwater Flow = 225,000 cfs
Sea = 0.5 ft
Wind = 3-5 knots
Tide:
Tide, ft
1
0
-1
data collection
0
12
24
36
48
Time, hr
SCALE
TSM, 7-9 July 1982

PLATE 15

PLATE 16

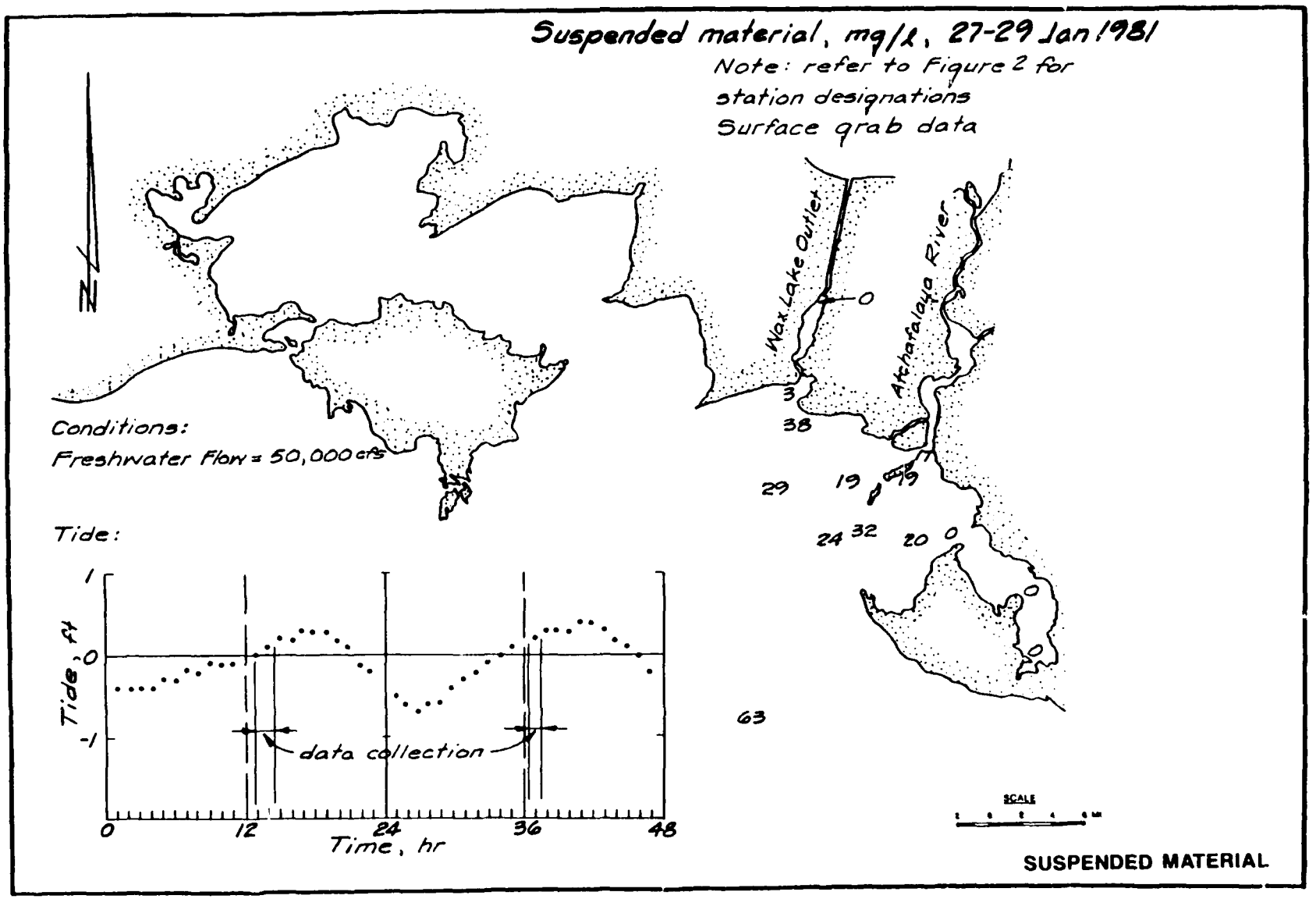
Suspended material, mg/l, 27-29 Jan 1981
Note: refer to Figure 2 for station designations
Surface grab data
Wax Lake Outlet
Atchafalaya River
0
3
38
29
19
24
32
20
0
0
0
63
Conditions:
Freshwater Flow = 50,000 cfs
Tide:
1
Tide, ft
0
-1
data collection
0
12
24
36
48
Time, hr
SCALE
SUSPENDED MATERIAL

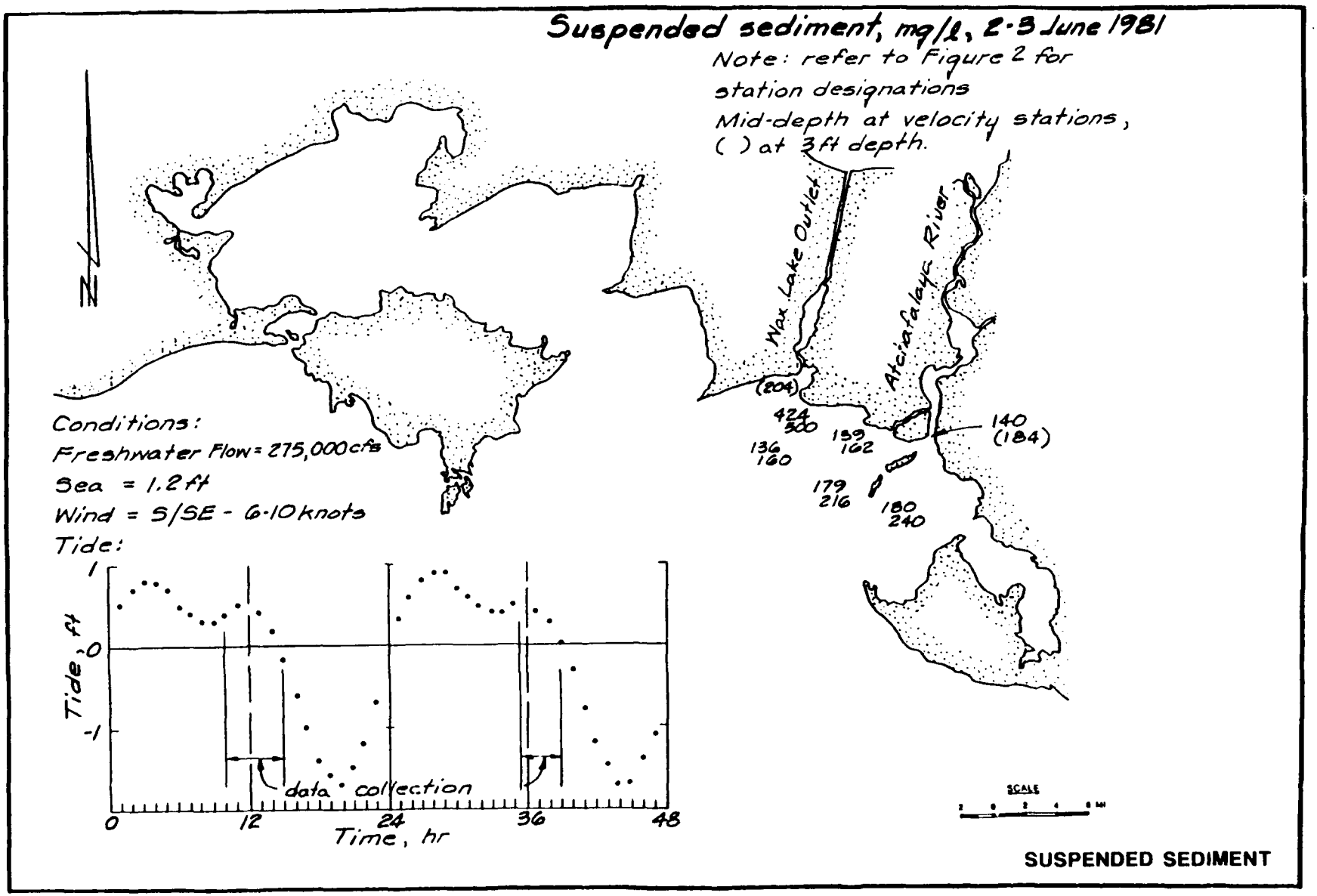
Suspended sediment, mg/l, 2-3 June 1981
Note: refer to Figure 2 for station designations
Mid-depth at velocity stations, ( ) at 3ft depth.
Wax Lake Outlet
Atchafalaya River
(204)
424
300
139
162
136
160
140
(184)
179
216
180
240
Conditions:
Freshwater Flow = 275,000cfs
Sea = 1.2ft
Wind = S/SE - 6-10knots
Tide:
Tide, ft
1
0
-1
data collection
0
12
24
36
48
Time, hr
SCALE
SUSPENDED SEDIMENT

PLATE 17

PLATE 18

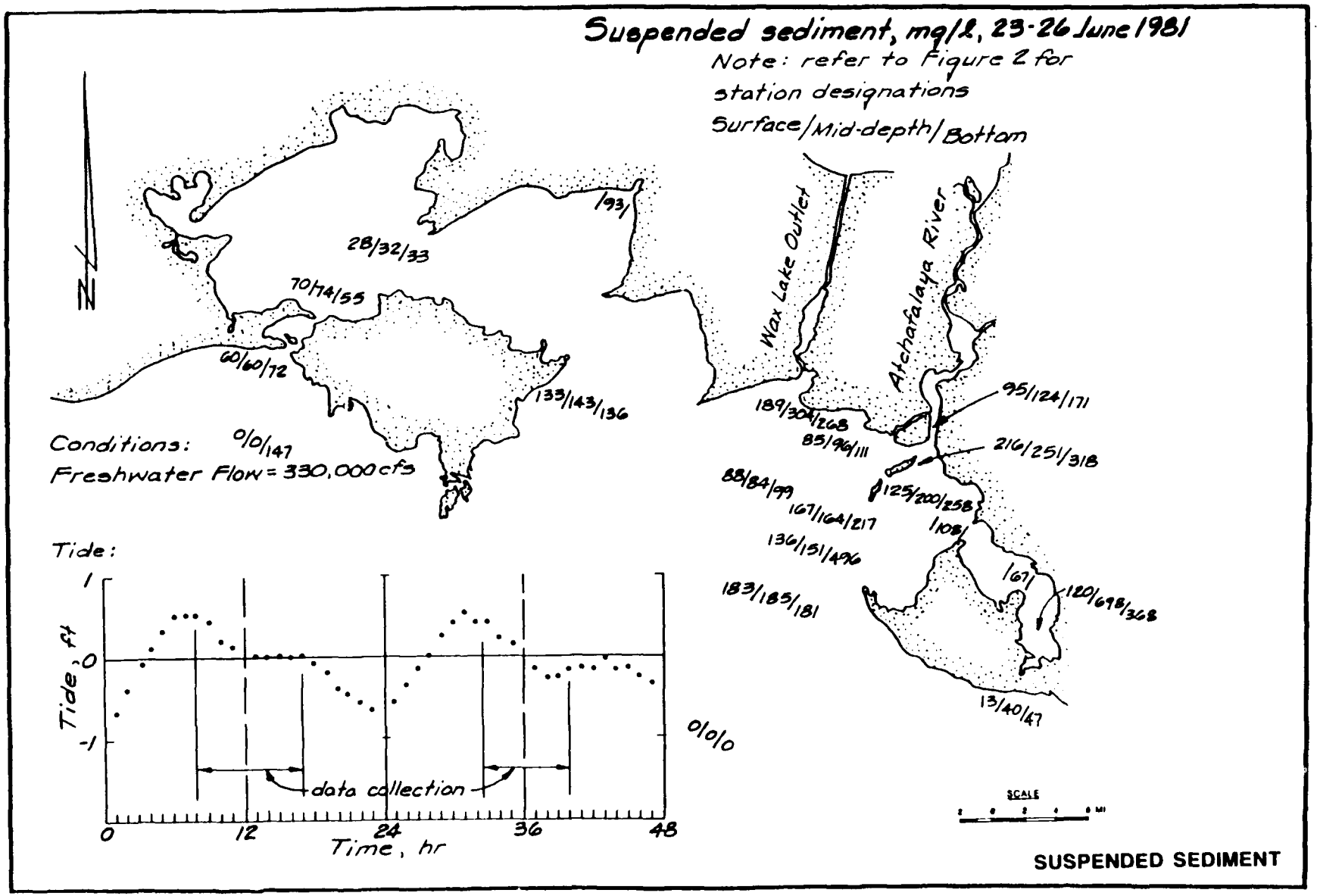
Suspended sediment, mg/l, 23-26 June 1981
Note: refer to Figure 2 for station designations
Surface/Mid-depth/Bottom
Wax Lake Outlet
Atchafalaya River
193
28/32/33
70/74/55
60/60/72
133/143/136
Conditions: 0/0/147
Freshwater Flow = 330,000 cfs
189/304/268
85/96/111
95/124/171
216/251/318
88/84/99
167/164/217
125/200/258
108
136/151/496
183/185/181
67
120/698/368
13/40/47
Tide:
Tide, ft
1
0
-1
data collection
0
12
24
36
48
Time, hr
0/0/0
SCALE
SUSPENDED SEDIMENT

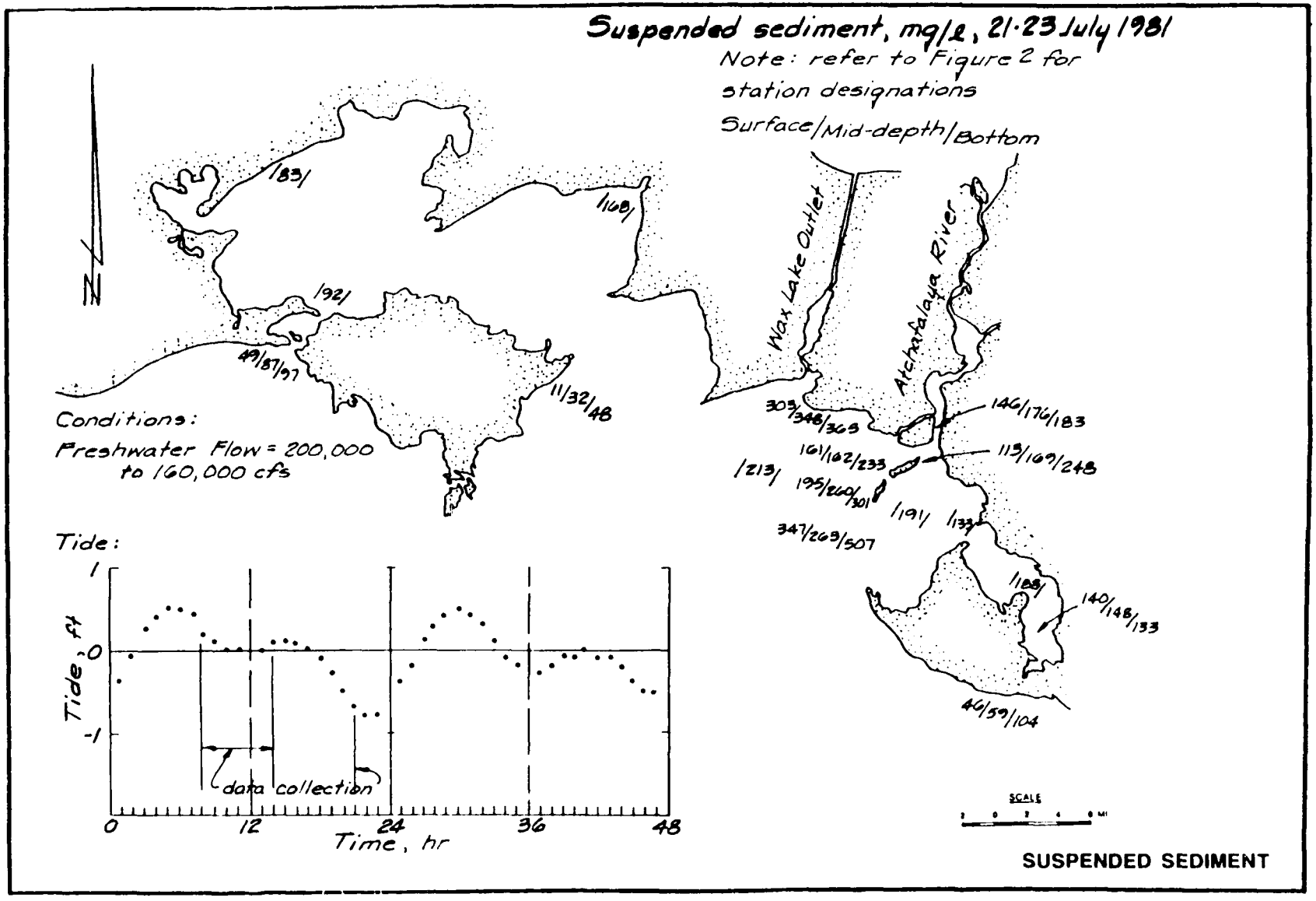
Suspended sediment, mg/L, 21-23 July 1981
Note: refer to Figure 2 for station designations
Surface/Mid-depth/Bottom
Wax Lake Outlet
Atchafalaya River
/183/
/168/
/192/
49/87/97
11/32/48
303/348/363
146/176/183
161/162/233
113/169/248
/213/
195/260/301
/191/
/133/
347/269/507
/188/
140/148/133
46/59/104
Conditions:
Freshwater Flow = 200,000 to 160,000 cfs
Tide:
Tide, ft
1
0
-1
data collection
0
12
24
36
48
Time, hr
SCALE
SUSPENDED SEDIMENT

PLATE 19

PLATE 20

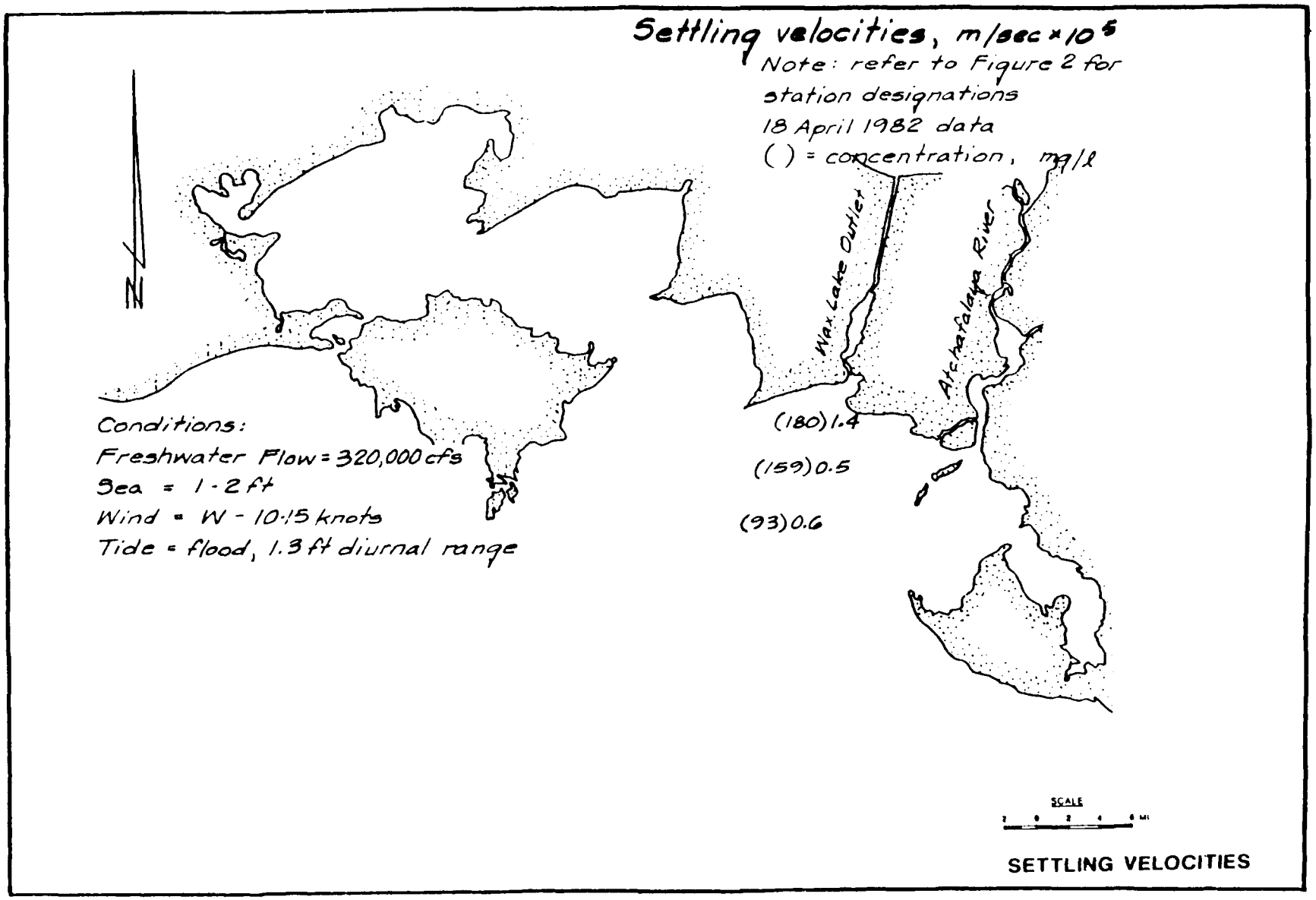
Settling velocities, m/sec x 10⁵
Note: refer to Figure 2 for station designations
18 April 1982 data
( ) = concentration, mg/l
Wax Lake Outlet
Atchafalaya River
(180) 1.4
(159) 0.5
(93) 0.6
Conditions:
Freshwater Flow = 320,000 cfs
Sea = 1-2 ft
Wind = W - 10-15 knots
Tide = flood, 1.3 ft diurnal range
SCALE
SETTLING VELOCITIES

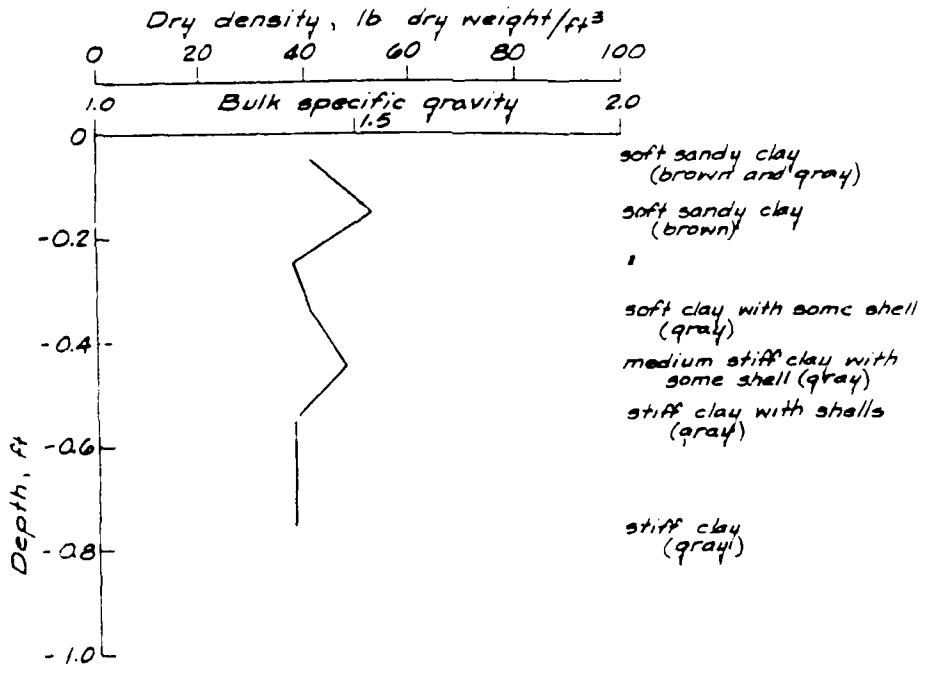

STATION A

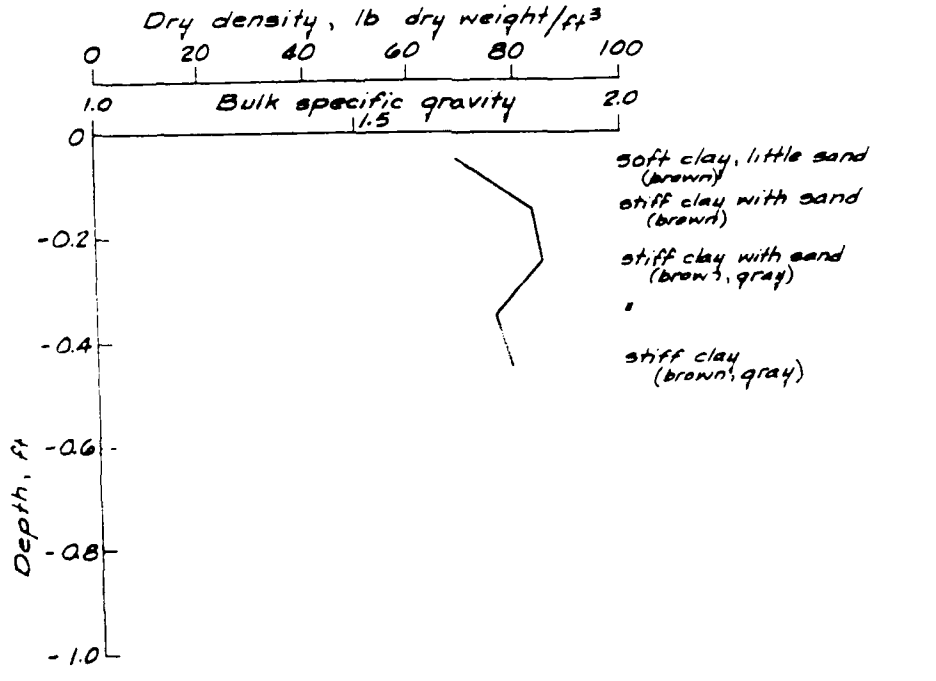

STATION C

BULK WET DENSITY
Stations A and C

PLATE 21

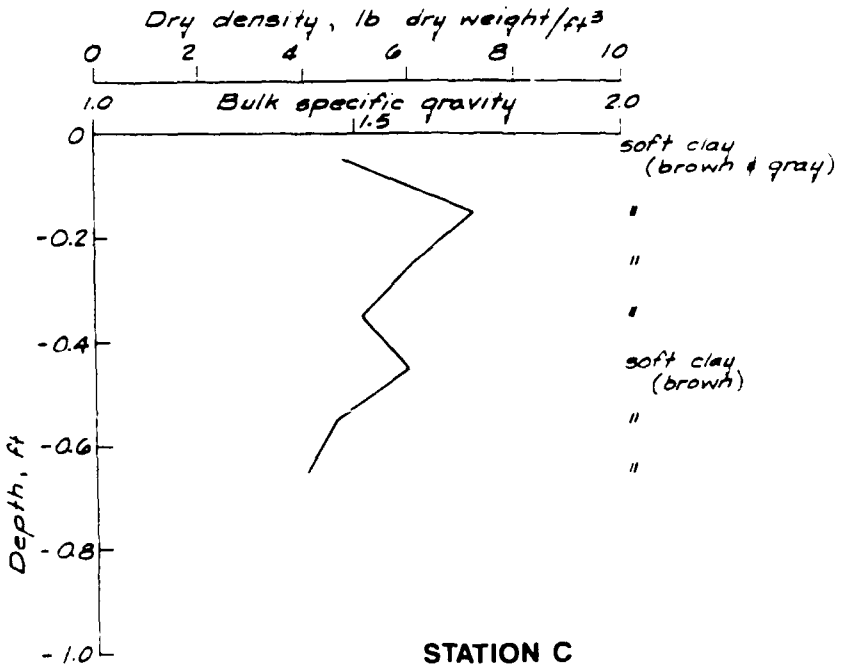

STATION C

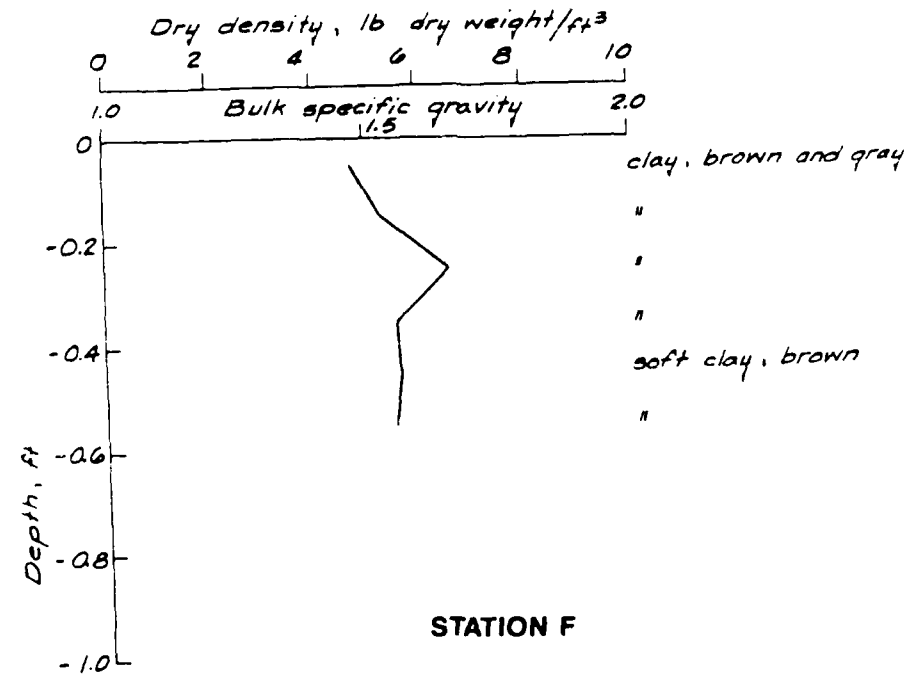

STATION F

BULK WET DENSITY

Stations C and F

PLATE 22

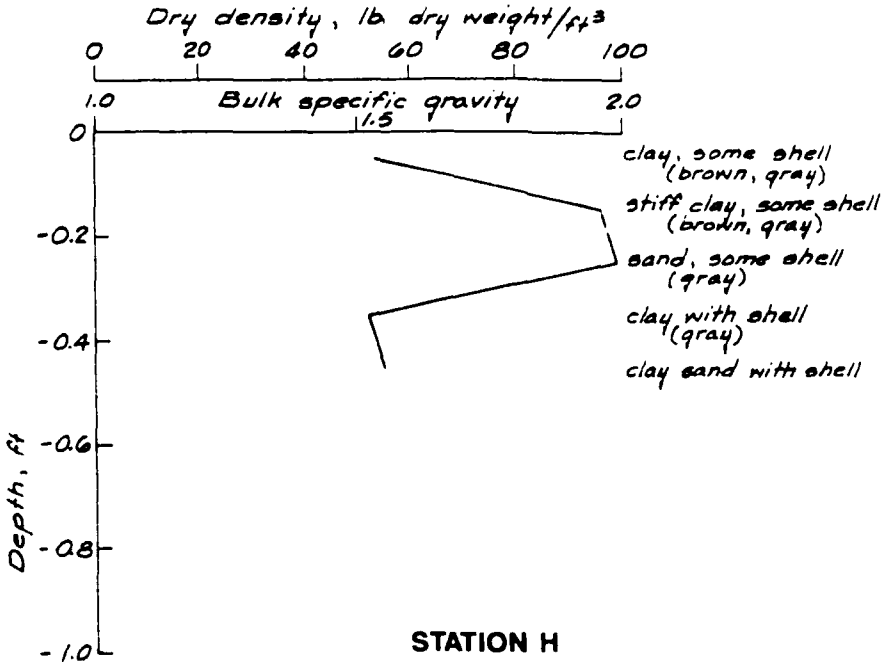

STATION H

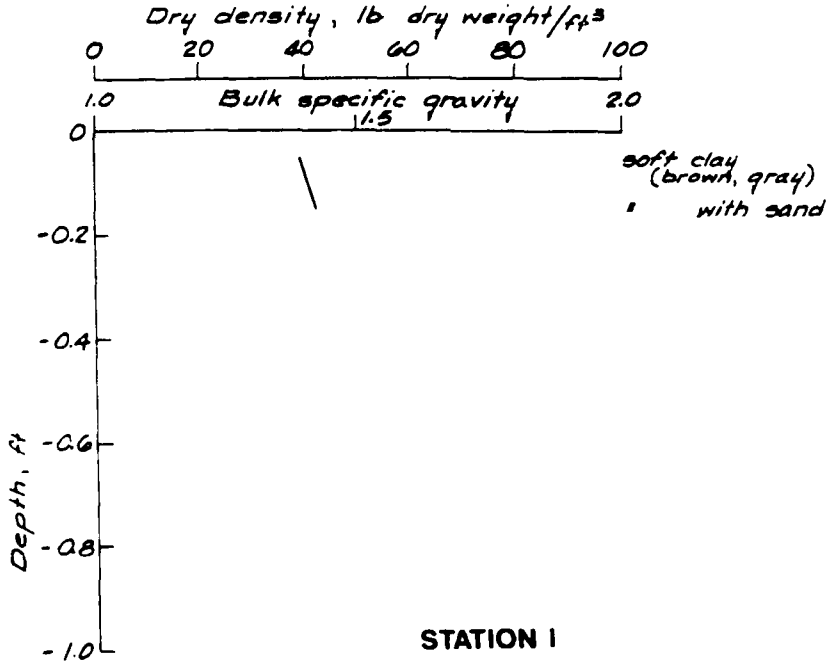

STATION I

BULK WET DENSITY
Stations H and I

PLATE 23

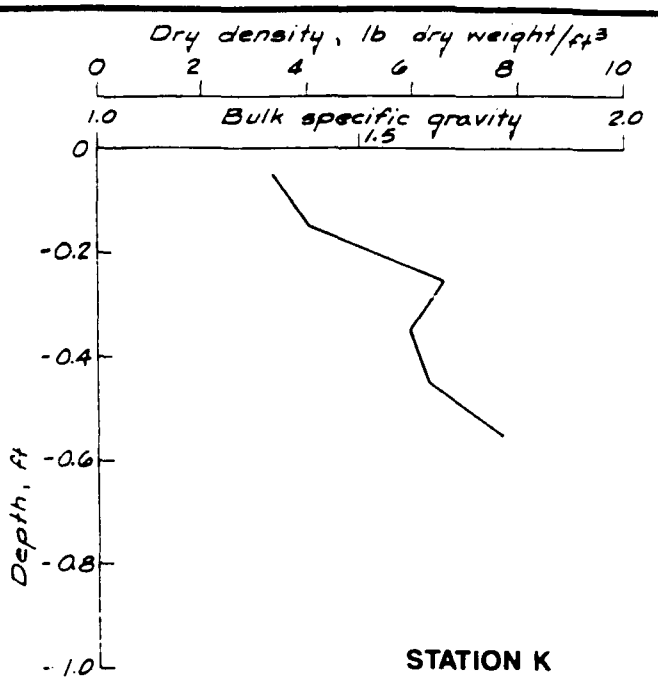

STATION K

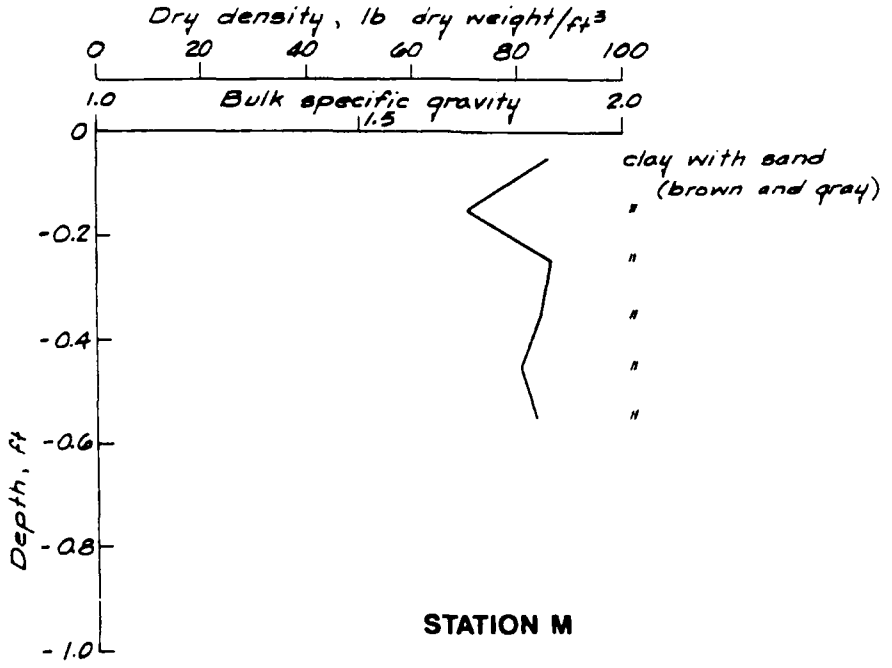

STATION M

BULK WET DENSITY

Stations K and M

PLATE 24

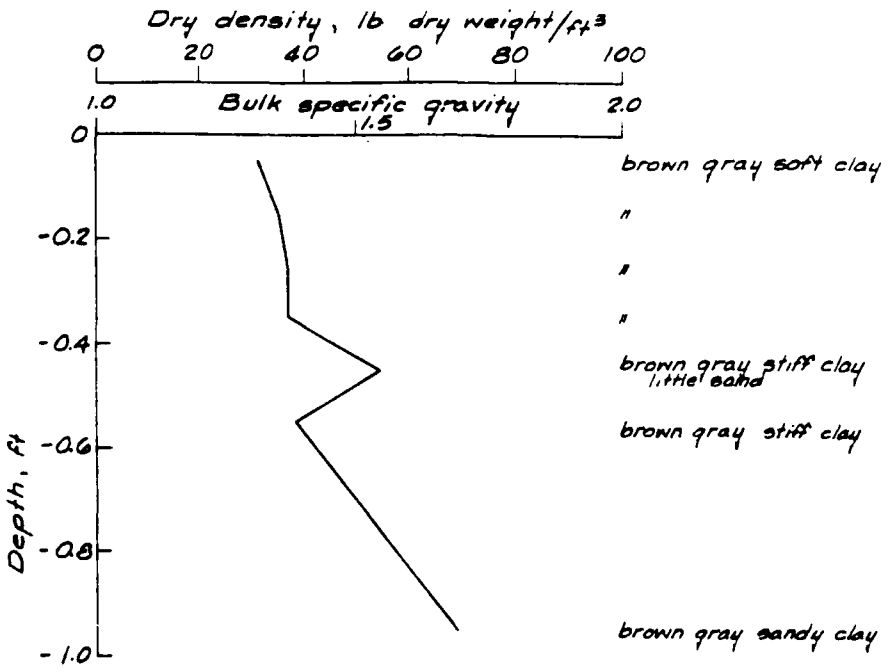

STATION N

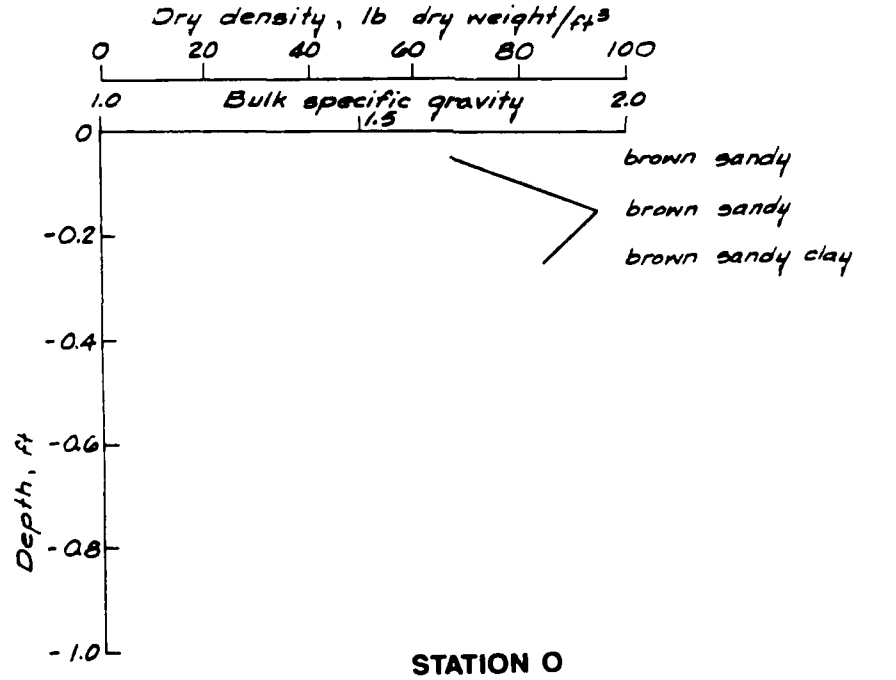

STATION O

BULK WET DENSITY

Stations N and O

PLATE 25

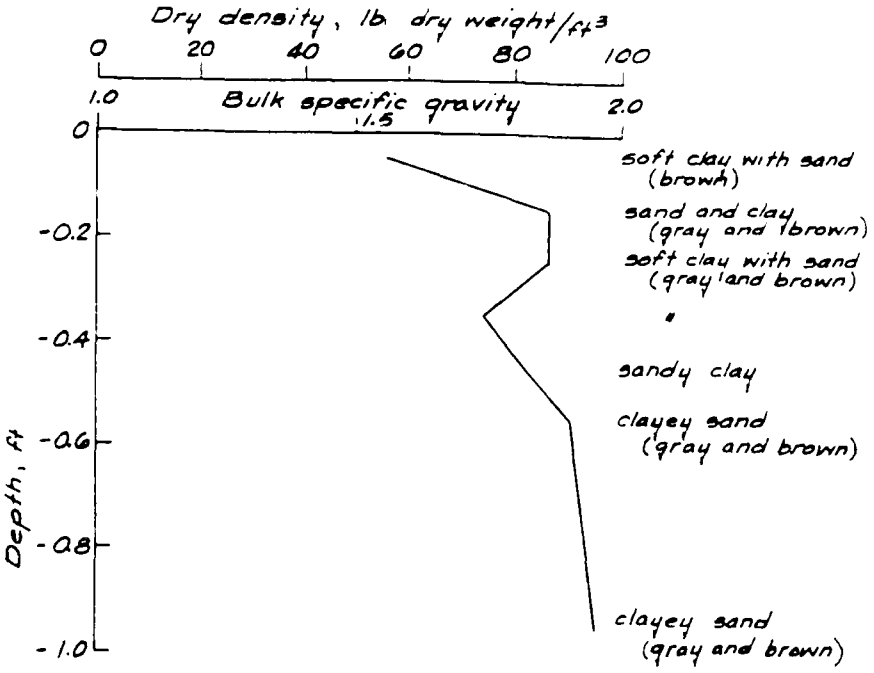

STATION O

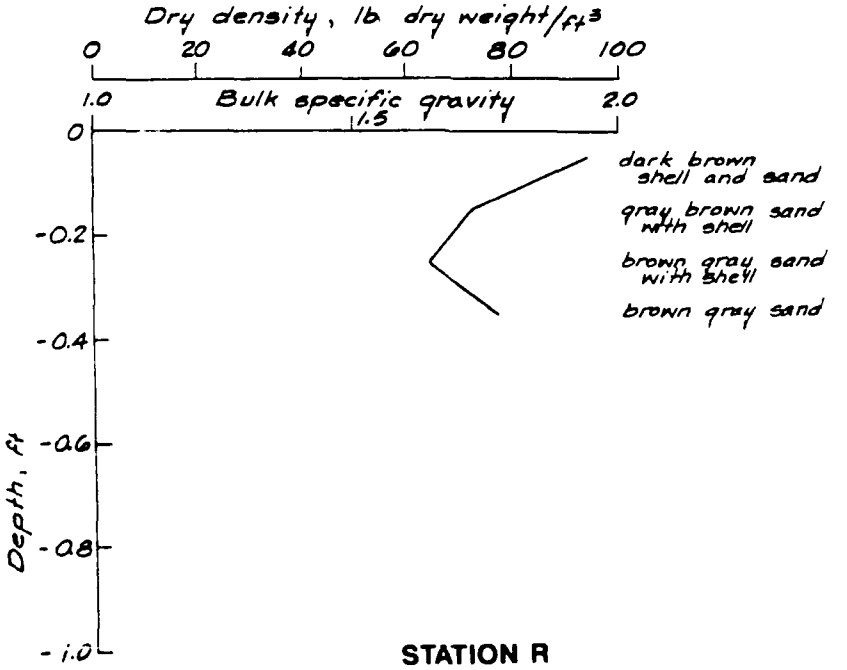

STATION R

BULK WET DENSITY
Stations O and R

PLATE 26

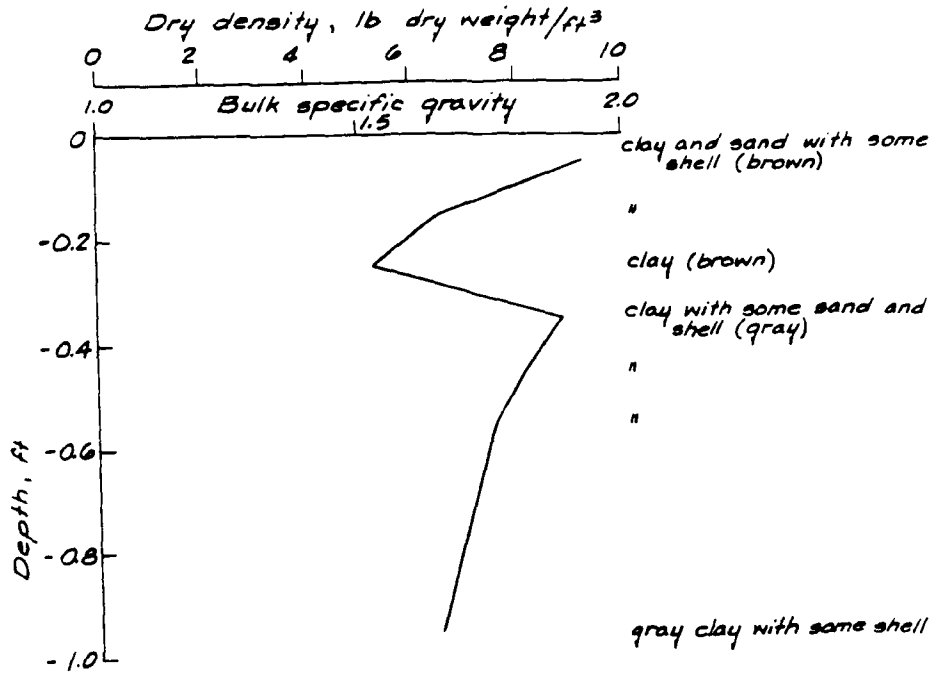

STATION R

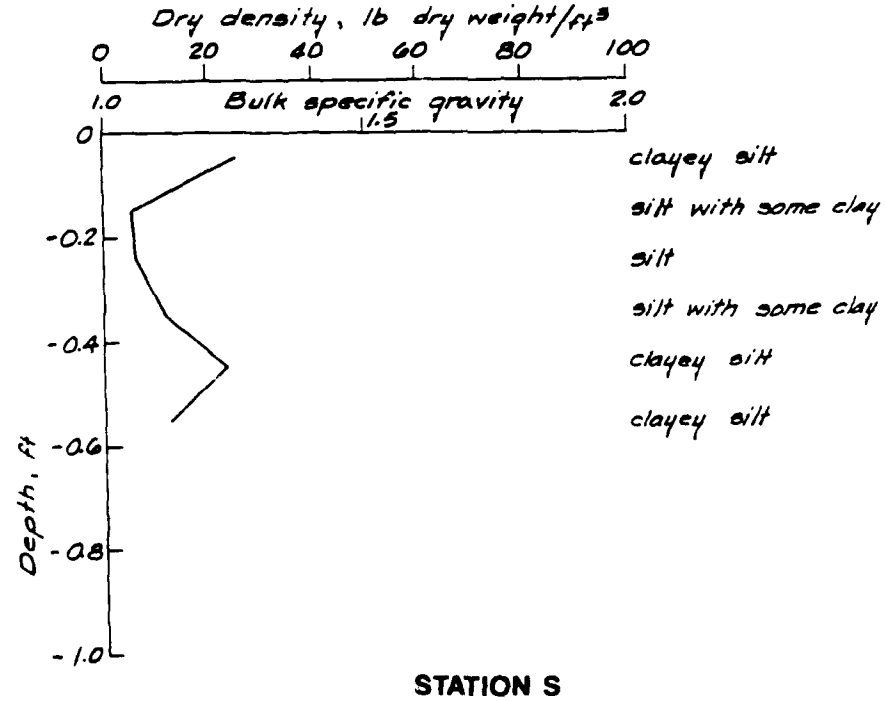

STATION S

BULK WET DENSITY
Stations R and S

PLATE 27

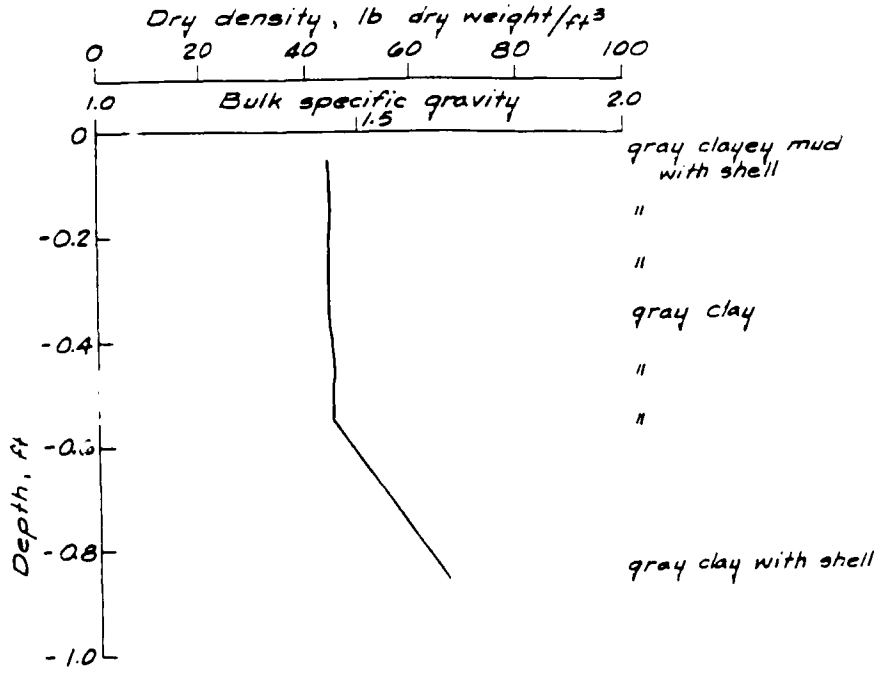

STATION U

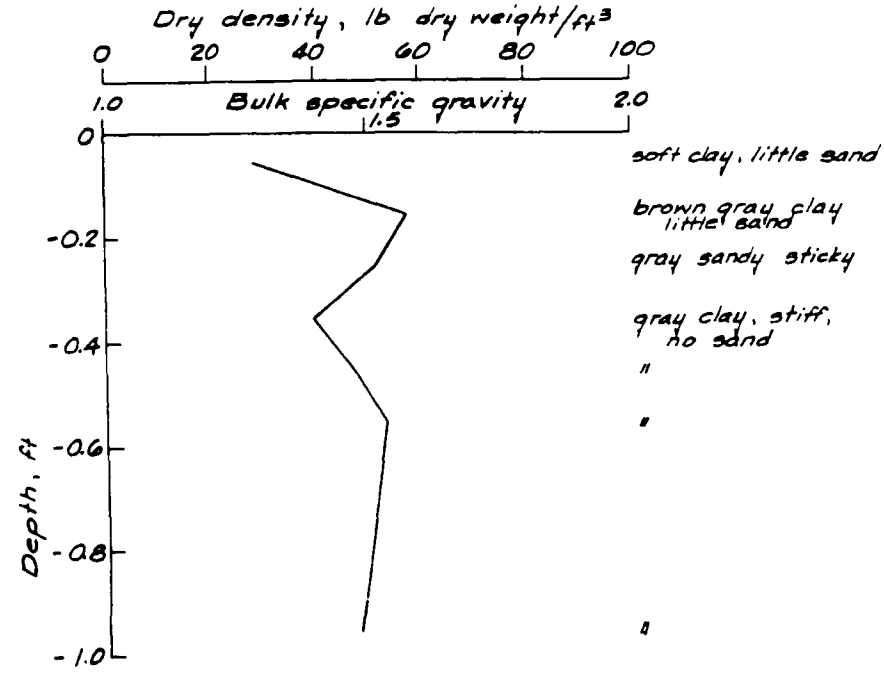

STATION "NEW"

BULK WET DENSITY

Stations U and "NEW"

PLATE 28

APPENDIX A: NOTATION

Subscripts and indices:

b	Bottom; bed
f	Fresh water
o	Indicates a depth average or vertically homogeneous
x	Horizontal coordinate
y	Vertical coordinate
z	Depth coordinate

Parameters:

a	Regression constant
BWD	Bulk wet density
C	Concentration of suspended sediment
$\bar{C}$	Depth-averaged concentration
C_o	Initial concentration
C_s	Concentration of bed sediments
CEC	Cation exchange capacity
D	Deposition
E	Erosion
g	Force due to gravity
h	Deviation from the mean tide level
H	Thickness of mud layer; total depth or height; settling height
k	An index, such as the number of sediment fractions
K	Empirical coefficient
K_z	Effective vertical eddy diffusivity
$\dot{m}$	Mass rate of erosion
m	Mass per unit surface area of the consolidating layer

n	Manning's friction coefficient
P	Probability of particle sticking to bed
P_e	Particle Peclet number
Q_f	Freshwater inflow
S	Salinity
t	Nondimensional time
T	Time, dimensional
TSM	Total suspended material
U	Horizontal velocity
U^*	Bed shear velocity
$\bar{U}$	Depth-averaged velocity
$U^*(fm)$	Shear velocity estimated using Manning's equation
W_s	Settling velocity
W_h	Hindered settling velocity
W_{s_g}	Geometric mean
W_{s_x}	Settling velocity at the x^{th} percentile
x	Nondimensional horizontal coordinate
z	Nondimensional vertical coordinate
Z	Vertical dimension measured upward from bed
Z_o	Roughness height
δC	Surface-to-bottom difference in concentration
ρ	Density
ρ_w	Density of water
ρ_o	Reference density (fresh water)
σ	Dye variance
σ_g	Geometric standard deviation

τ	Shear stress
τ_b	Bed shear stress
τ_{cd}	Critical shear stress for deposition